

Dedicated gravity satellite missions



Lóránt Földvály

Geodesy

Tasks of **geodesy**:

Determination of the topography, and of the position of artificial / natural objects on the surface of the Earth.

geometry

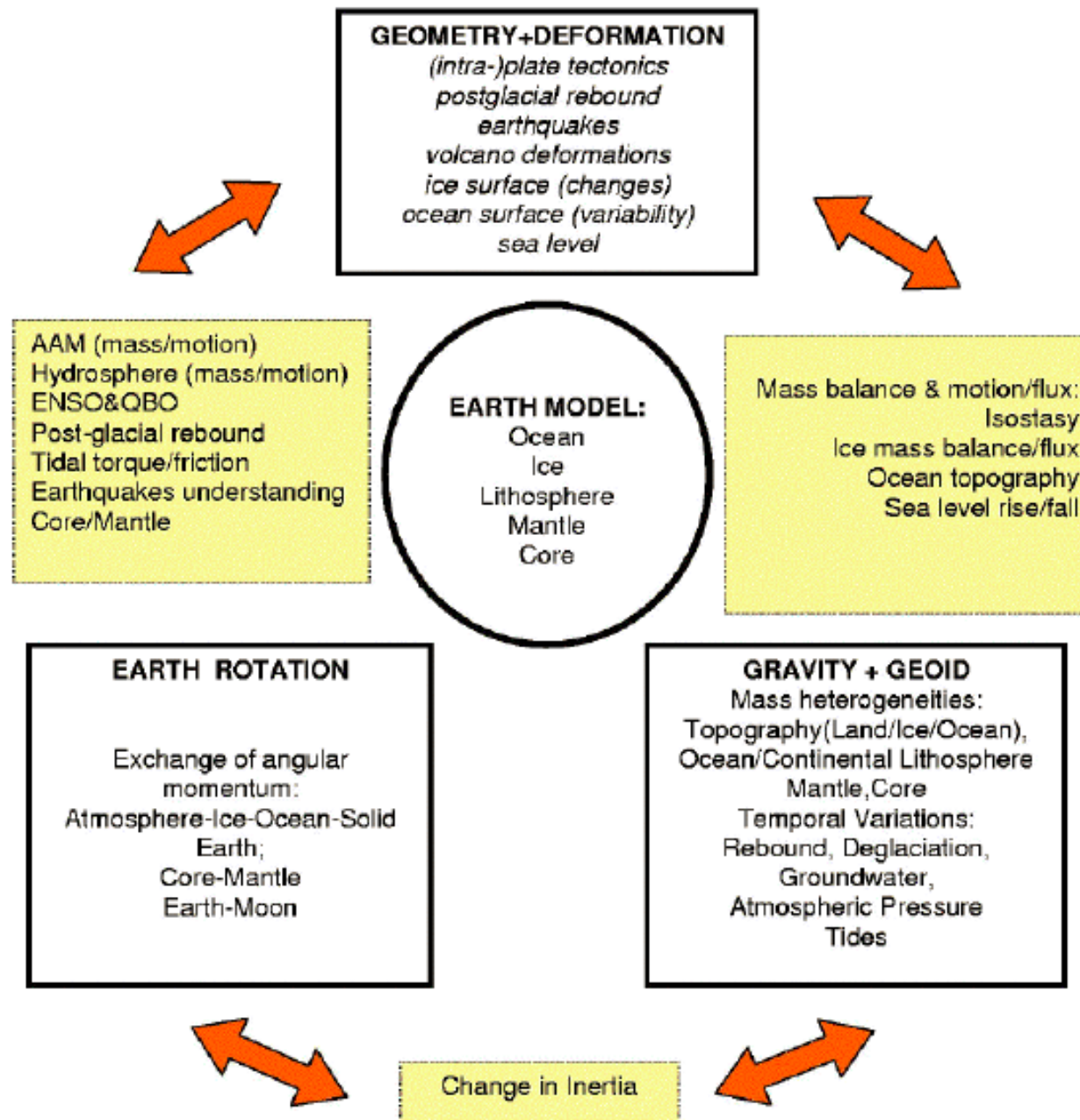
Determination of the global height reference, the geoid

geoid, gravity field

Determination of the Earth rotation parameters

Earth rotation

These tasks may be extended with the temporally varying counterparts of the features: deformation, temporal gravity variations, etc.



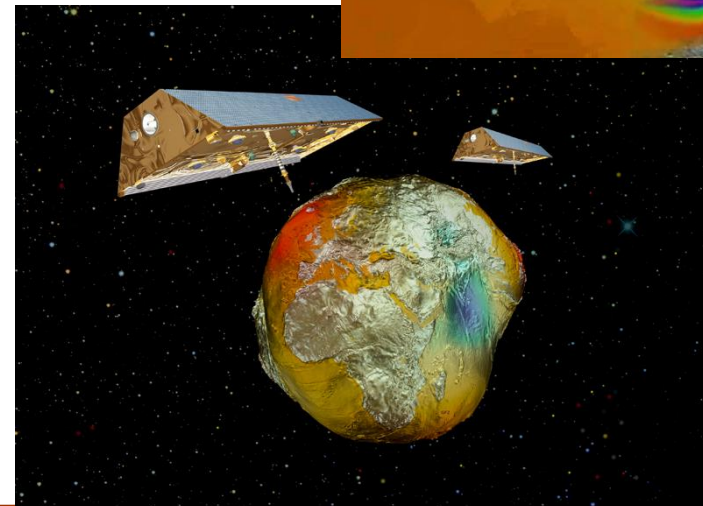
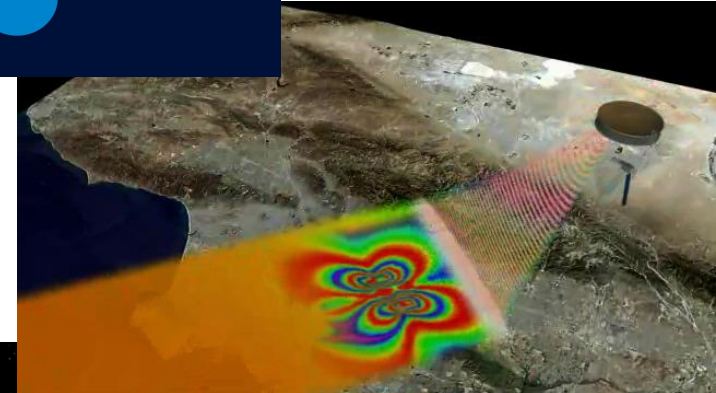
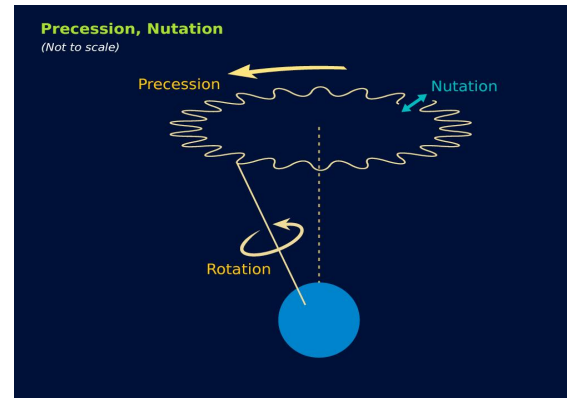
Dedicated gravity satellite missions
 Mostar, 19.10.2017

Tasks of Geodesy

Earth rotation

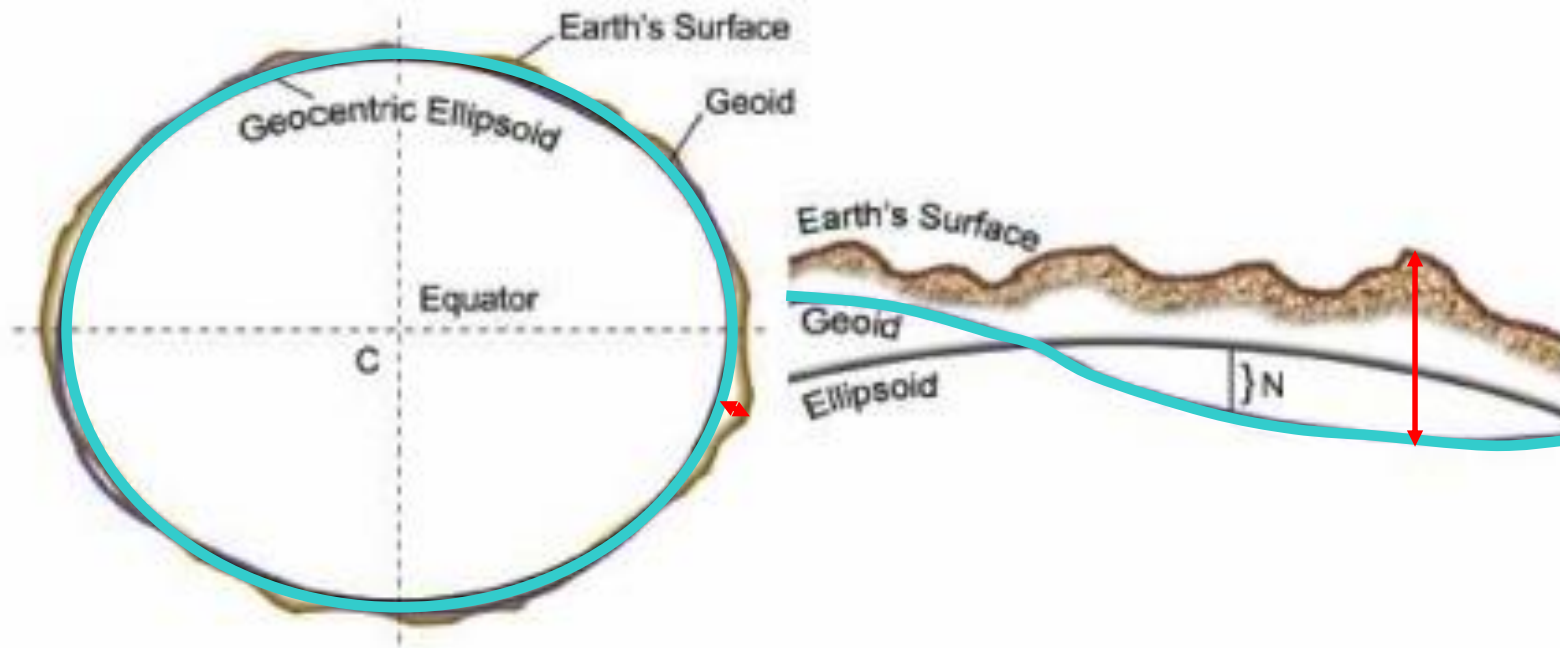
geometry, deformation

geoid, gravity field



Dedicated gravity satellite missions
Mostar, 19.10.2017

Need of geoid determination



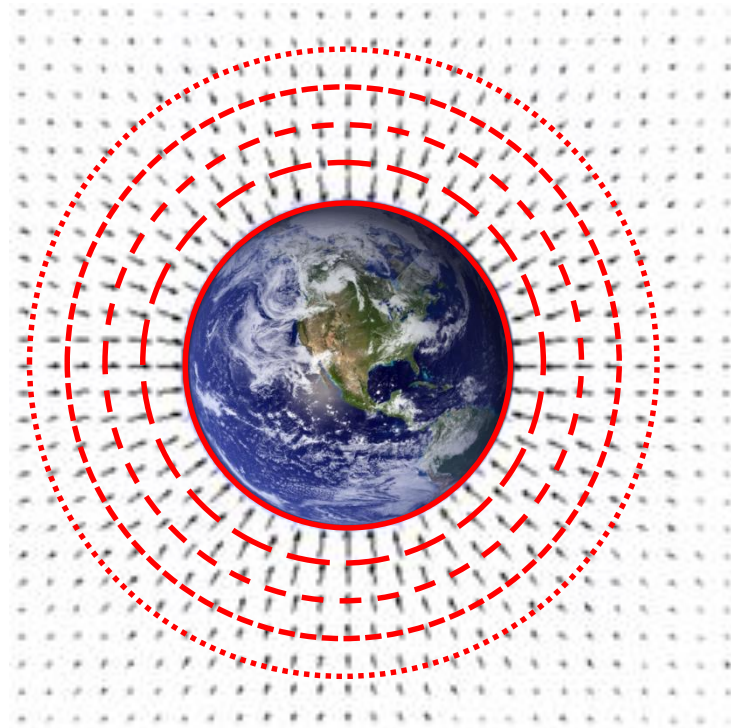
For engineering applications separation of **horizontal** and **vertical** directions can be defined by the knowledge of a geoid model.

Determination of the geoid

The **geoid** is a equipotential surface of the gravity field.

Therefore:

determination of the geoid = determination of the gravity field

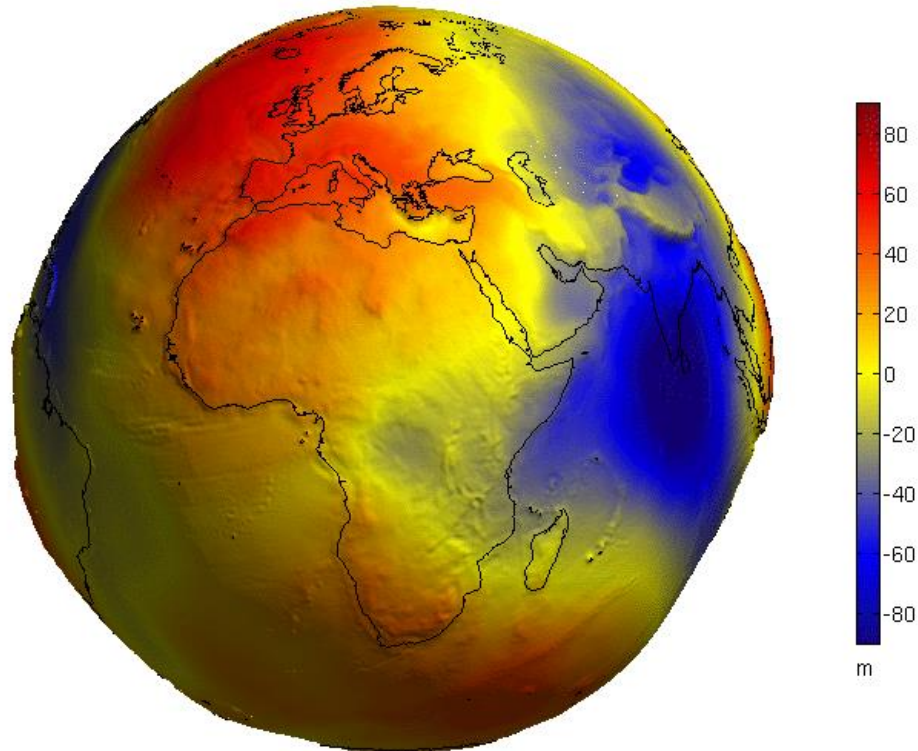


Determination of the geoid

The geoid is nearly a spherical, closed surface.

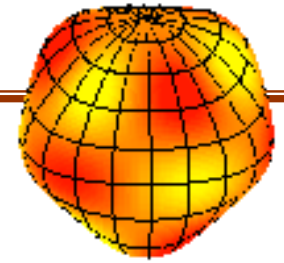
It's maximal deviation from a sphere is 21 km

It's maximal deviation from an ellipsoid is 100 m



Thus, it makes sense to describe this surface with a spherical function.

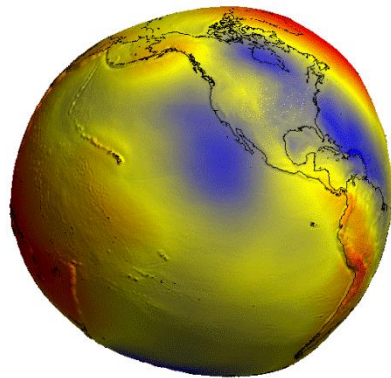
Spherical harmonics



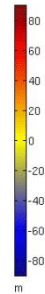
Spherical harmonics:

It is a mathematical tool to describes ‘bumps’ and ‘dimples’ with its differences from a sphere.

Spherical harmonics are a set of surface (2D) wavefunctions with different wavelength. Summation infinite number of spherical harmonics can describe any surface pattern.

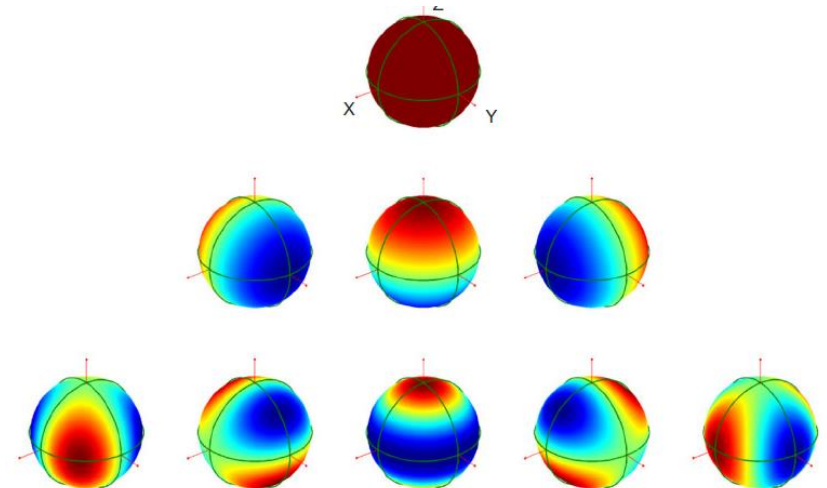


Geoid height (EGM2008, nmax=500)



=

Σ



Geoid model

Geoid model:

$$N = f(r, \varphi, \lambda, C_{nm}, S_{nm})$$

Spherical harmonic coefficients describe that at a certain „waveform” what is the size (amplitude) of the signal. The amplitude: C_{nm}, S_{nm}

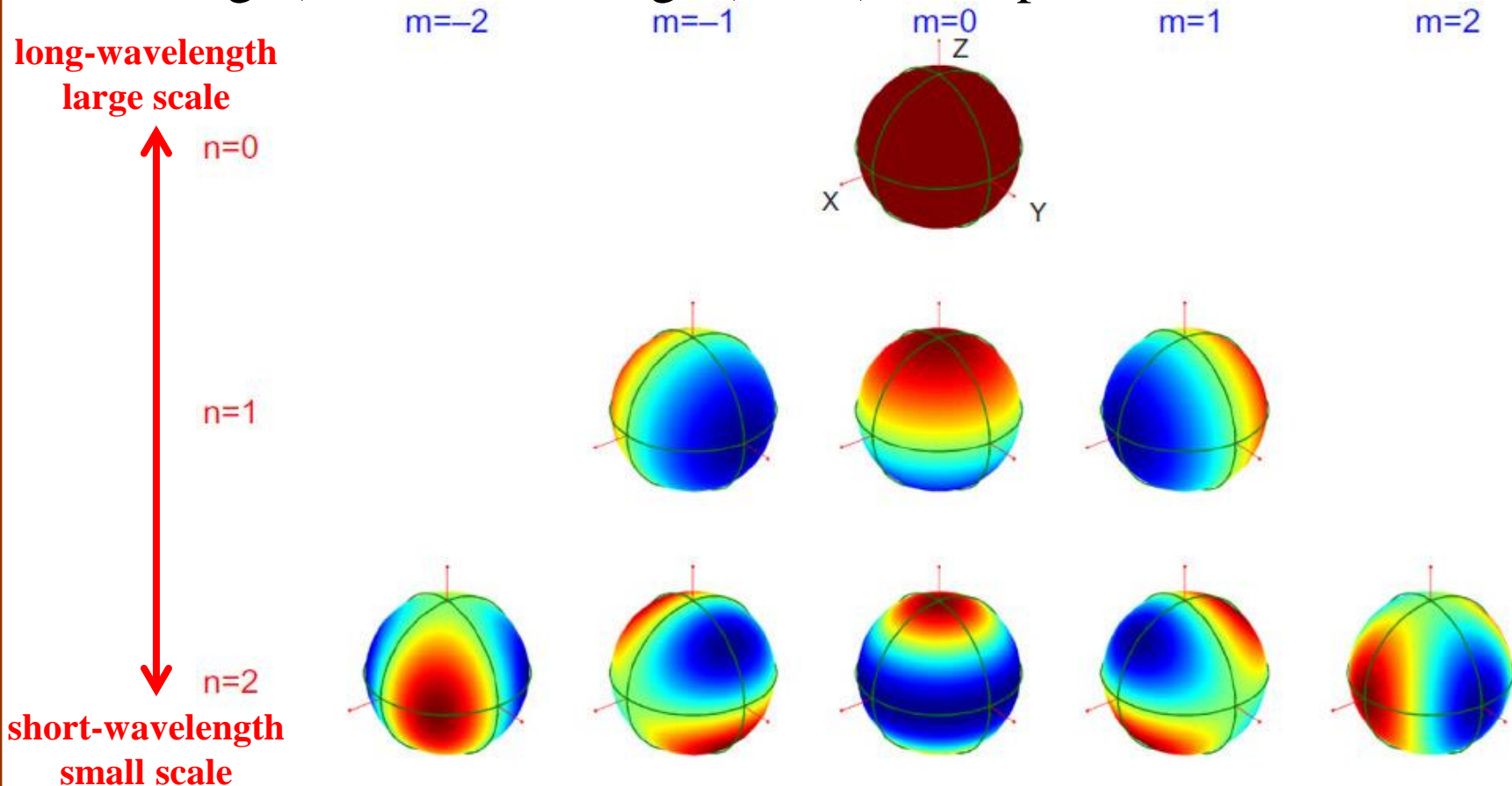
By defining the size of each wavelength component, the equation provides an unambiguous function between position (r, φ, λ) and distance (N) of geoid and sphere.

A geoid-model in fact is a set of spherical harmonic *coefficients*:

$$C_{nm}, S_{nm}$$

Geoid model

Wavelength of a spherical harmonic is described by the degree, n and order, m . Large (small) values of n refers to long-wavelength (short-wavelength) terms, thus large (small) scale patterns.



Determination of the geoid

Determination of a geoid model by satellite geodesy:

$$N = f(r, \varphi, \lambda, C_{nm}, S_{nm})$$

Geoid-related measurements are performed at known locations by **satellites** covering the whole globe.

Measurements: N at r, φ, λ

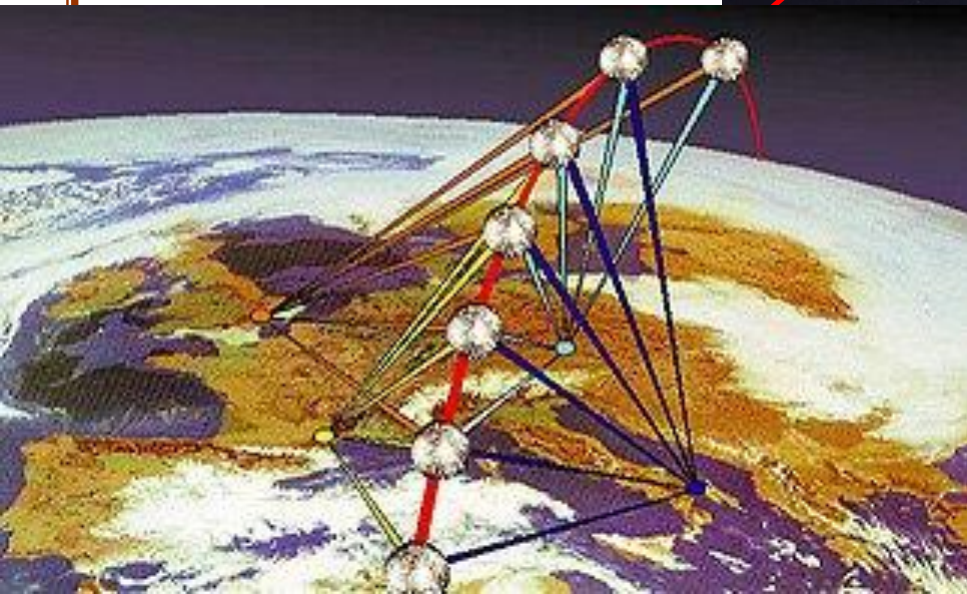
Unknown: C_{nm}, S_{nm}

The number of determinable unknowns (spherical harmonic coefficients) depends on the number and the spatial arrangement of measurements.

Determination of the geoid by satellite geodesy

Geoid determination in the XX century

Satellites revolving around the planet are tracked from observatories on the ground. Based on arcs of the orbits of satellites, a priori gravity field models can be refined.



Determination of the geoid by satellite geodesy

Geoid determination in the XX century

Satellites revolving around the planet are tracked from observatories on the ground. Based on arcs of the orbits of satellites, a priori gravity field models can be refined.

Techniques of tracking the orbits of satellites are done

1. optically
2. by Doppler
3. by laser (Satellite Laser Ranging)



Further contribution to gravity field determination has been added by the GNSS (GPS, Glonass) satellite systems and satellite altimetry missions (TOPEX/Poseidon, GPS/MET)

Determination of the geoid by satellite geodesy

Geoid determination in the XX century

The fundamental background of determining the gravity field from (arcs of) orbit is Newton's equation of motion:

$$\vec{F} = m\vec{a}$$

\vec{F} - (gravitational) force

\vec{a} - (gravitational) acceleration

The acceleration is related to the orbit (position, \vec{r}), as it is its second derivative by time. The relation between gravitational force and orbit reads

$$\vec{F} = m \frac{\partial^2 \vec{r}}{\partial t^2}$$

Determination of the geoid by satellite geodesy

Geoid determination in the XXI century

Dedicated gravity satellite missions have been implemented, which have already been simulated in the 80ies.

These missions have essentially improved both the precision and the spatial resolution of the gravity field models.

Fundamental background:

Several different methods tested at Universities and Research Institutes.

- integrating short-arcs of the orbit
- energy integral
- kinematic accelerations
- etc.

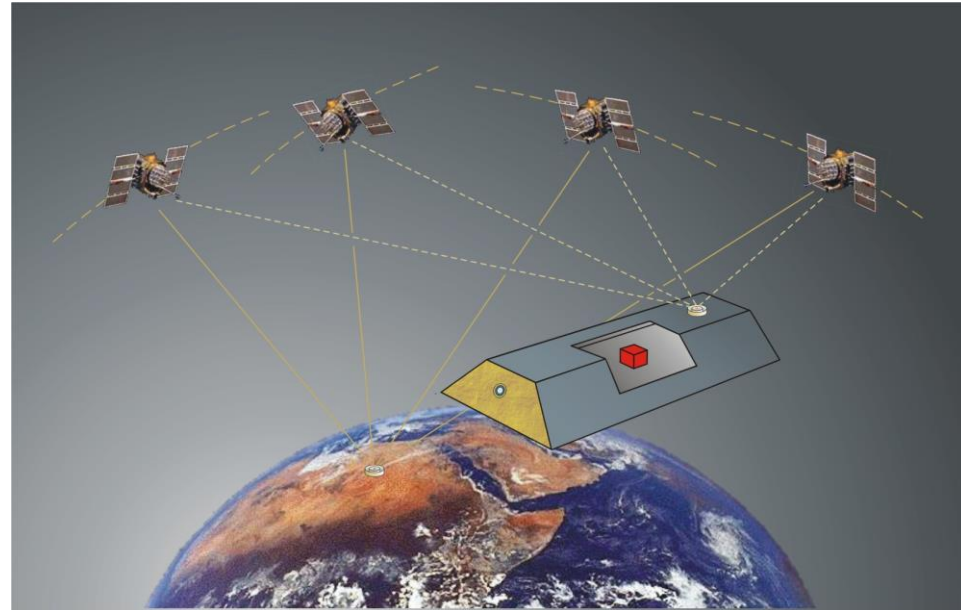
Dedicated gravity satellite missions

Satellite gravimetry:

Satellite-borne observation of the Earth's gravity field.

From the 80ies, several arrangements for satellite gravimetry have been developed:

1. High-Low SST
2. Low-Low SST
3. SGG



SST - Satellite-to-Satellite Tracking
SGG - Satellite Gravity Gradiometry

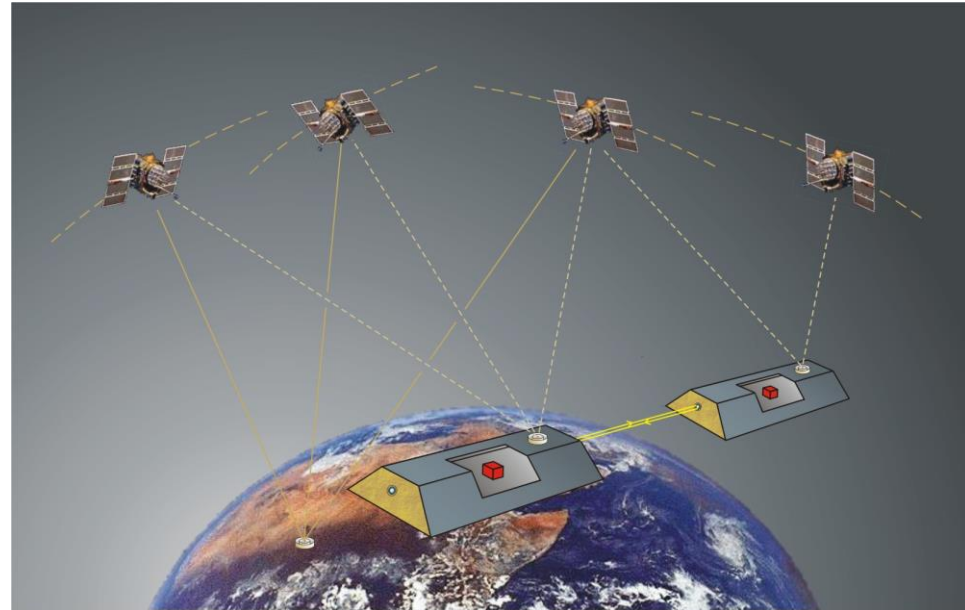
Dedicated gravity satellite missions

Satellite gravimetry:

Satellite-borne observation of the Earth's gravity field.

From the 80ies, several arrangements for satellite gravimetry have been developed:

1. High-Low SST
2. Low-Low SST
3. SGG



SST - Satellite-to-Satellite Tracking
SGG - Satellite Gravity Gradiometry

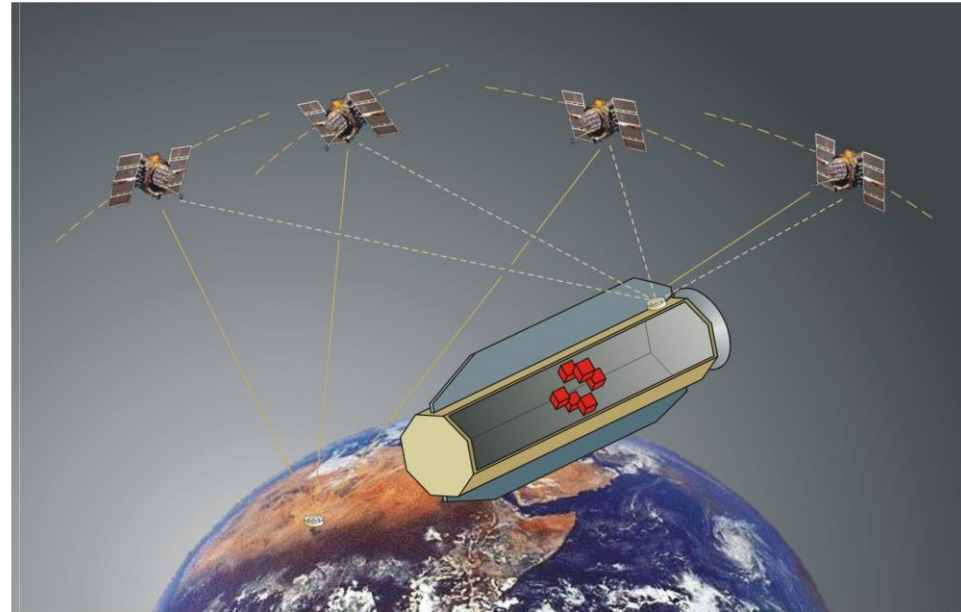
Dedicated gravity satellite missions

Satellite gravimetry:

Satellite-borne observation of the Earth's gravity field.

From the 80ies, several arrangements for satellite gravimetry have been developed:

1. High-Low SST
2. Low-Low SST
3. SGG

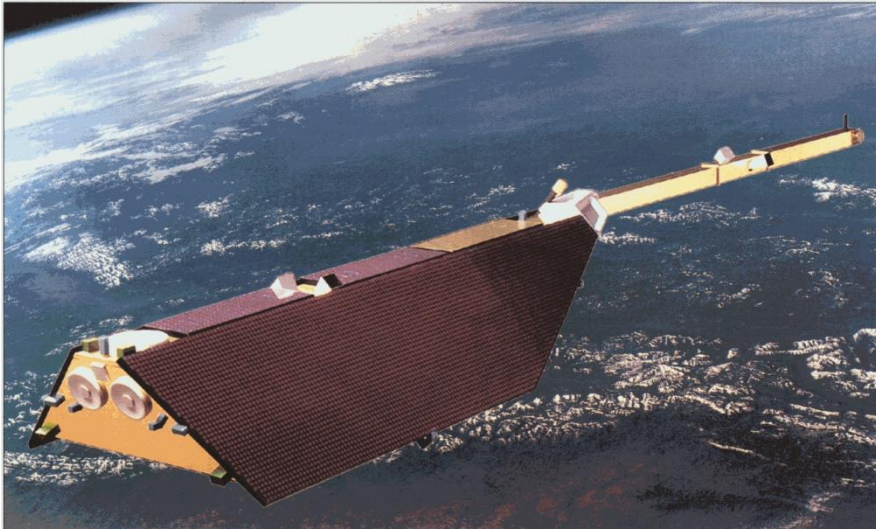


SST - Satellite-to-Satellite Tracking
SGG - Satellite Gravity Gradiometry

CHAMP

The High-Low SST mission

CHAMP



Orbit:

- nearly circular
- nearly polar ($i = 87^\circ$)
- altitude: 454 km, then lowered to 200 km

Launch:

- 15 July 2000

Mission duration:

- it was planned for 5 years, actually it was on orbit for more than 10 years

The High-Low SST concept

The orbit of a **LEO** (Low Earth Orbiter) is tracked continuously by a satellite (or a satellite system) at a high altitude.

If the LEO would be in free fall, the observed orbit would be generated only by the gravity field.

Fact: LEOs are *not* in free fall.

Solution: taking into account all other forces either by measurement or by modelling.

Forces acting on a satellite

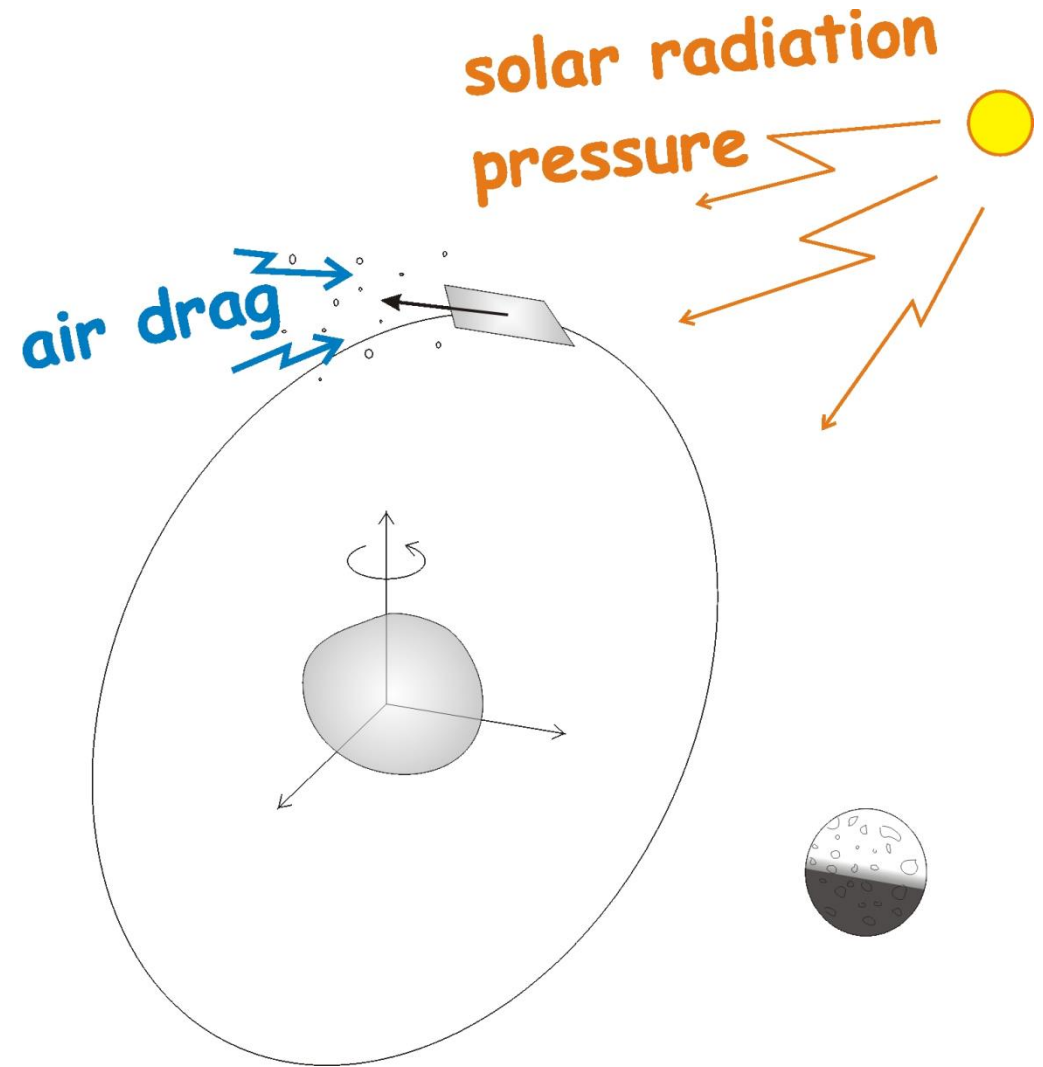
1. Gravity field of the Earth
2. Direct tides (gravity field of the Sun and the Moon)
3. Indirect tides
 - » mass variations due to the tidal forces
 - solid Earth tide
 - ocean tide
 - polar motion
4. Non-gravitational forces
 - atmospheric drag
 - solar radiation pressure

Dissipative forces

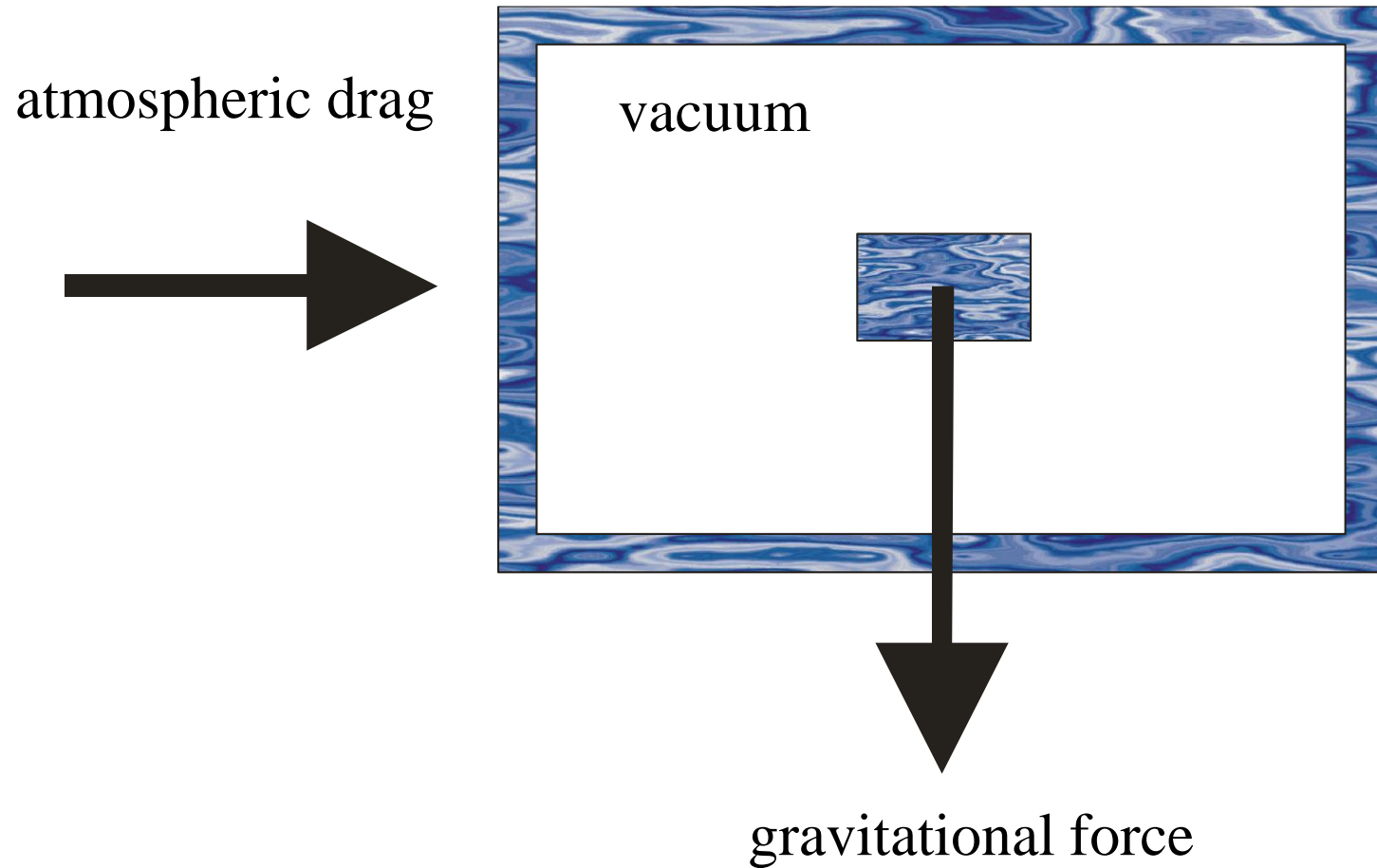
**Dissipative forces
(non-gravitational
forces; surface
forces):**

**1. Solar radiation
pressure**

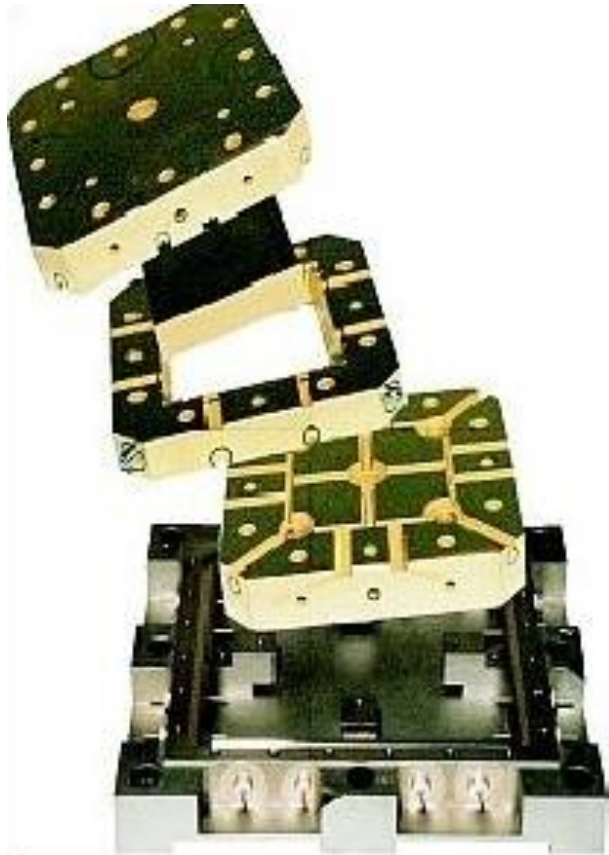
2. Atmospheric drag



Basic concept of accelerometers

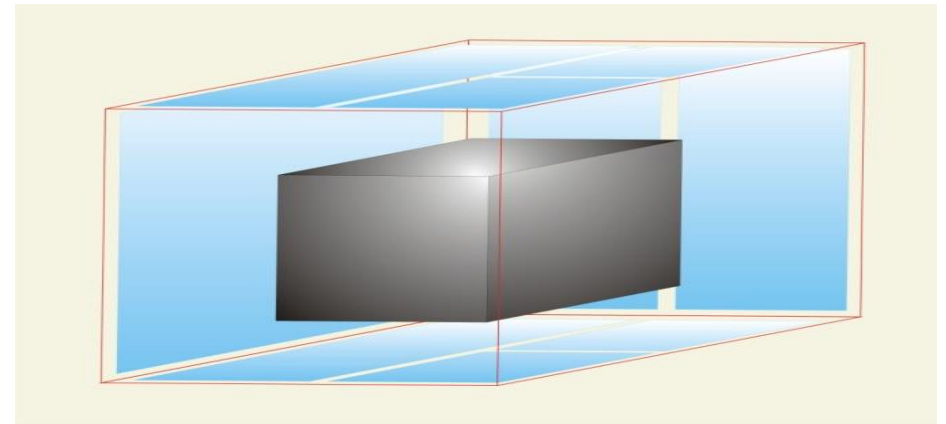


Accelerometers



A test mass is capacitively kept at the CoM of the satellite.

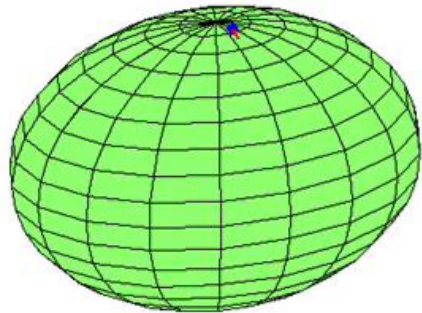
The observable is the feedback voltage.



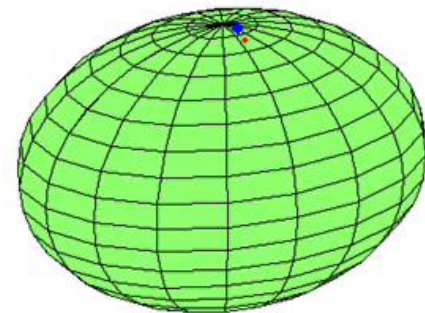
The accelerometer is built on 6 pairs of capacitors
-> linear and angular accelerations can be determined

Processing CHAMP observations

Orbit data: kinematic orbit, meaning quasi-independent positions determined from GPS observations with $10\text{ s} / 30\text{ s}$ sampling.



actual orbit



sampled orbit

Processing CHAMP observations

Energy balance approach

$$V_{pot} + V_{kin} = H$$

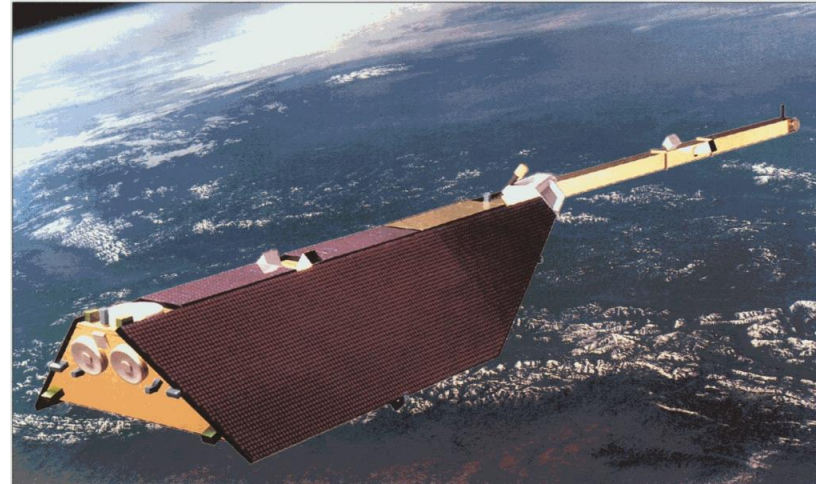
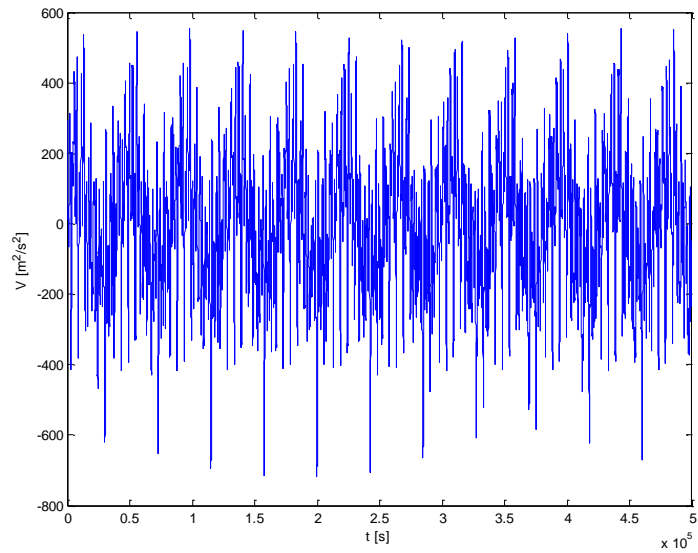
$$T_{grav} = V_{kin} - V_{grav}^{normal} - V_{dir.tides} - V_{ind.tides} - H - V_{non-grav.}$$

$$V_{pot} = T_{grav} + V_{grav}^{normal} \quad - \text{gravitational potential}$$

$$V_{kin} = \frac{1}{2} \dot{\vec{r}}^2 \quad - \text{kinetic energy}$$

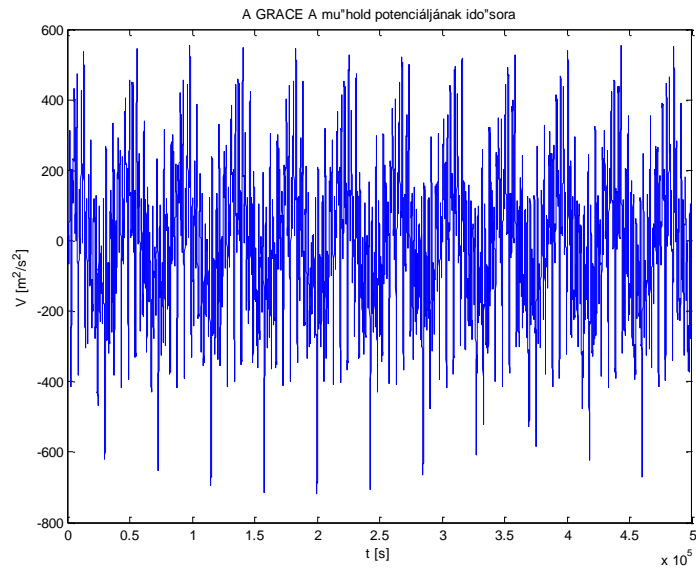
$$V_{non-grav.} = \int \bar{a}_{non-grav.} d\vec{r} \quad - \text{dissipative energy}$$

Processing CHAMP observations

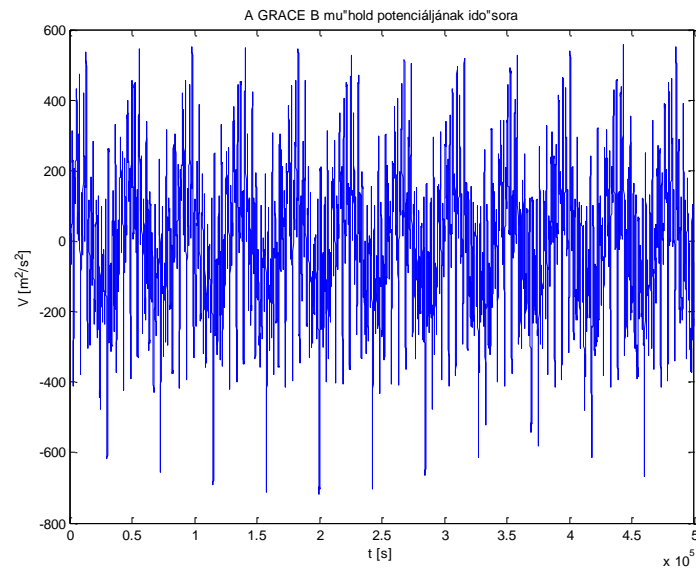


$$V_{pot}$$

Processing GRACE observations



V_{pot}



Processing CHAMP observations

Adjustment by the Least Squares Method. Observation equation:

$$V(r, \varphi, \lambda) = \frac{GM}{R} \sum_{l=0}^{L_{\max}} \left(\frac{R}{r}\right)^{l+1} \sum_{m=0}^l (C_{lm} \cos m\lambda + S_{lm} \sin m\lambda) P_{lm}(\sin \varphi)$$

Unknowns: C_{lm} , S_{lm}

Observation: $V(r, \varphi, \lambda)$

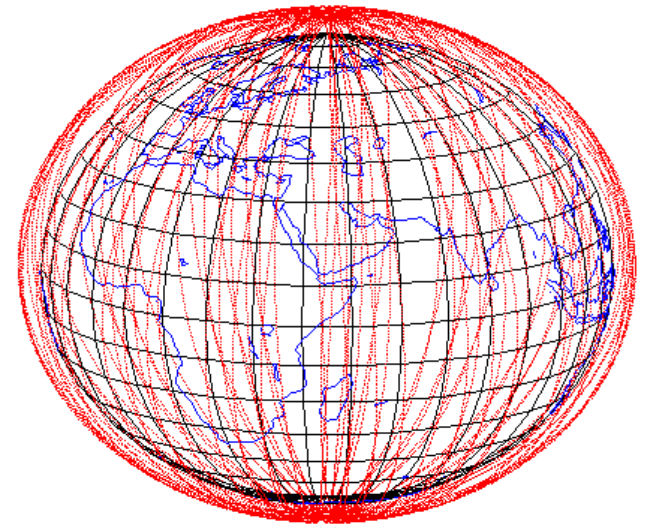
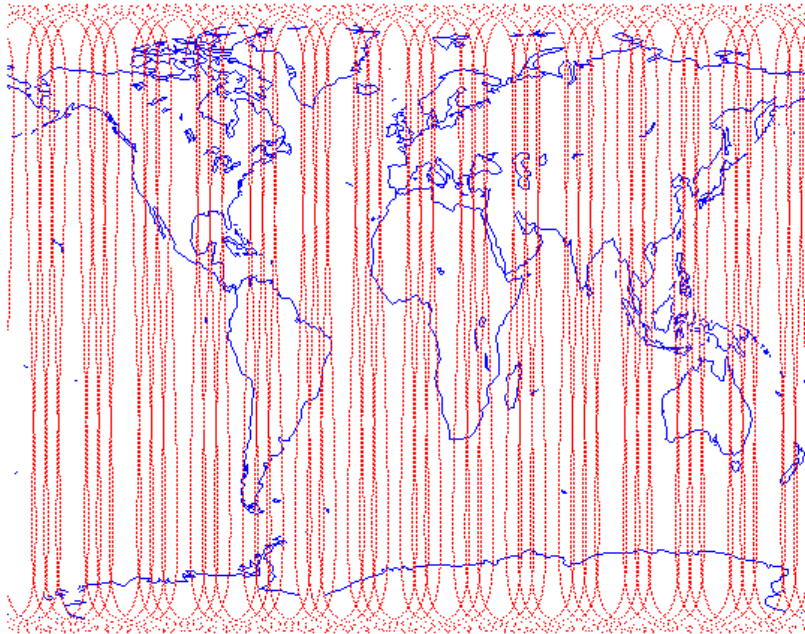
Number of unknowns: $(L_{\max} + 1) \frac{(L_{\max} + 2)}{2} + L_{\max} \frac{(L_{\max} + 1)}{2} = (L_{\max} + 1)^2$

Number of observations: N

Processing CHAMP observations

Distribution of observations:

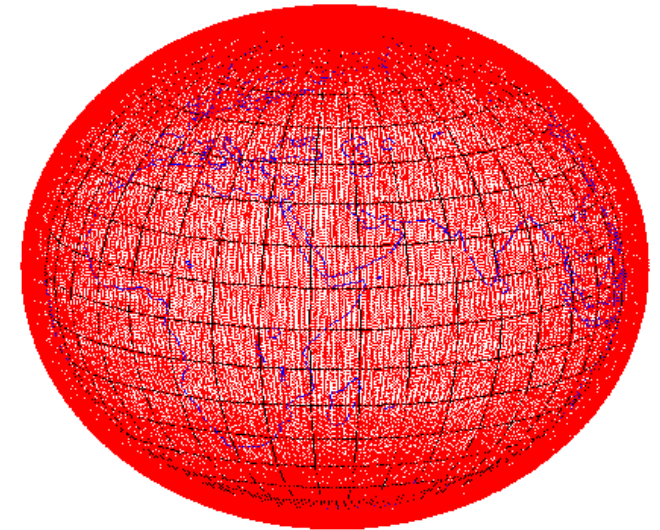
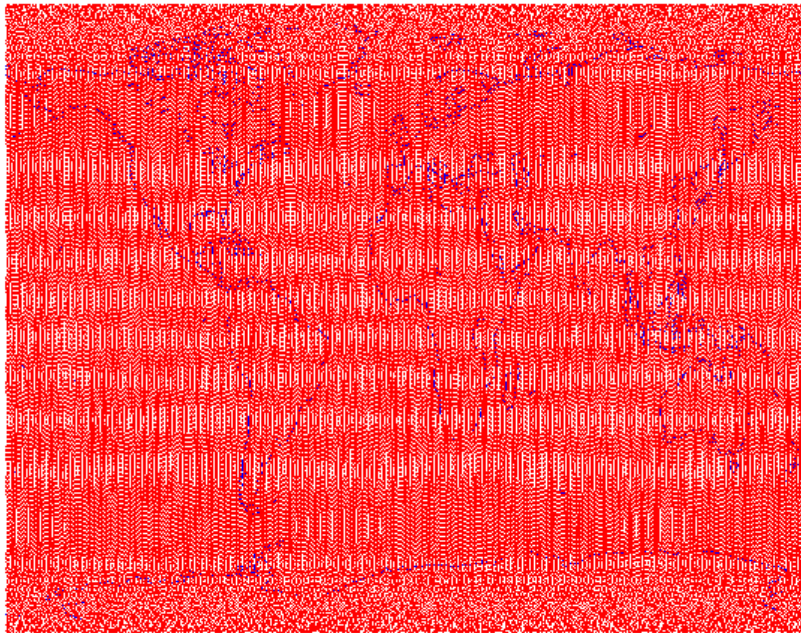
3 days



Processing CHAMP observations

Distribution of observations:

15 days



Processing CHAMP observations

Observation equation:

$$V(C_{lm}, S_{lm}) = \frac{GM}{R} \sum_{l=0}^{L_{\max}} \left(\frac{R}{r}\right)^{l+1} \sum_{m=0}^l (C_{lm} \cos m\lambda + S_{lm} \sin m\lambda) P_{lm}(\sin \varphi)$$

Design matrix:

$$A = \begin{pmatrix} \left. \frac{\partial V}{\partial C_{00}} \right|_{t_1} & \left. \frac{\partial V}{\partial C_{10}} \right|_{t_1} & \cdots & \left. \frac{\partial V}{\partial C_{L_{\max}0}} \right|_{t_1} & \left. \frac{\partial V}{\partial C_{11}} \right|_{t_1} & \cdots & \left. \frac{\partial V}{\partial C_{L_{\max}1}} \right|_{t_1} & \cdots & \left. \frac{\partial V}{\partial C_{L_{\max}L_{\max}}} \right|_{t_1} & \left. \frac{\partial V}{\partial S_{11}} \right|_{t_1} & \cdots & \left. \frac{\partial V}{\partial S_{L_{\max}L_{\max}}} \right|_{t_1} \\ \left. \frac{\partial V}{\partial C_{00}} \right|_{t_2} & \left. \frac{\partial V}{\partial C_{10}} \right|_{t_2} & \cdots & \left. \frac{\partial V}{\partial C_{L_{\max}0}} \right|_{t_2} & \left. \frac{\partial V}{\partial C_{11}} \right|_{t_2} & \cdots & \left. \frac{\partial V}{\partial C_{L_{\max}1}} \right|_{t_2} & \cdots & \left. \frac{\partial V}{\partial C_{L_{\max}L_{\max}}} \right|_{t_2} & \left. \frac{\partial V}{\partial S_{11}} \right|_{t_2} & \cdots & \left. \frac{\partial V}{\partial S_{L_{\max}L_{\max}}} \right|_{t_2} \\ \cdots & \cdots & \cdots & \cdots & \cdots & \cdots & \cdots & \cdots & \cdots & \cdots & \cdots & \cdots \\ \left. \frac{\partial V}{\partial C_{00}} \right|_{t_N} & \left. \frac{\partial V}{\partial C_{10}} \right|_{t_N} & \cdots & \left. \frac{\partial V}{\partial C_{L_{\max}0}} \right|_{t_N} & \left. \frac{\partial V}{\partial C_{11}} \right|_{t_N} & \cdots & \left. \frac{\partial V}{\partial C_{L_{\max}1}} \right|_{t_N} & \cdots & \left. \frac{\partial V}{\partial C_{L_{\max}L_{\max}}} \right|_{t_N} & \left. \frac{\partial V}{\partial S_{11}} \right|_{t_N} & \cdots & \left. \frac{\partial V}{\partial S_{L_{\max}L_{\max}}} \right|_{t_N} \end{pmatrix}$$

Processing CHAMP observations

Size of the design matrix: $(N, (L_{\max} + 1)^2)$

N after 4 month observations: 1.036.800

Adjusting up to d/o $L_{\max} = 100$ the size of the design matrix:

(1.036.800, 10.201)

Memory and time consuming → alternative solutions

SEMI-ANALYTICAL APPROACH

Processing CHAMP observations

Legendre-polynomial:

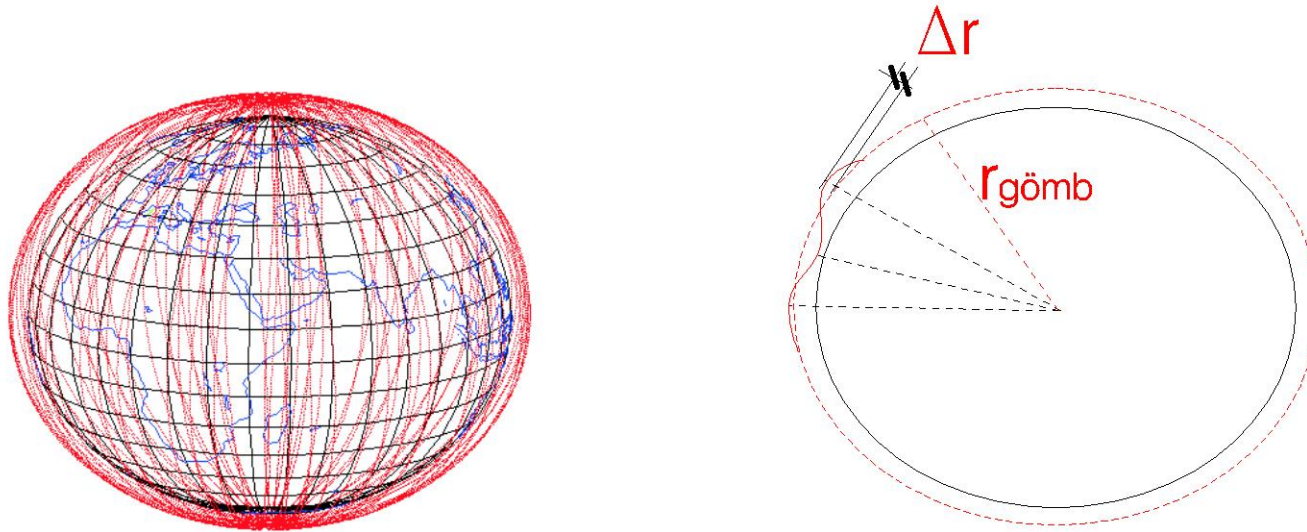
$$P_{lm}(\cos \theta) = \sum_{k=-l}^l a_{lmk} \begin{cases} \cos k\theta & (k > 0) \\ \sin k\theta & (k < 0) \end{cases}$$

This way it can be converted to a 2D Fourier transformation:

$$\begin{aligned} V(r, \varphi, \lambda) &= \frac{GM}{R} \sum_{l=0}^{L_{\max}} \left(\frac{R}{r}\right)^{l+1} \sum_{m=0}^l (C_{lm} \cos m\lambda + S_{lm} \sin m\lambda) P_{lm}(\cos \theta) = \\ &= \frac{GM}{R} \sum_{l=0}^{L_{\max}} \sum_{m=0}^l \sum_{k=-l}^l a_{lmk} \left(\frac{R}{r}\right)^{l+1} (C_{lm} \cos m\lambda + S_{lm} \sin m\lambda) \begin{cases} \cos k\theta & (k > 0) \\ \sin k\theta & (k < 0) \end{cases} \end{aligned}$$

Processing CHAMP observations

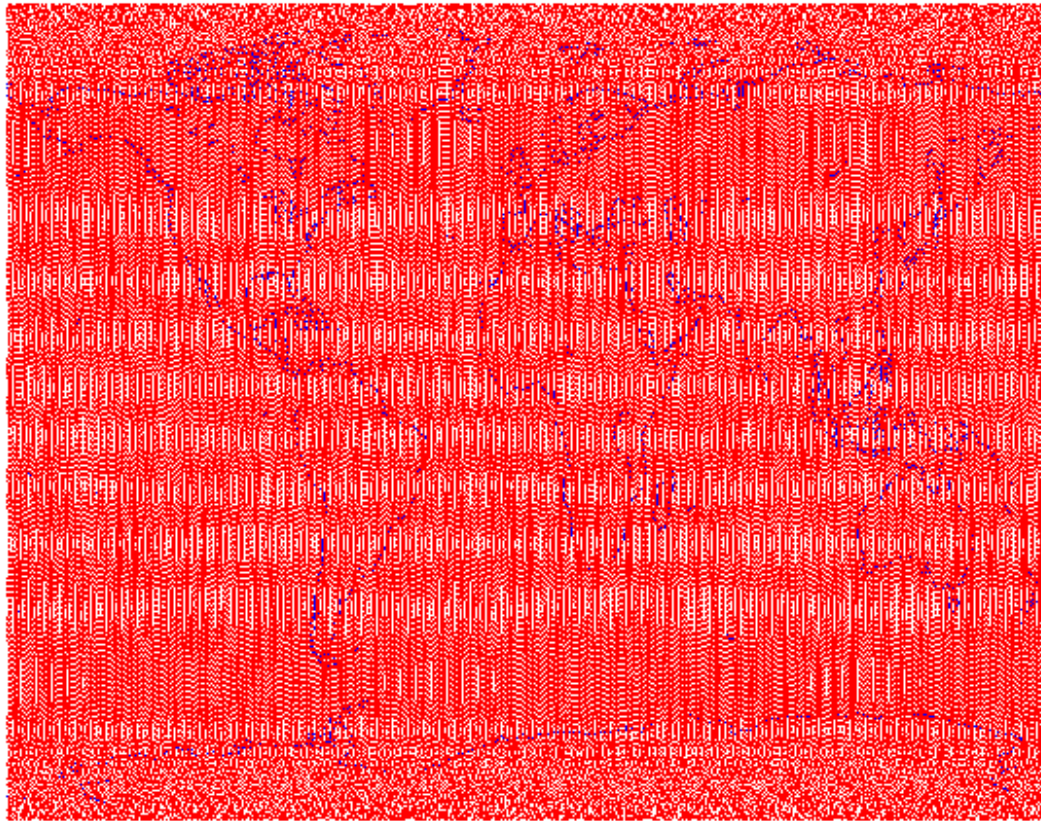
Reduction of the observations to a mean sphere:



$$V(r_{\text{gömb}}, \varphi, \lambda) = V(r, \varphi, \lambda) + \frac{\partial V(r_{\text{gömb}}, \varphi, \lambda)}{\partial r} \Delta r + \frac{1}{2} \frac{\partial^2 V(r_{\text{gömb}}, \varphi, \lambda)}{\partial r^2} \Delta r^2 + \dots$$

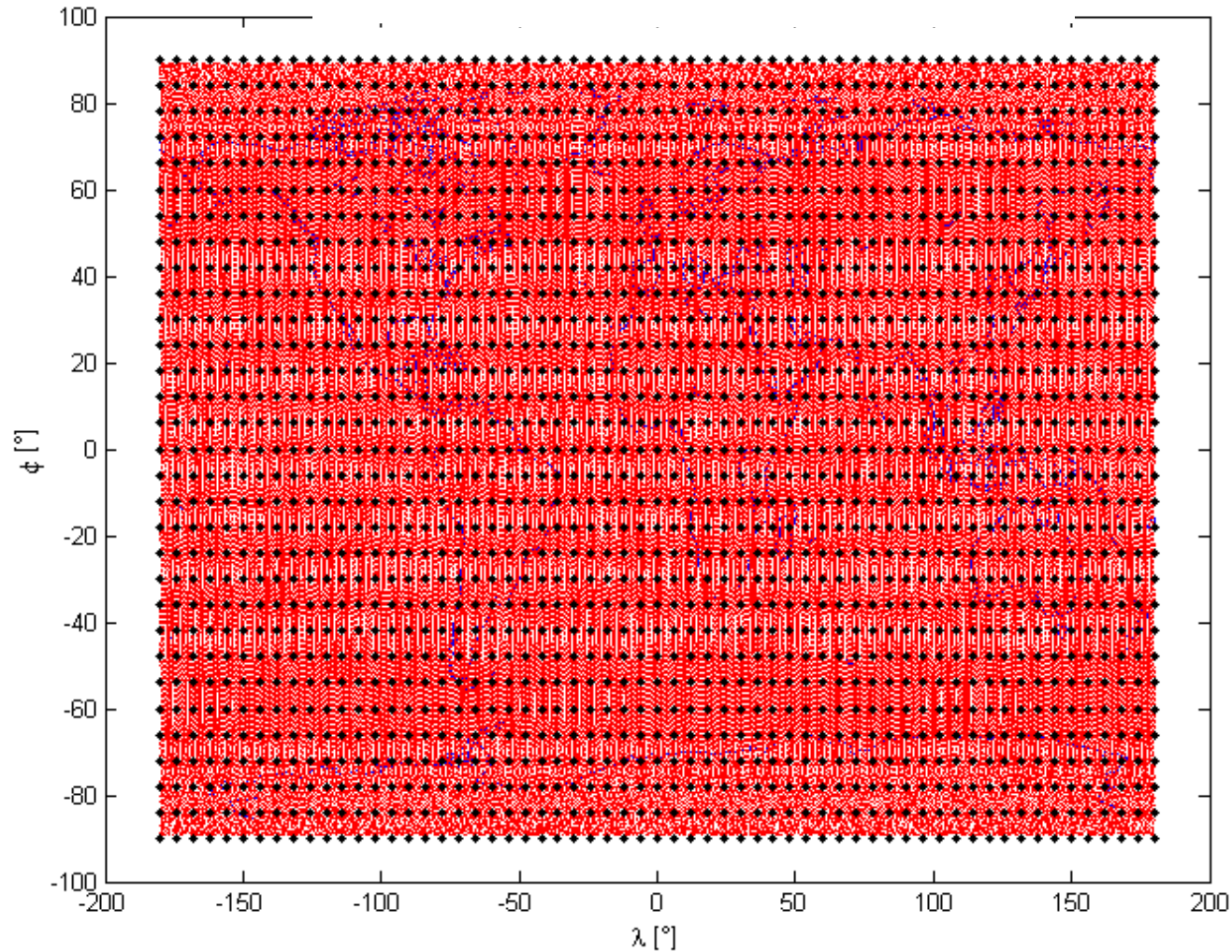
Processing CHAMP observations

data



Processing CHAMP observations

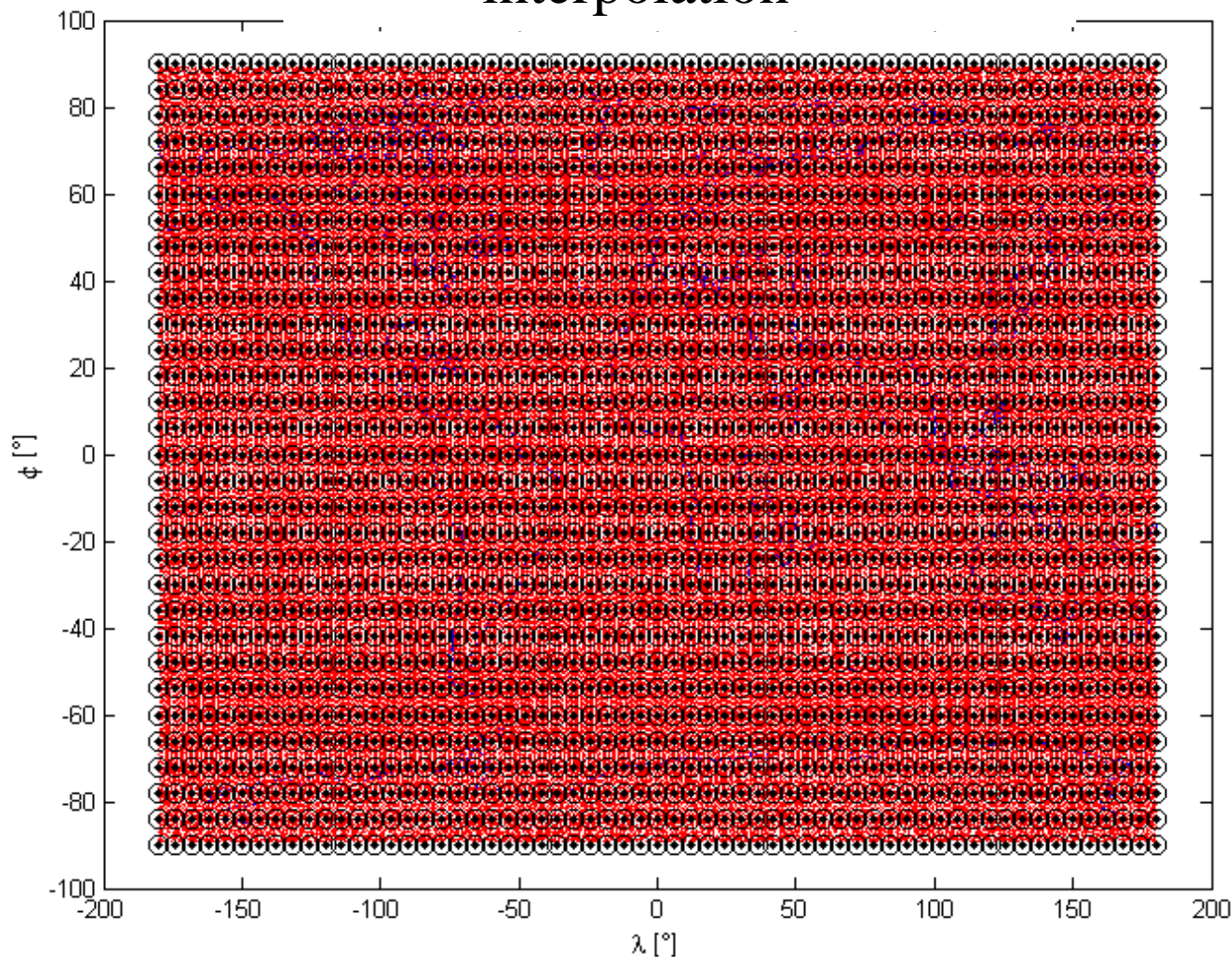
reduction



$$V(r_{sphere}, \varphi, \lambda)$$

Processing CHAMP observations

interpolation



$$V(r_{sphere}, \varphi, \lambda)$$



$$V(r_{sphere}, \varphi_{grid}, \lambda_{grid})$$

$$\varphi_{grid} = \sum k \Delta \varphi$$

$$\lambda_{grid} = \sum_m^k m \Delta \lambda$$

Processing CHAMP observations

$$V = \frac{GM}{R} \sum_{l=0}^{L_{\max}} \left(\frac{R}{r_{\text{gömb}}} \right)^{l+1} \sum_{m=0}^l \sum_{k=-l}^l (C_{lm} \cos m\lambda + S_{lm} \sin m\lambda) \begin{cases} \cos k\theta & (k > 0) \\ \sin k\theta & (k < 0) \end{cases}$$

Exchanging summation:

$$V = \frac{GM}{R} \sum_{m=0}^{L_{\max}} \sum_{k=-L_{\max}}^{L_{\max}} \sum_{l=\max(|m|, |k|)}^{L_{\max}} \left(\frac{R}{r_{\text{gömb}}} \right)^{l+1} (C_{lm} \cos m\lambda + S_{lm} \sin m\lambda) \begin{cases} \cos k\theta \\ \sin k\theta \end{cases}$$

Deriving new coefficients containing the summation by degree, l :

$$\begin{Bmatrix} A_{mk} \\ B_{mk} \end{Bmatrix} = \frac{GM}{R} \sum_{l=\max(|m|, |k|)}^{L_{\max}} \left(\frac{R}{r_{\text{gömb}}} \right)^{l+1} \begin{Bmatrix} C_{lm} \\ S_{lm} \end{Bmatrix}$$

The resulting equation depends on m and k but not on l (c.f. next page):

Processing CHAMP observations

$$V = \sum_{m=0}^{L_{\max}} \sum_{k=-L_{\max}}^{L_{\max}} (A_{mk} \cos m\lambda + B_{mk} \sin m\lambda) \begin{cases} \cos k\theta \\ \sin k\theta \end{cases}$$

All observations can be involved using a design matrix with a size of $(L_{\max}+1, 2L_{\max}+1)$, independently on the length of the observations.

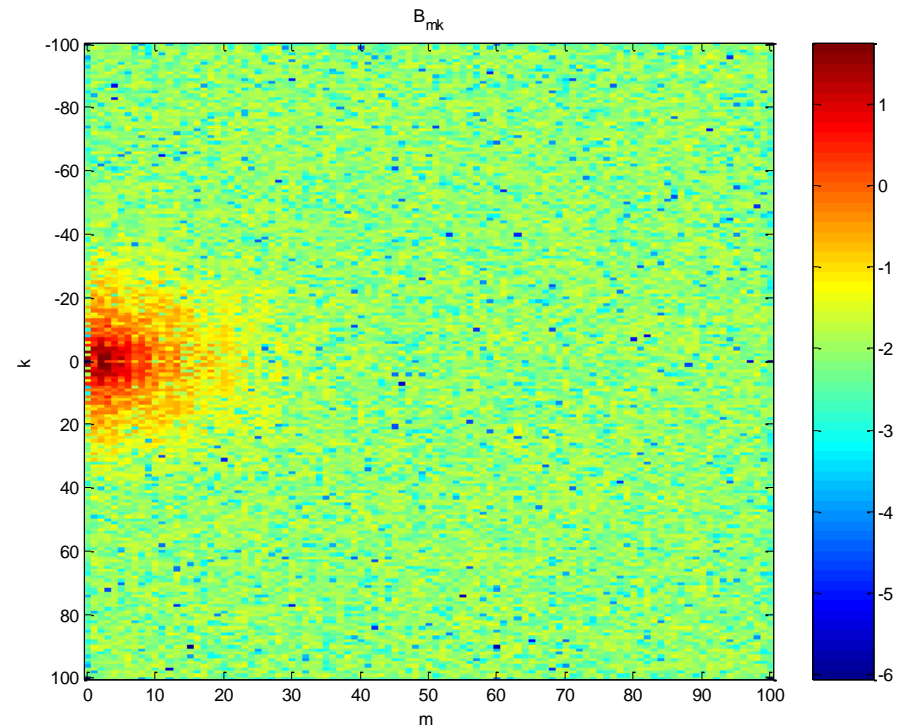
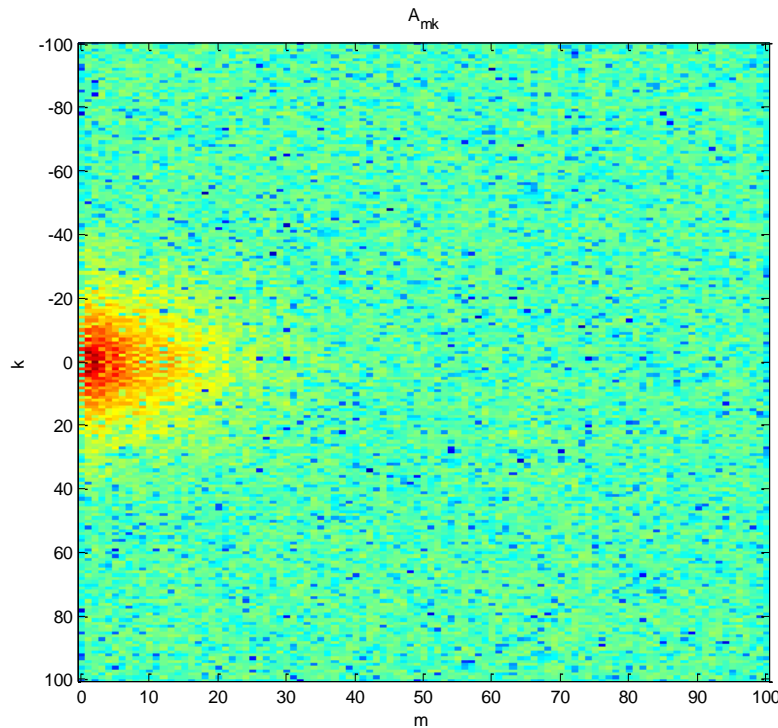
The observation equation is
$$\begin{cases} A_{mk} \\ B_{mk} \end{cases} = \frac{GM}{R} \sum_{l=\max(|m|,|k|)}^{L_{\max}} \left(\frac{R}{r_{gömb}} \right)^{l+1} \begin{cases} C_{lm} \\ S_{lm} \end{cases}$$

The coefficients called lumped coefficients, in which coefficients all observations are lumped in. The size of the design matrix with this approach for $L_{\max} = 100$ becomes only (101,201).

Processing CHAMP observations

lumped coefficients

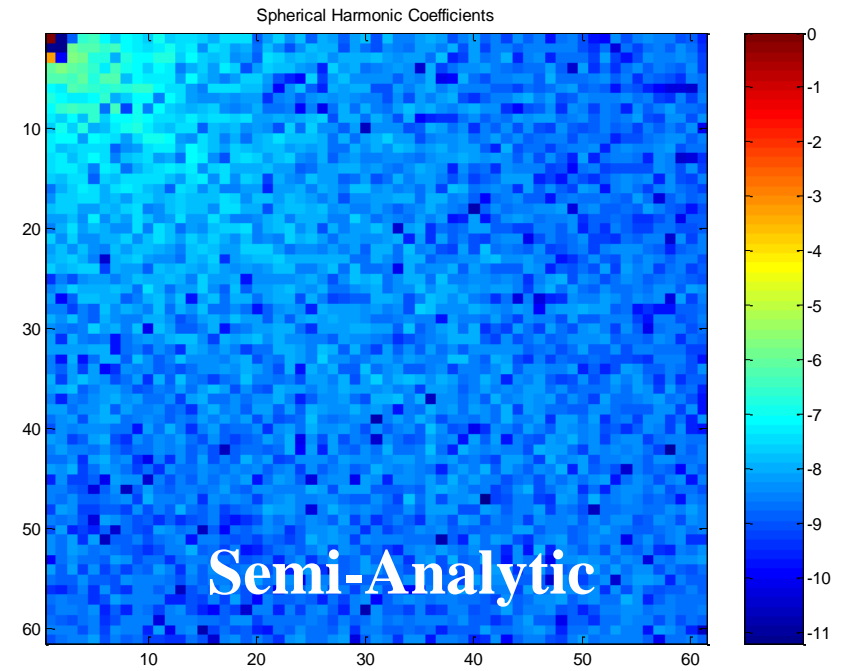
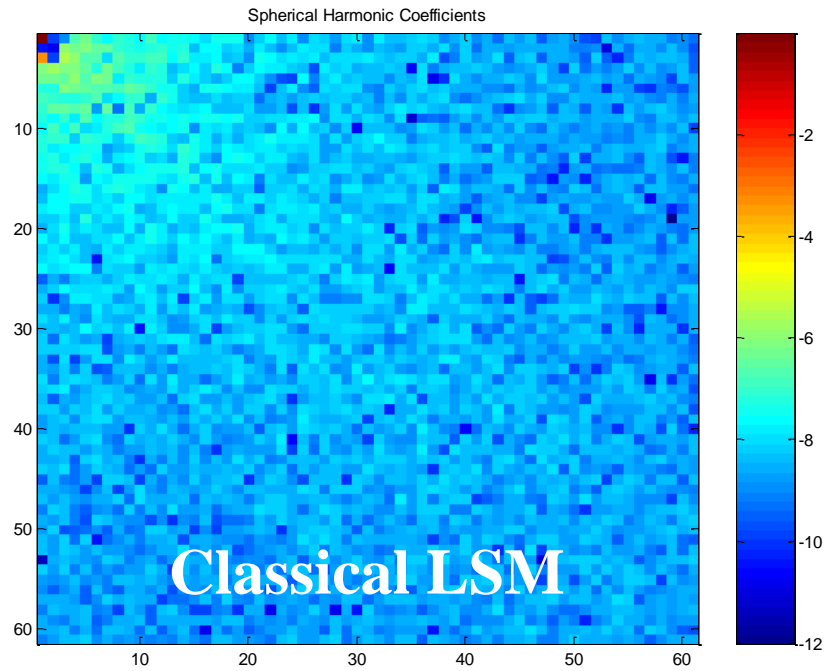
$$\left. \begin{matrix} A_{mk} \\ B_{mk} \end{matrix} \right\} = \frac{GM}{R} \sum_{l=\max(|m|,|k|)}^{L_{\max}} \left(\frac{R}{r_{\text{gömb}}} \right)^{l+1} \left\{ \begin{matrix} C_{lm} \\ S_{lm} \end{matrix} \right.$$



When lumped coefficients are derived, the data was interpolated. This involved errors, which can be reduced by an **iterative** solution.

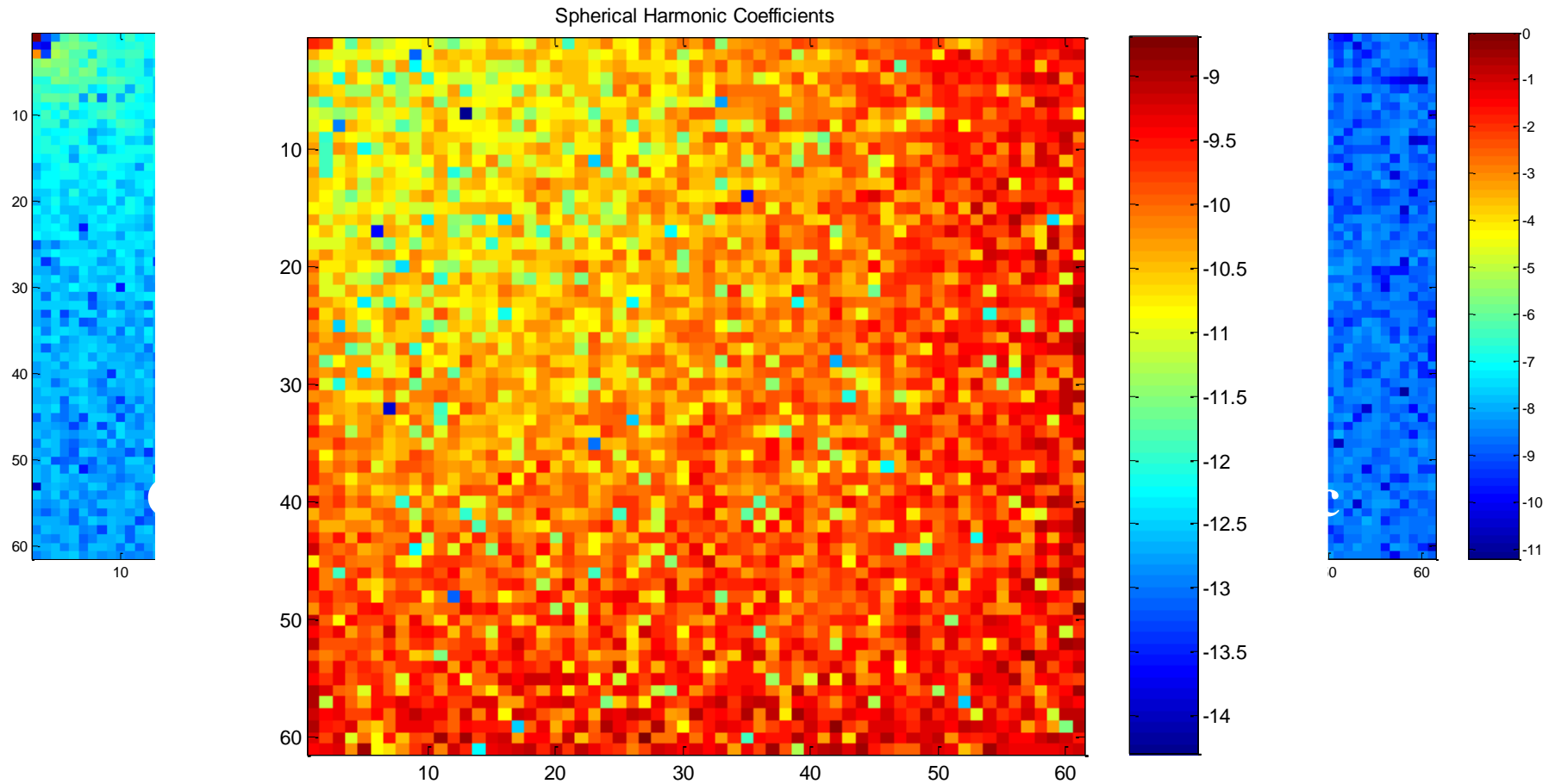
Processing CHAMP observations

Validation of semi-analytical approach



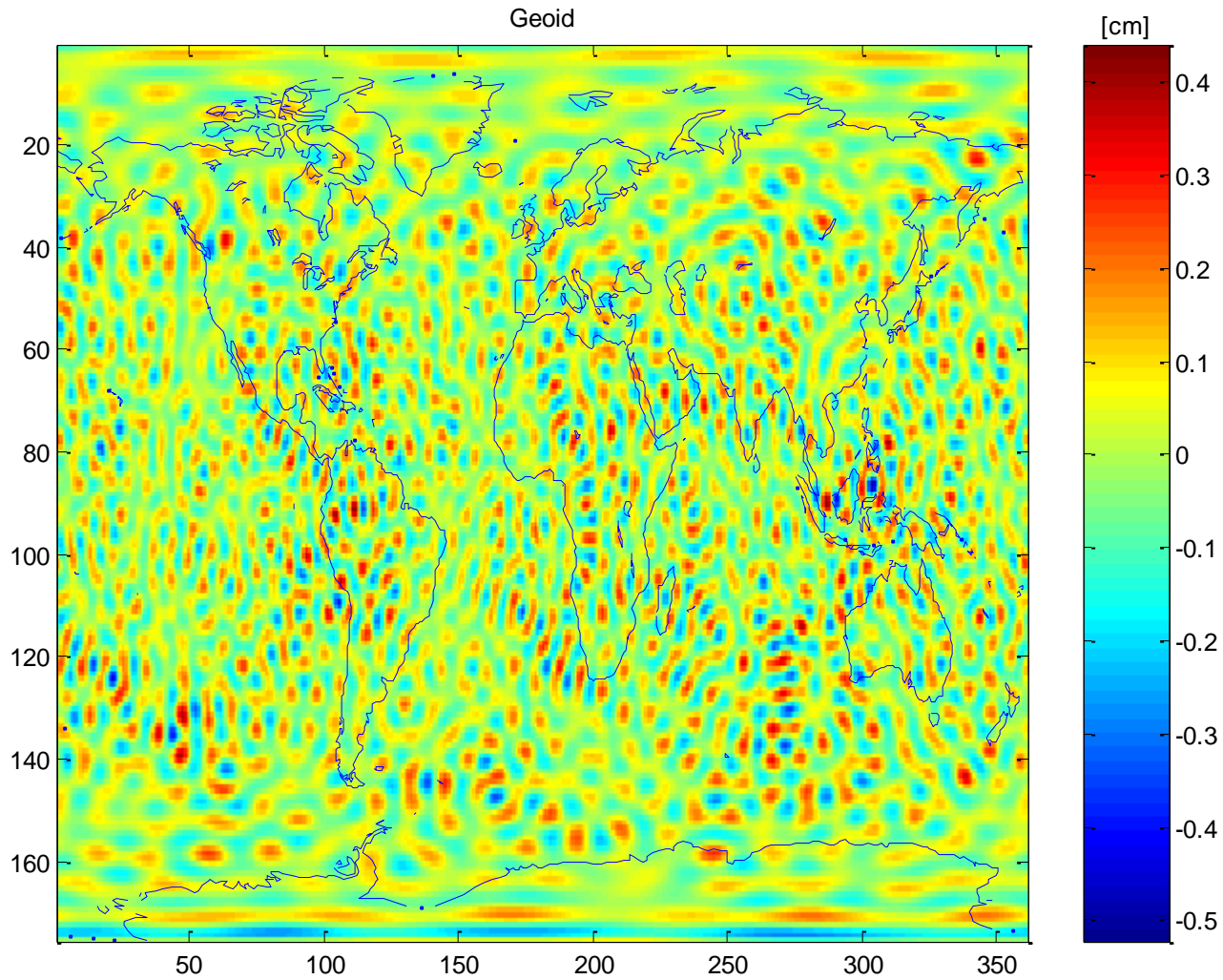
Processing CHAMP observations

Validation of semi-analytical approach



Error of Semi-Analytic

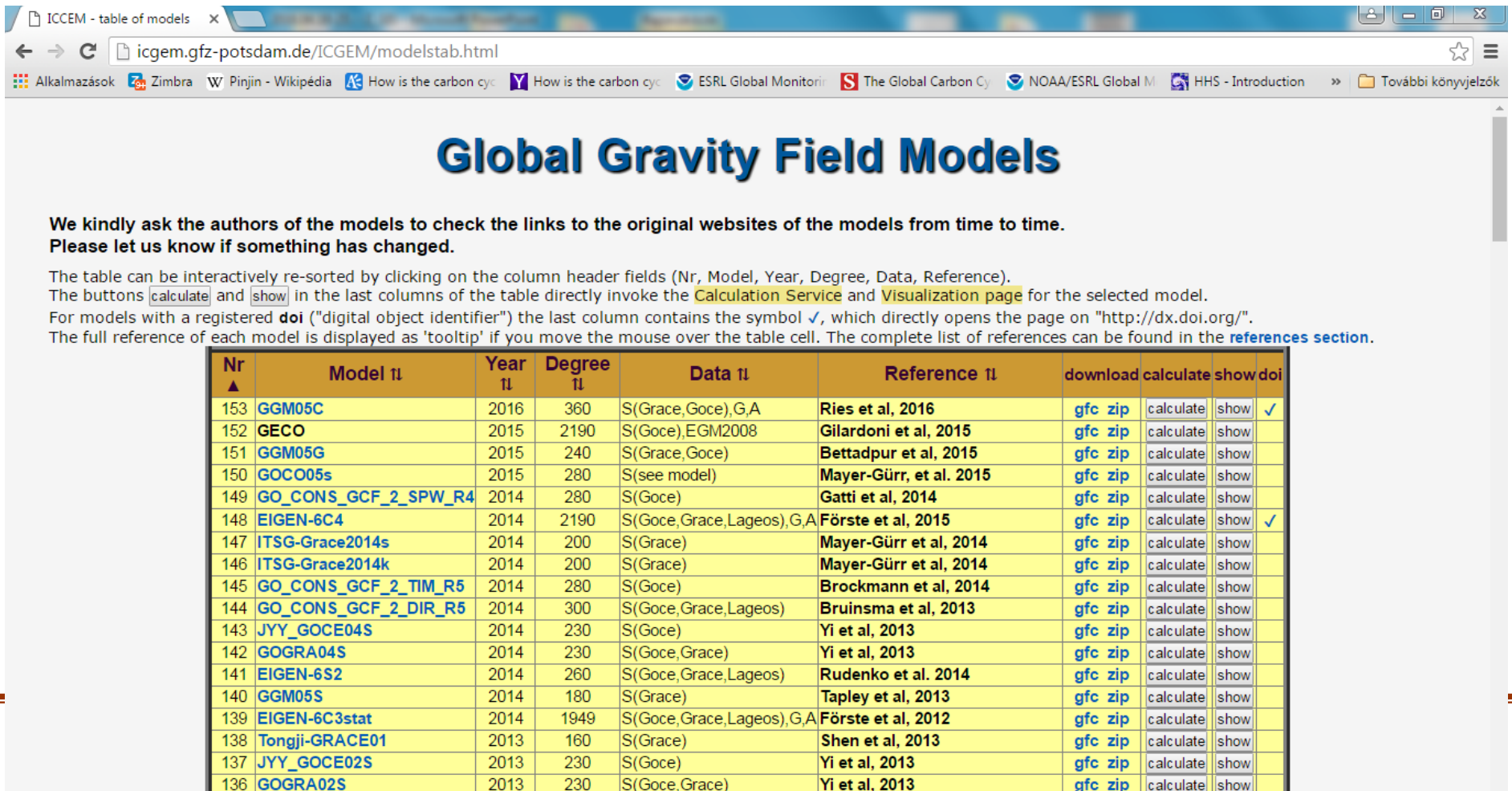
Processing CHAMP observations



Dedicated gravity satellite missions
Mostar, 19.10.2017

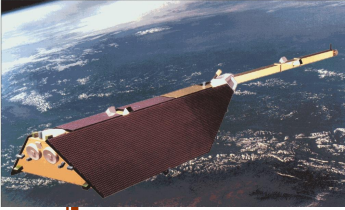
CHAMP gravity field models

Data base of global gravity field models are available at
International Center for Global Gravity Field Models
Homepage: <http://icgem.gfz-potsdam.de/ICGEM/modelstab.html>



The screenshot shows a web browser window with the URL icgem.gfz-potsdam.de/ICGEM/modelstab.html. The page title is "Global Gravity Field Models". Below the title, there is a message: "We kindly ask the authors of the models to check the links to the original websites of the models from time to time. Please let us know if something has changed." Below this message, there is a paragraph explaining the table's interactivity: "The table can be interactively re-sorted by clicking on the column header fields (Nr, Model, Year, Degree, Data, Reference). The buttons [calculate](#) and [show](#) in the last columns of the table directly invoke the [Calculation Service](#) and [Visualization page](#) for the selected model. For models with a registered [doi](#) ('digital object identifier') the last column contains the symbol ✓, which directly opens the page on 'http://dx.doi.org/'. The full reference of each model is displayed as 'tooltip' if you move the mouse over the table cell. The complete list of references can be found in the [references section](#)."

Nr ▲	Model ††	Year ††	Degree ††	Data ††	Reference ††	download	calculate	show	doi
153	GGM05C	2016	360	S(Grace,Goce),G,A	Ries et al, 2016	gfc zip	calculate	show	✓
152	GECO	2015	2190	S(Goce),EGM2008	Gilardoni et al, 2015	gfc zip	calculate	show	
151	GGM05G	2015	240	S(Grace,Goce)	Bettadpur et al, 2015	gfc zip	calculate	show	
150	GOCO05s	2015	280	S(see model)	Mayer-Gürr, et al. 2015	gfc zip	calculate	show	
149	GO_CONS_GCF_2_SPW_R4	2014	280	S(Goce)	Gatti et al, 2014	gfc zip	calculate	show	
148	EIGEN-6C4	2014	2190	S(Goce,Grace,Lageos),G,A	Förste et al, 2015	gfc zip	calculate	show	✓
147	ITSG-Grace2014s	2014	200	S(Grace)	Mayer-Gürr et al, 2014	gfc zip	calculate	show	
146	ITSG-Grace2014k	2014	200	S(Grace)	Mayer-Gürr et al, 2014	gfc zip	calculate	show	
145	GO_CONS_GCF_2_TIM_R5	2014	280	S(Goce)	Brockmann et al, 2014	gfc zip	calculate	show	
144	GO_CONS_GCF_2_DIR_R5	2014	300	S(Goce,Grace,Lageos)	Bruinsma et al, 2013	gfc zip	calculate	show	
143	JYY_GOCE04S	2014	230	S(Goce)	Yi et al, 2013	gfc zip	calculate	show	
142	GOGRA04S	2014	230	S(Goce,Grace)	Yi et al, 2013	gfc zip	calculate	show	
141	EIGEN-6S2	2014	260	S(Goce,Grace,Lageos)	Rudenko et al. 2014	gfc zip	calculate	show	
140	GGM05S	2014	180	S(Grace)	Tapley et al, 2013	gfc zip	calculate	show	
139	EIGEN-6C3stat	2014	1949	S(Goce,Grace,Lageos),G,A	Förste et al, 2012	gfc zip	calculate	show	
138	Tongji-GRACE01	2013	160	S(Grace)	Shen et al, 2013	gfc zip	calculate	show	
137	JYY_GOCE02S	2013	230	S(Goce)	Yi et al, 2013	gfc zip	calculate	show	
136	GOGRA02S	2013	230	S(Goce,Grace)	Yi et al. 2013	gfc zip	calculate	show	



CHAMP gravity field models

Based on the *International Center for Global Gravity Field Models* data, the list of the CHAMP-only gravity field models:

Nr	Name	Year	Degree	Data	Reference
80	EIGEN-1	2002	119	S(Champ)	Reigber et al, 2003a
81	EIGEN-2	2003	140	S(Champ)	Reigber et al, 2003b
82	EIGEN-CHAMP03Sp	2003	140	S(Champ)	Reigber et al, 2004a
86	TUM-1S	2003	60	S(Champ)	Gerlach et al, 2003
87	TUM-2Sp	2003	60	S(Champ)	Földvary et al, 2003
88	ITG Champ01E	2003	75	S(Champ)	Ilk et al, 2003
89	ITG Champ01S	2003	70	S(Champ)	Ilk et al, 2003
90	ITG Champ01K	2003	70	S(Champ)	Ilk et al, 2003
91	DEOS_CHAMP-01C	2004	70	S(Champ)	Ditmar et al, 2006
92	TUM-2S	2004	70	S(Champ)	Wermuth et al., 2004
94	EIGEN-CHAMP03S	2004	140	S(Champ)	Reigber et al, 2005b
102	AIUB-CHAMP01S	2007	90	S(Champ)	Prange et al, 2009
112	EIGEN-CHAMP05S	2010	150	S(Champ)	Flechtner et al, 2010
113	AIUB-CHAMP03S	2010	100	S(Champ)	Prange, 2011
135	ULux_CHAMP2013s	2013	120	S(Champ)	Weigelt et al, 2013

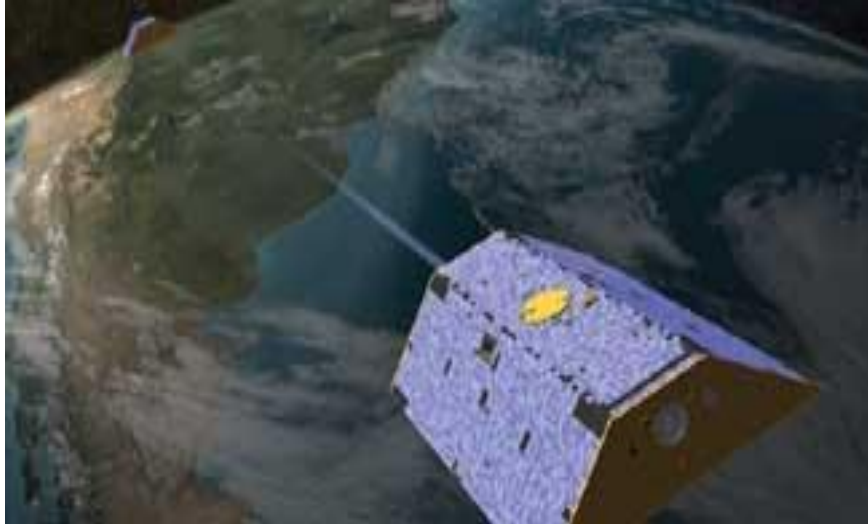
GRACE

The Low-Low SST mission (+High-Low SST)

GRACE

Orbit:

- nearly circular
- nearly polar ($i = 89^\circ$)
- altitude: between 300 km and 500 km
- nominal distance between satellites is 220 km



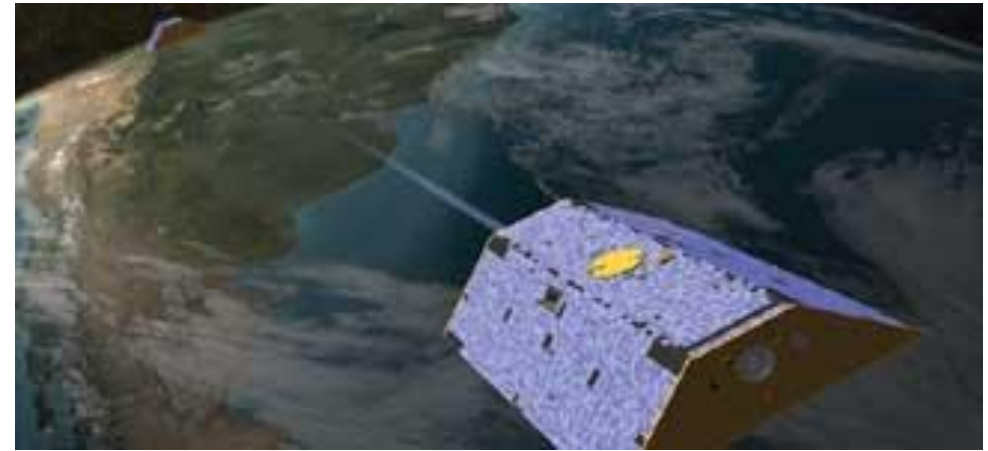
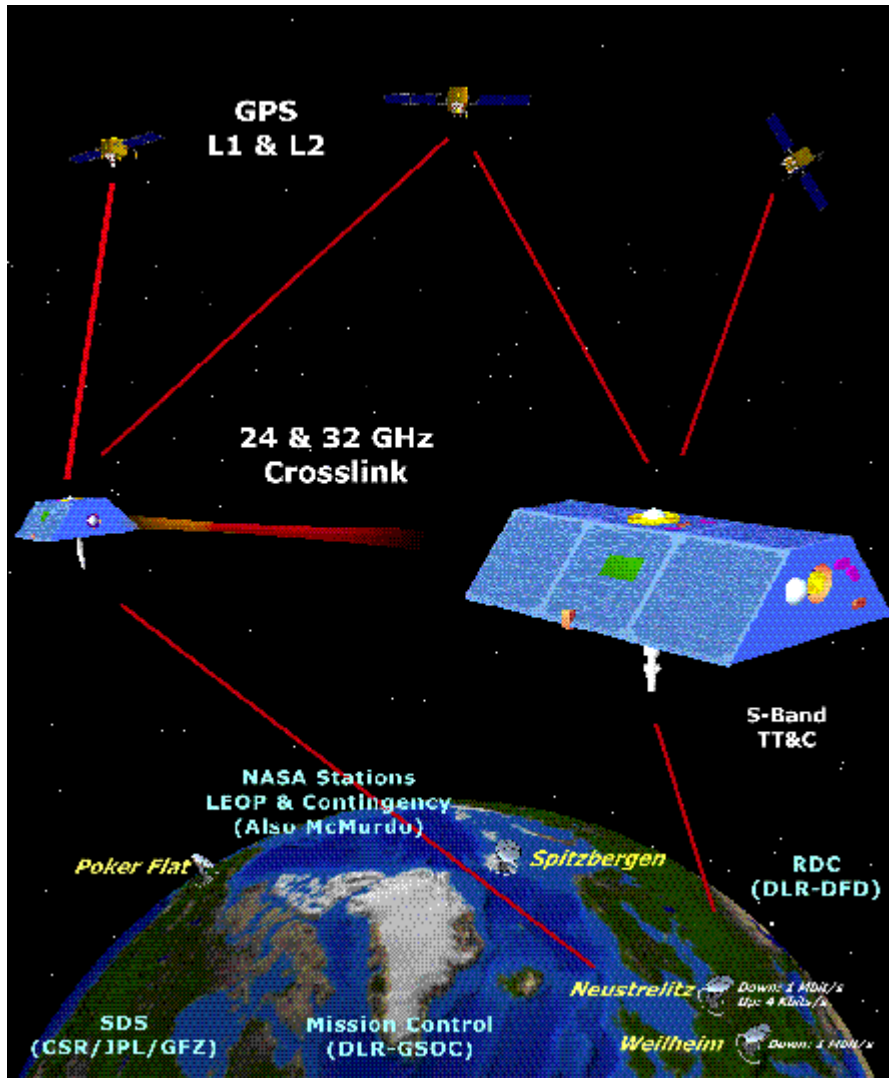
Launch:

- 17 March 2002

Mission duration :

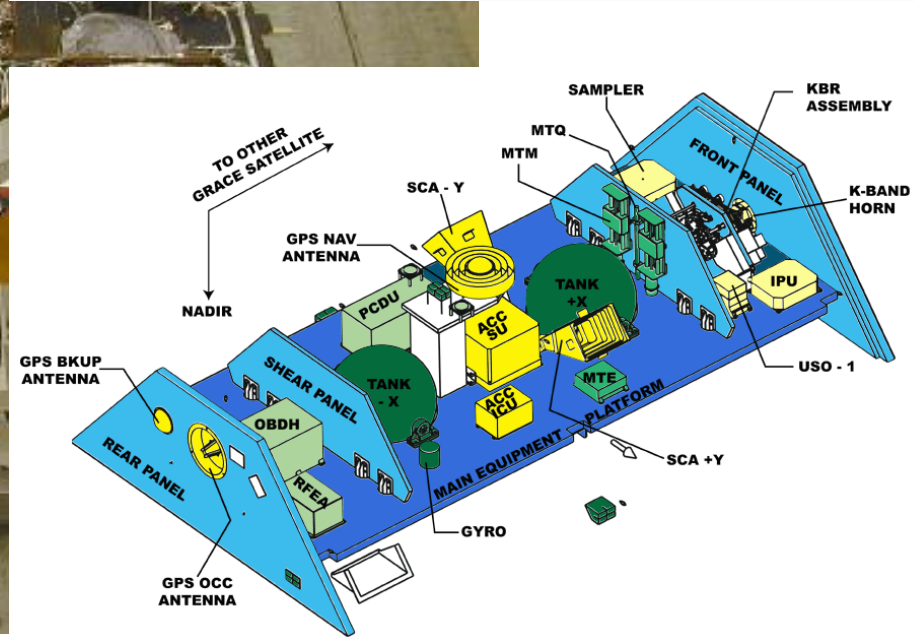
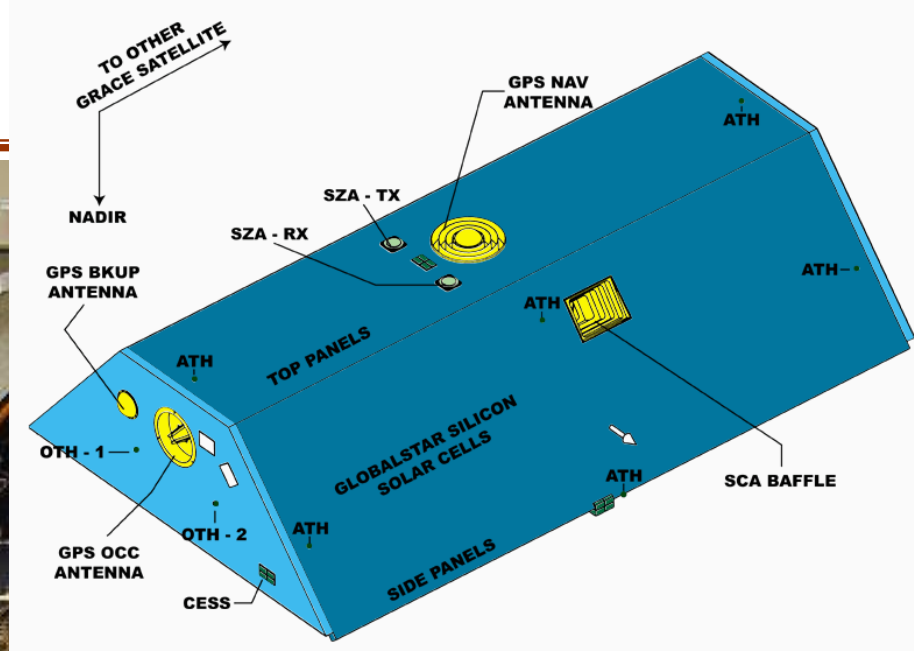
- 5 years was planned, but it is still active

GRACE



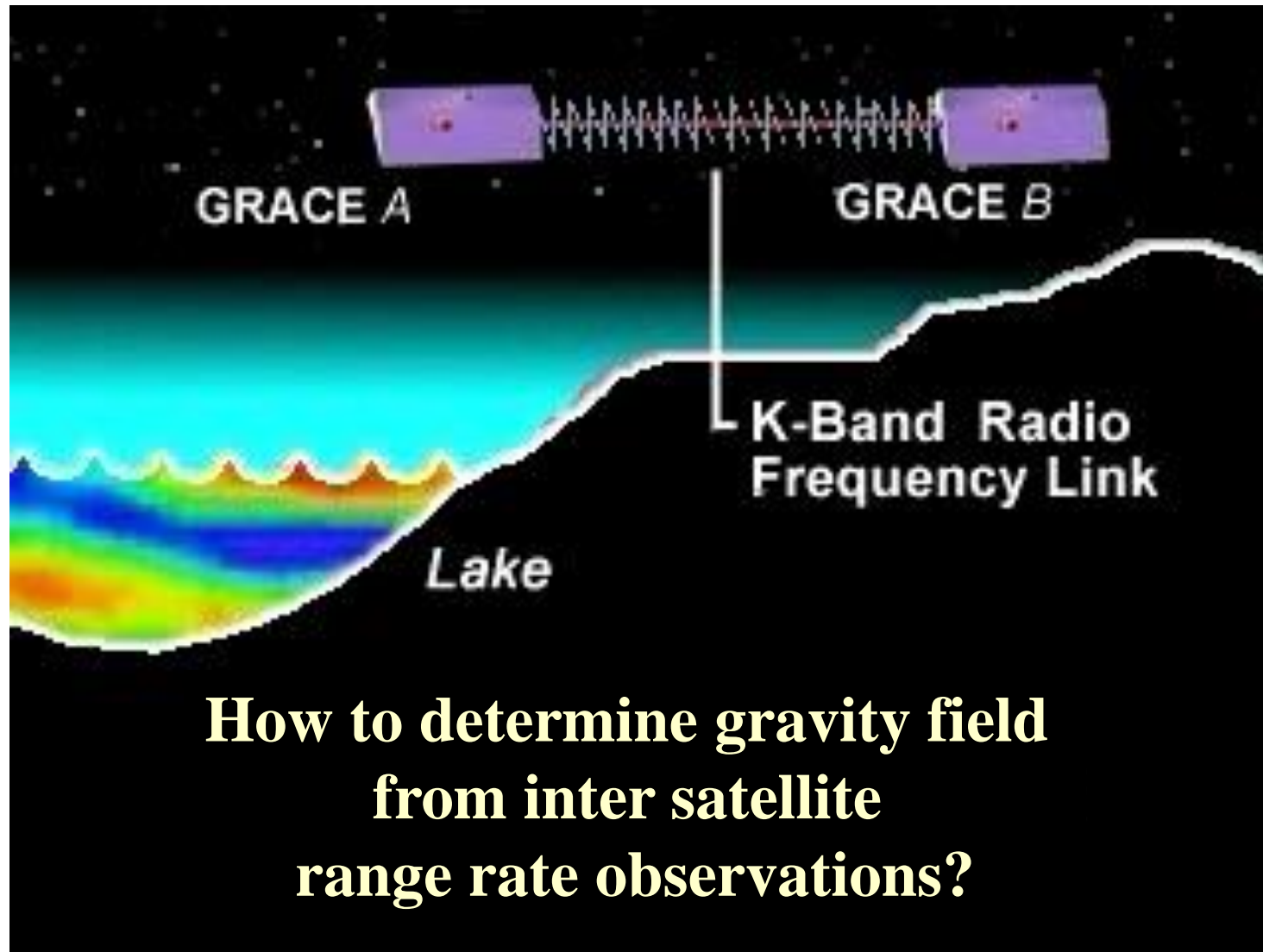
Key science instrument:
continuous interferometric
range rate observation
between the the satellites
in the K-band (μ wave) with
 $1 \mu\text{m/s}$ precision (!)

GRACE

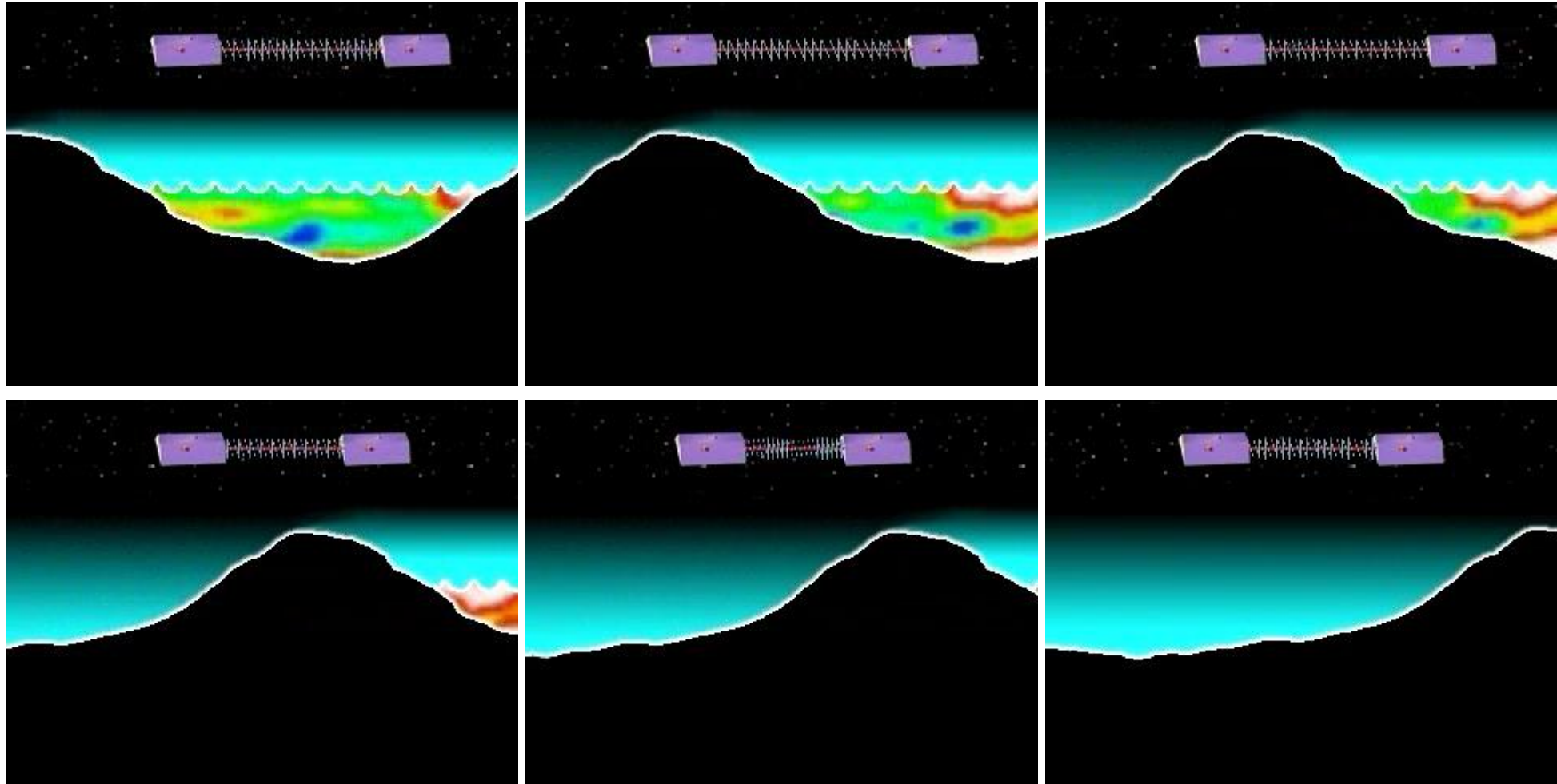


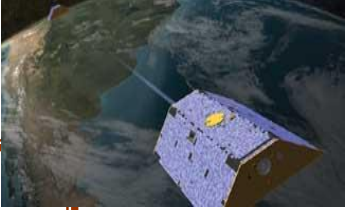
Dedicated gravity satellite missions
Mostar, 19.10.2017

GRACE



How to determine gravity field from intersatellite range rate observations?

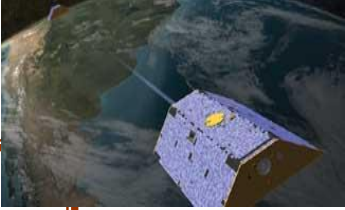




GRACE gravity field models

Based on the *International Center for Global Gravity Field Models* data, the list of the GRACE-only gravity field models:

Nr	Name	Year	Degree	Data	Reference
83	EIGEN-GRACE01S	2003	140	S(Grace)	Reigber et al, 2003c
84	GGM01S	2003	120	S(Grace)	Tapley et al, 2003
93	EIGEN-GRACE02S	2004	150	S(Grace)	Reigber et al, 2005a
96	GGM02S	2004	160	S(Grace)	UTEX CSR, 2004
101	ITG-Grace02s	2006	170	S(Grace)	Mayer-Gürr et al, 2006
103	ITG-Grace03	2007	180	S(Grace)	Mayer-Gürr et al, 2007
107	AIUB-GRACE01S	2008	120	S(Grace)	Jäggi et al, 2008
108	GGM03S	2008	180	S(Grace)	Tapley et al, 2007
110	AIUB-GRACE02S	2009	150	S(Grace)	Jäggi et al, 2009
111	ITG-Grace2010s	2010	180	S(Grace)	Mayer-Gürr et al, 2010
122	AIUB-GRACE03S	2011	160	S(Grace)	Jäggi et al, 2011
138	Tongji-GRACE01	2013	160	S(Grace)	Shen et al, 2013
140	GGM05S	2014	180	S(Grace)	Tapley et al, 2013
146	ITSG-Grace2014k	2014	200	S(Grace)	Mayer-Gürr et al, 2014
147	ITSG-Grace2014s	2014	200	S(Grace)	Mayer-Gürr et al, 2014



GRACE gravity field models

Based on the *International Center for Global Gravity Field Models* data, the list of combined GRACE and CHAMP gravity field models:

Nr	Name	Year	Degree	Data	Reference
95	EIGEN-CG01C	2004	360	S(Champ,Grace),G,A	Reigber et al, 2006
98	EIGEN-CG03C	2005	360	S(Champ,Grace),G,A	Förste et al, 2005c
97	GGM02C	2004	200	S(Grace),G,A	UTEX CSR, 2004
104	EGM2008	2008	2190	S(Grace),G,A	Pavlis et al, 2008
109	GGM03C	2009	360	S(Grace),G,A	Tapley et al, 2007
126	GIF48	2011	360	S(Grace),G,A	Ries et al, 2011
114	EIGEN-51C	2010	359	S(Grace,Champ),G,A	Bruinsma et al, 2010
100	EIGEN-GL04S1	2006	150	S(Grace,Lageos)	Förste et al, 2006
106	EIGEN-5S	2008	150	S(Grace,Lageos)	Förste et al, 2008
99	EIGEN-GL04C	2006	360	S(Grace,Lageos),G,A	Förste et al, 2006
105	EIGEN-5C	2008	360	S(Grace,Lageos),G,A	Förste et al, 2008

GRACE – temporal gravity variations

Gravity field models with monthly resolution are presented by

- University Texas, Center for Space Research (CSR)
- GeoForschungsZentrum (GFZ)
- NASA Jet Propulsion Laboratory (JPL)
- and others.

These models have lower spatial resolution, but enables the investigation of mass variation processes, which corresponds to the monthly temporal resolution.

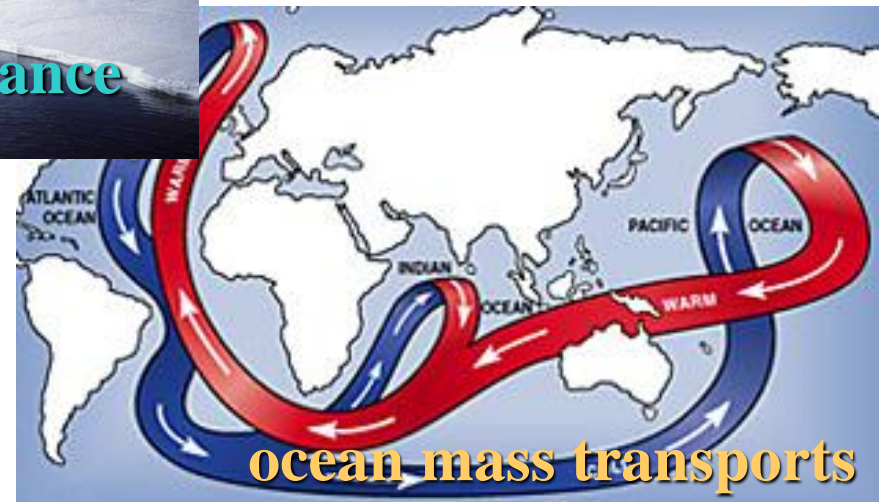
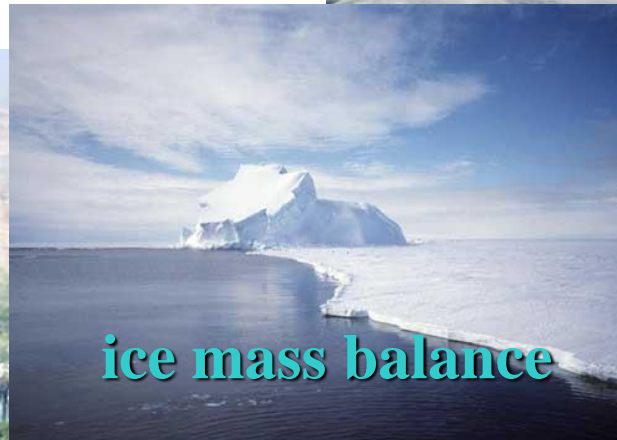
These are:

- annual
- semi-annual
- long-term periodic
- secular

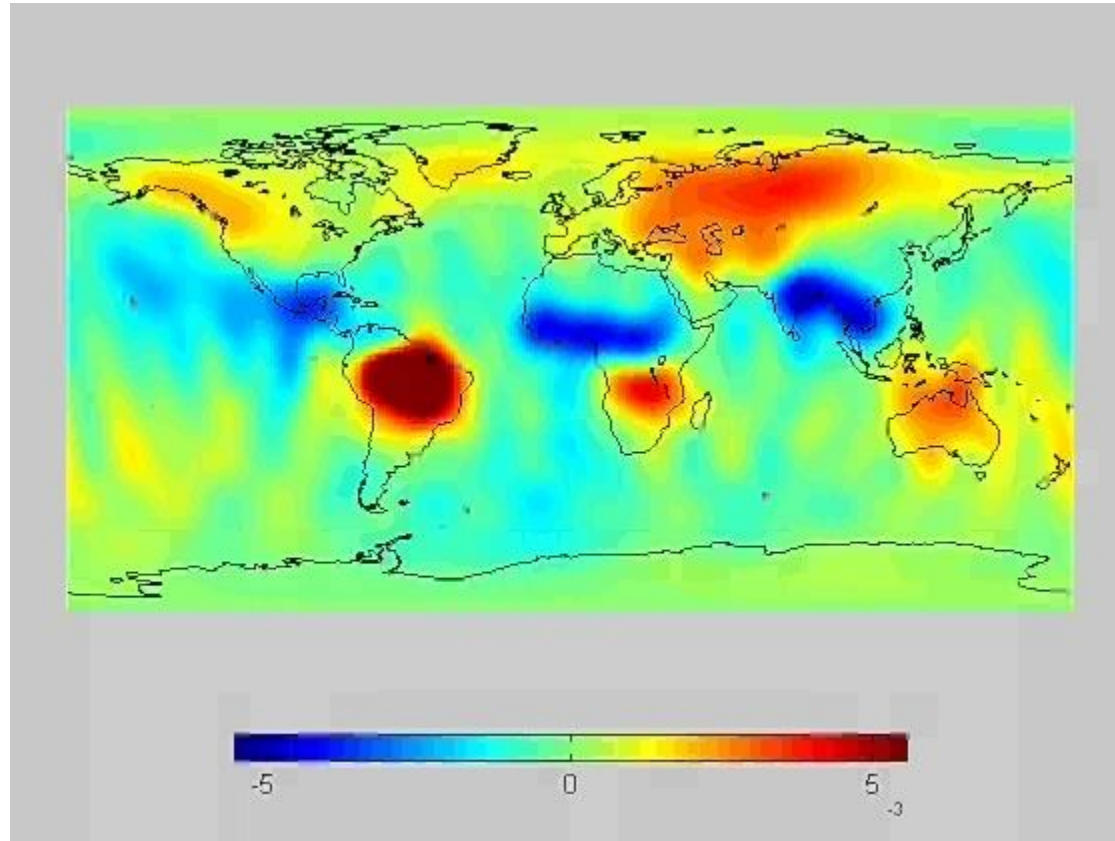
GRACE – temporal gravity variations

Temporal variations of gravity field

- (semi-)annual
- secular



GRACE – temporal gravity variations



GRACE – temporal gravity variations

Annual and semi-annual mass variations:

Atmosphere	16.50	} · 10 ¹⁵ kg
Ocean	13.37	
Hydrology	4.73	

Annual variations:

1. atmosphere
2. hydrology
3. ocean

Semi-annual variations:

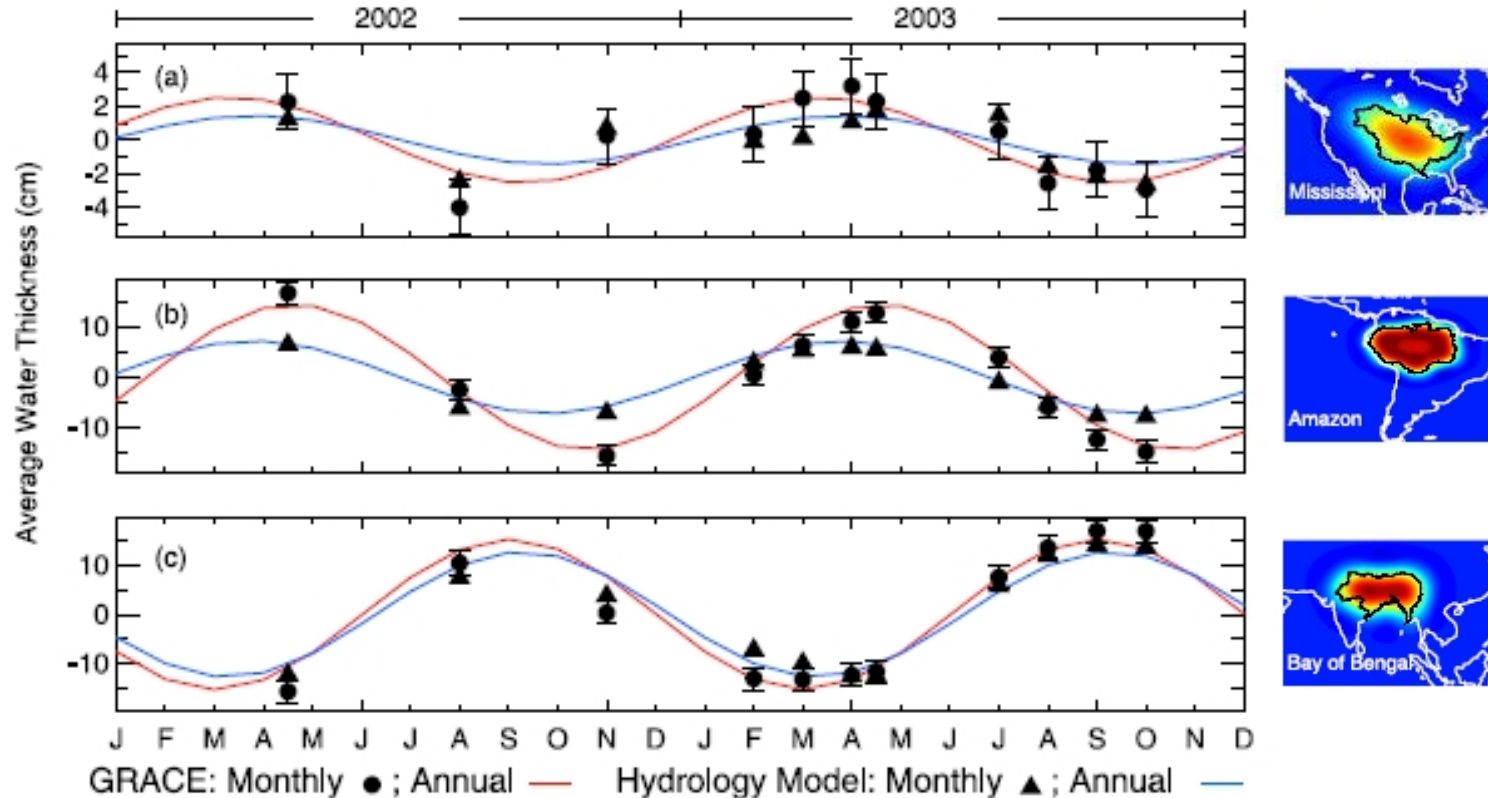
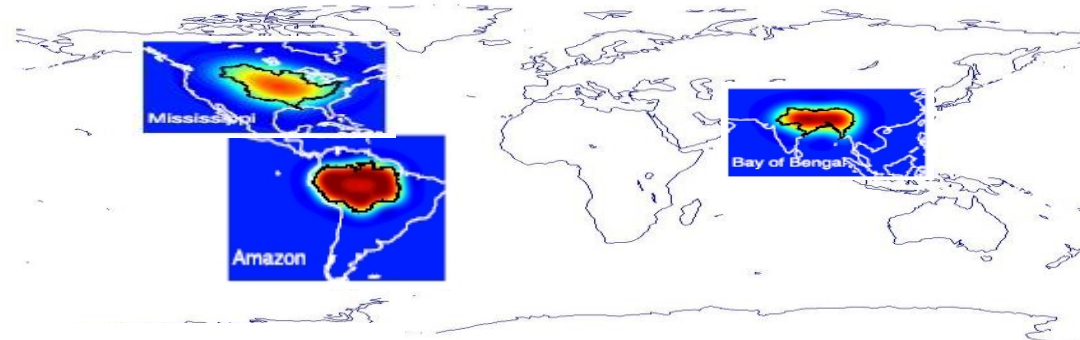
1. atmosphere
2. ocean
3. hydrology

Separation of the contributions:

- by the period of the variation
- by the location of the variation
- by correction with the most known contribution

GRACE – temporal gravity variations

Application for hydrology



GRACE – temporal gravity variations

Application for hydrology

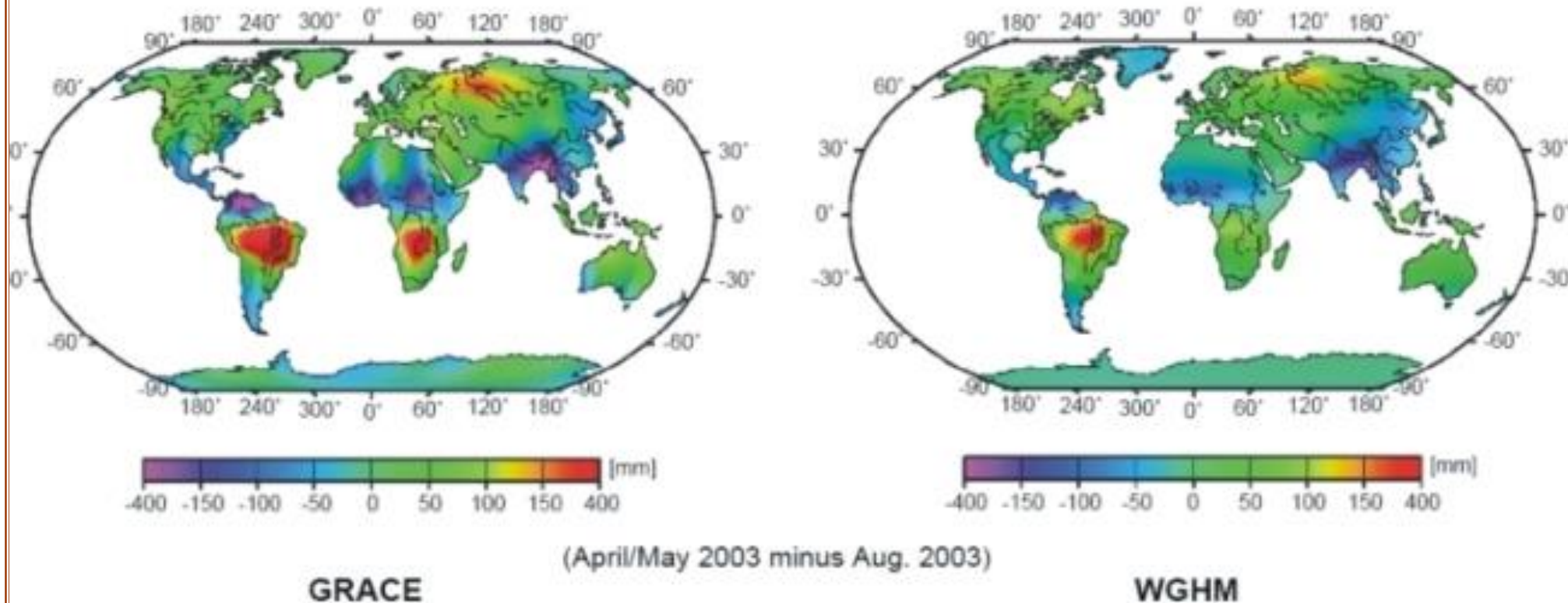
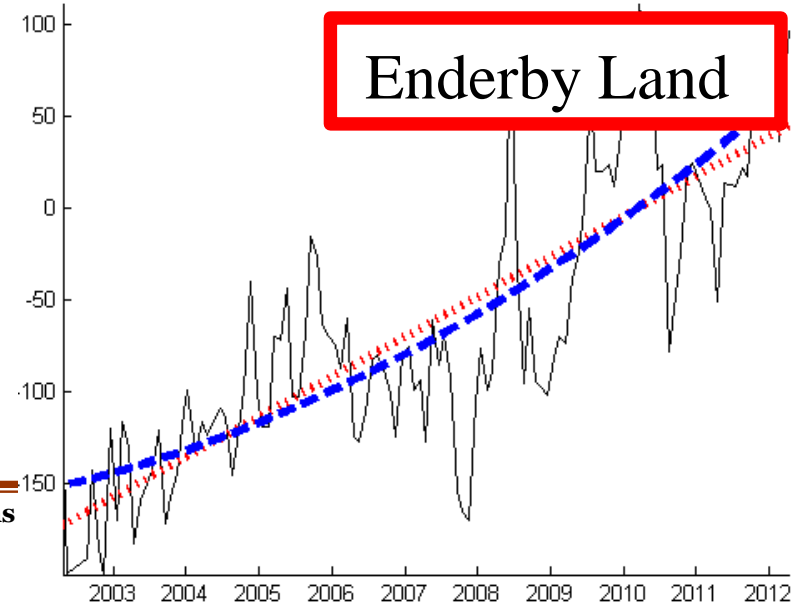
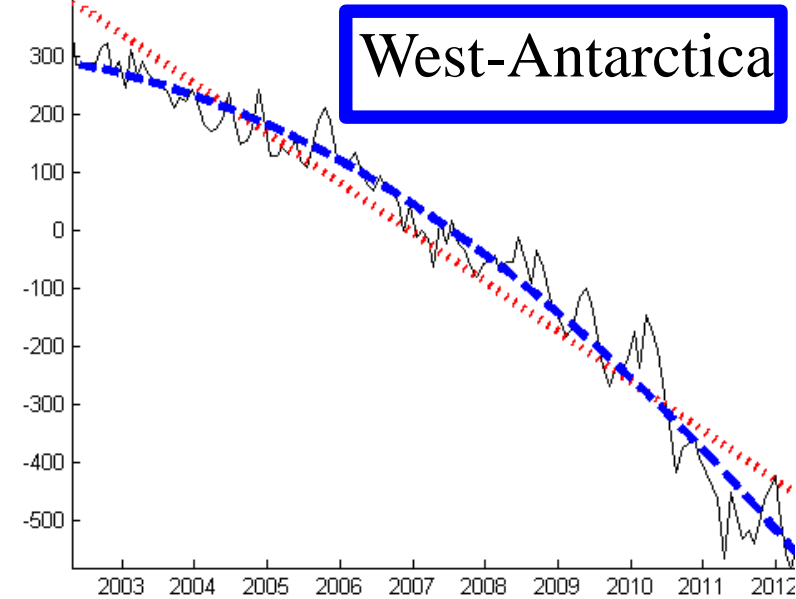
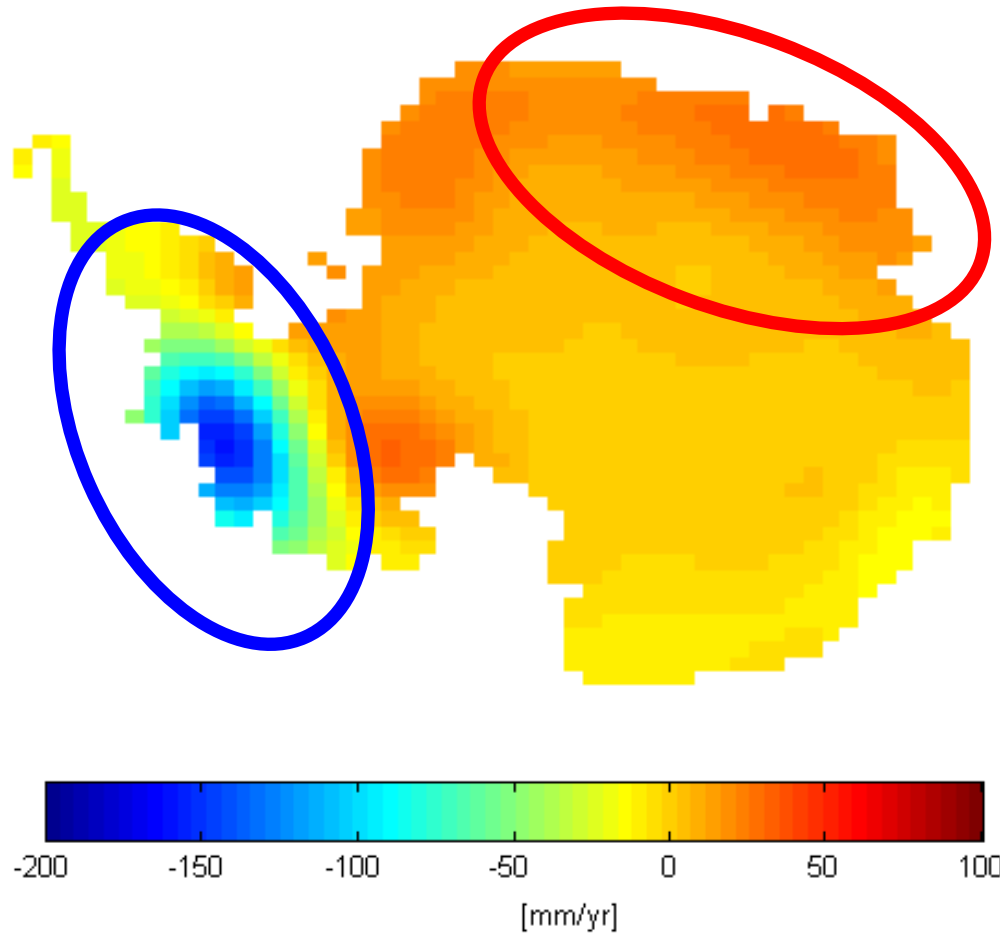


Fig. 1- Geographical distribution of differences over continents between GRACE gravity field solutions and those predicted by the WGHM continental hydrological model (in mm of equivalent water column height); averaging radius 750 km [Schmidt et al.(2006); GRACE observations of changes in continental water storage, Global and Planetary Change, Vol 50/1-2, 112-126]

GRACE – temporal gravity variations

Application for ice mass balance investigations



GRACE – temporal gravity variations

Application for ice mass balance investigations

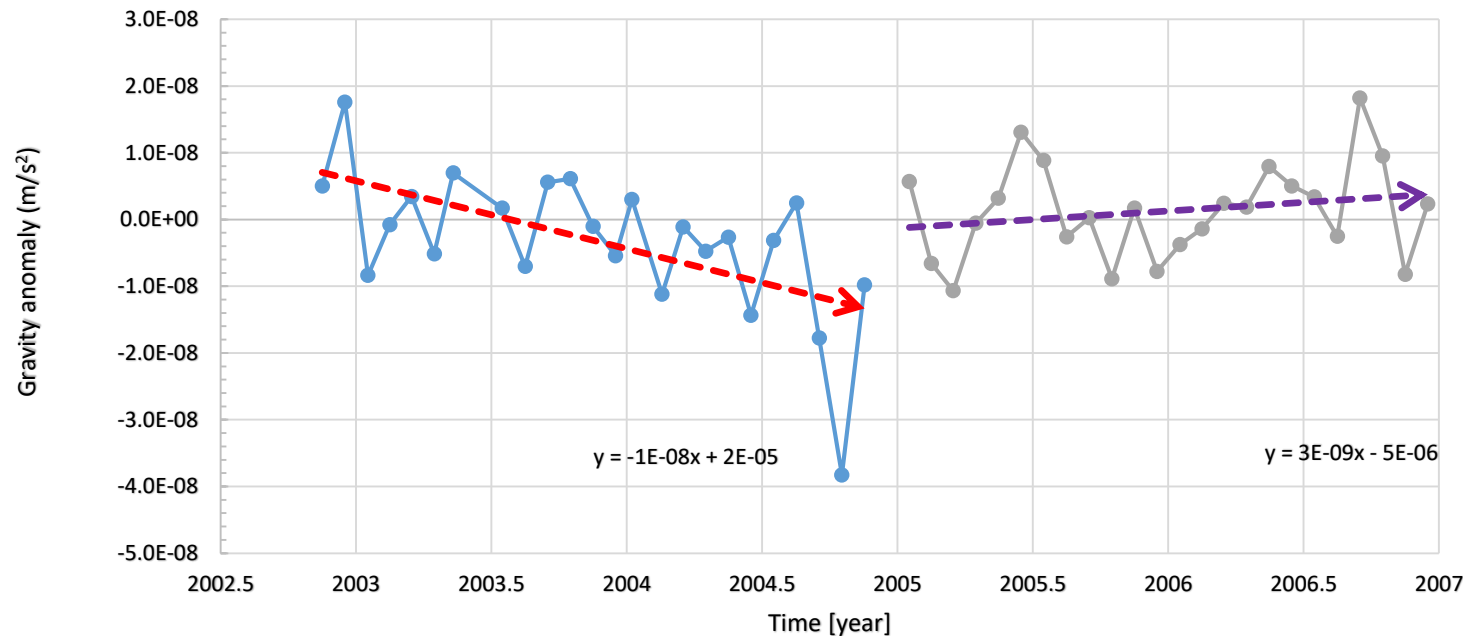
Greenland: Within 100 years, it will be „green”.

Antarctica: More stable ice mass, which contains the 70% of fresh water of the Earth. It seems, around 2008 a melting process has been started, but it is too early to draw ultimate conclusions.

GRACE – temporal gravity variations

Application for modeling co- and post-seismic crustal deformations

Event: Sumatra-Andaman earthquake, 2004.12.26.



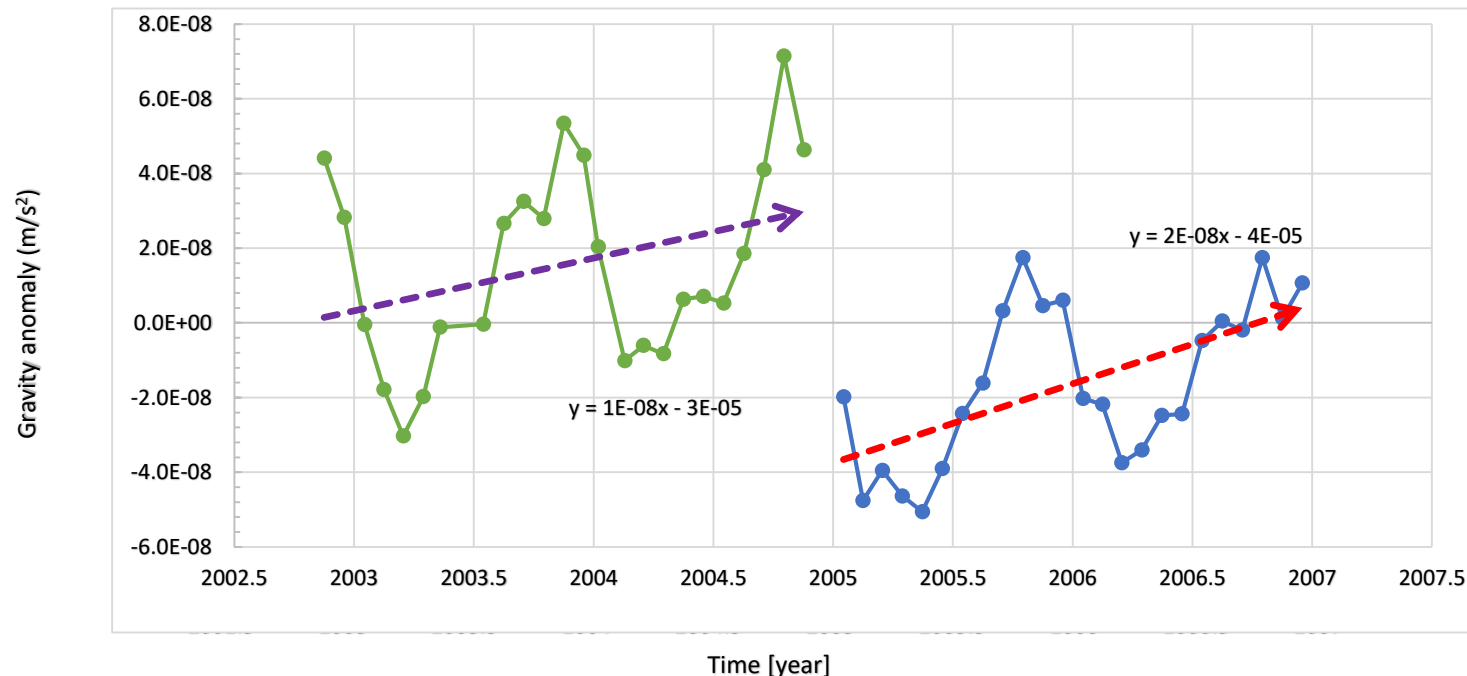
Location: $\varphi=0^\circ$, $\lambda=93^\circ$



GRACE – temporal gravity variations

Application for modeling co- and post-seismic crustal deformations

Event: Sumatra-Andaman earthquake, 2004.12.26.



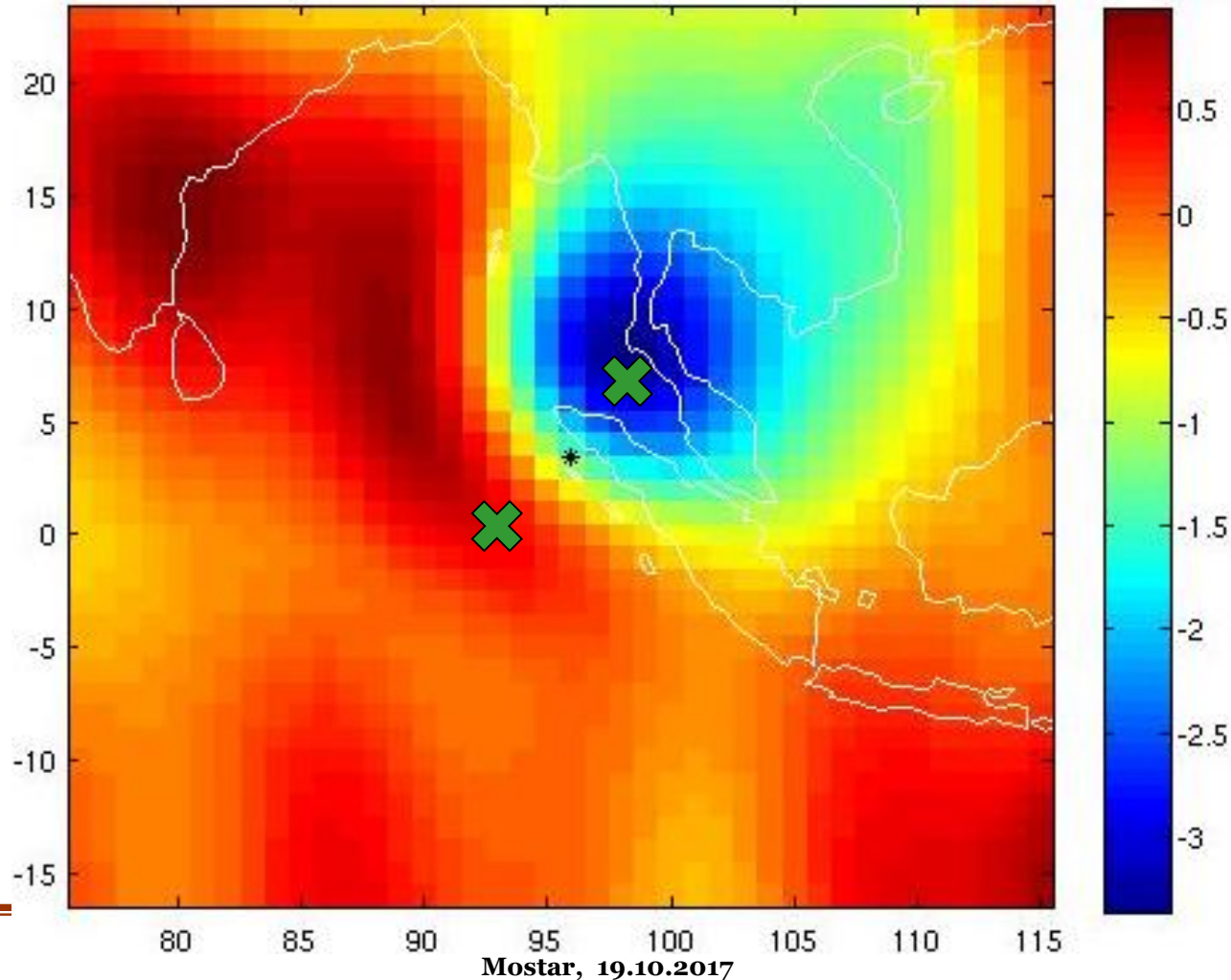
Location: $\varphi=8^\circ$, $\lambda=100^\circ$



GRACE – temporal gravity variations

Application for modeling co- and post-seismic crustal deformations

Event: Sumatra-Andaman earthquake, 2004.12.26.

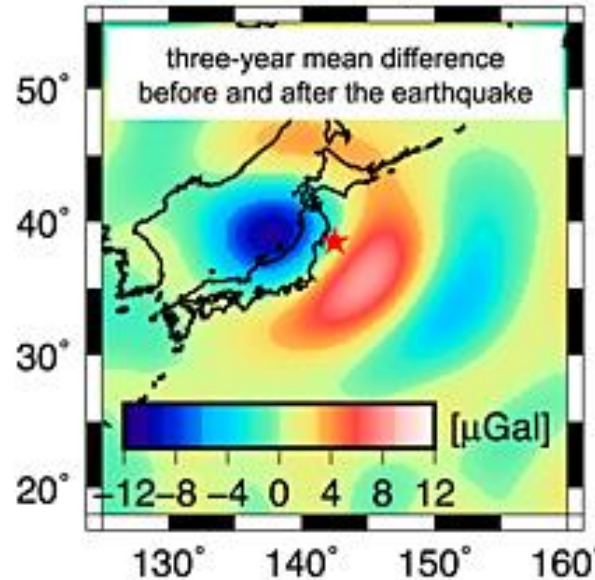


GRACE – temporal gravity variations

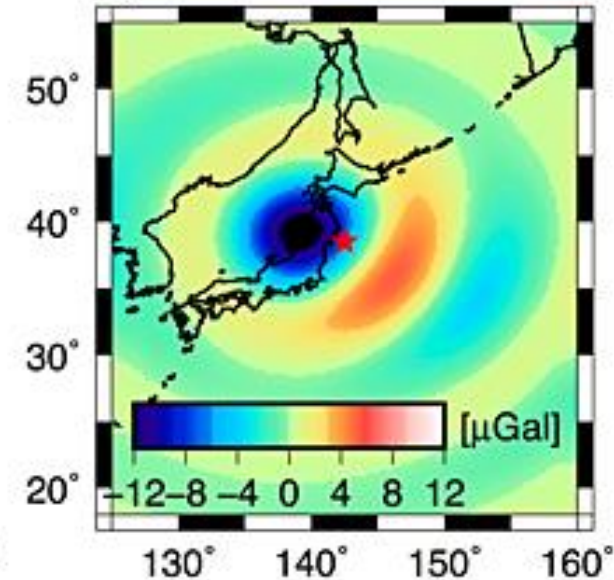
Application for modeling
co- and postseismic
crustal deformations

Event: Tohoku-Oki
earthquake, 2011.03.11.

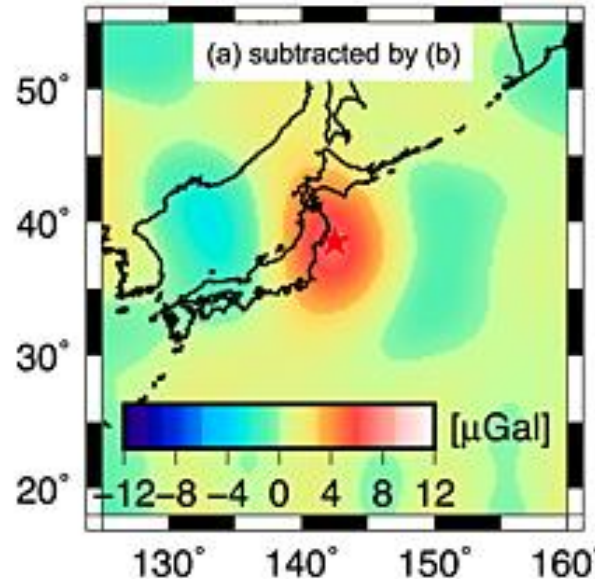
(a) Observed gravity change



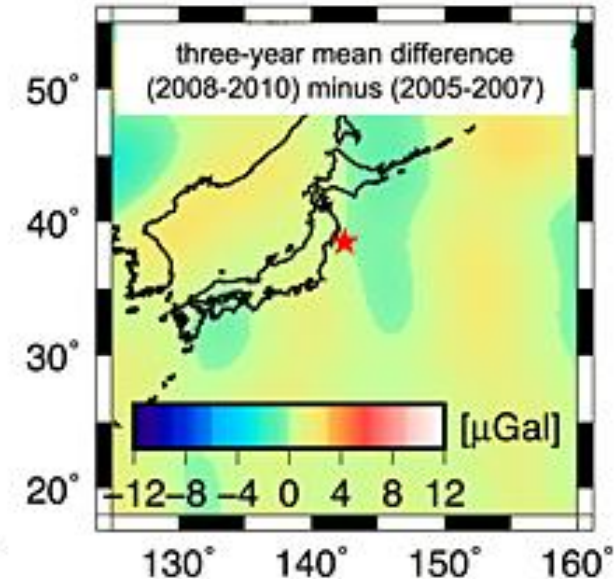
(b) Seismic model



(c) Postseismic gravity change



(d) Background data noise



Han, S.-C., J. Sauber, and F. Pollitz (2014), Broadscale postseismic gravity change following the 2011 Tohoku-Oki earthquake and implication for deformation by viscoelastic relaxation and afterslip, *Geophys. Res. Lett.*, 41, 5797–5805, doi:10.1002/2014GL060905.

GOCE

**The SGG mission
(+High-Low SST)**

GOCE



Orbit:

- nearly circular
- polar gap ($i = 96.7^\circ$)
- altitude: 260 km

Launch:

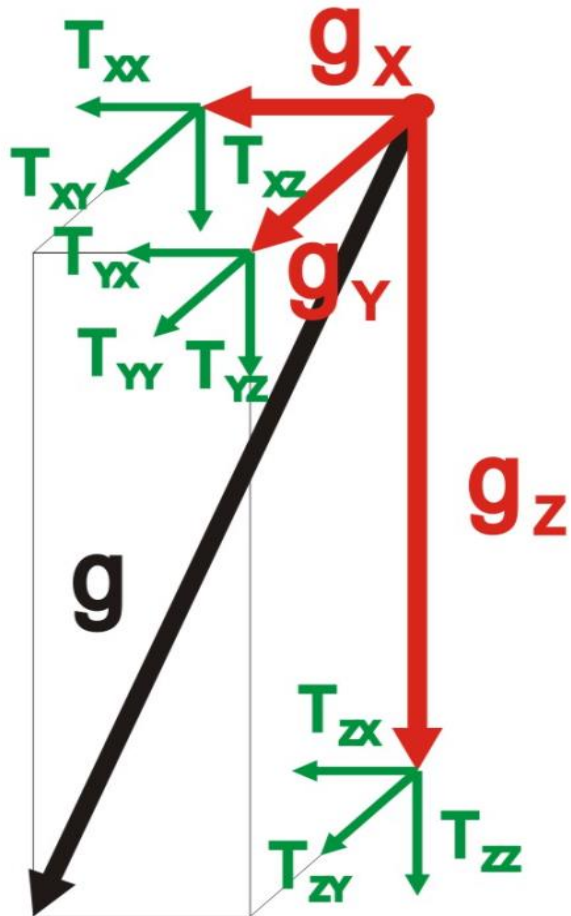
- 17 March 2009

Mission duration:

- planned for 20 months,
but it was on orbit until
19 November, 2013

Gradiometry

Gradiometry: observation of gravity gradients



$$\mathbf{g} = [g_x \ g_y \ g_z]$$

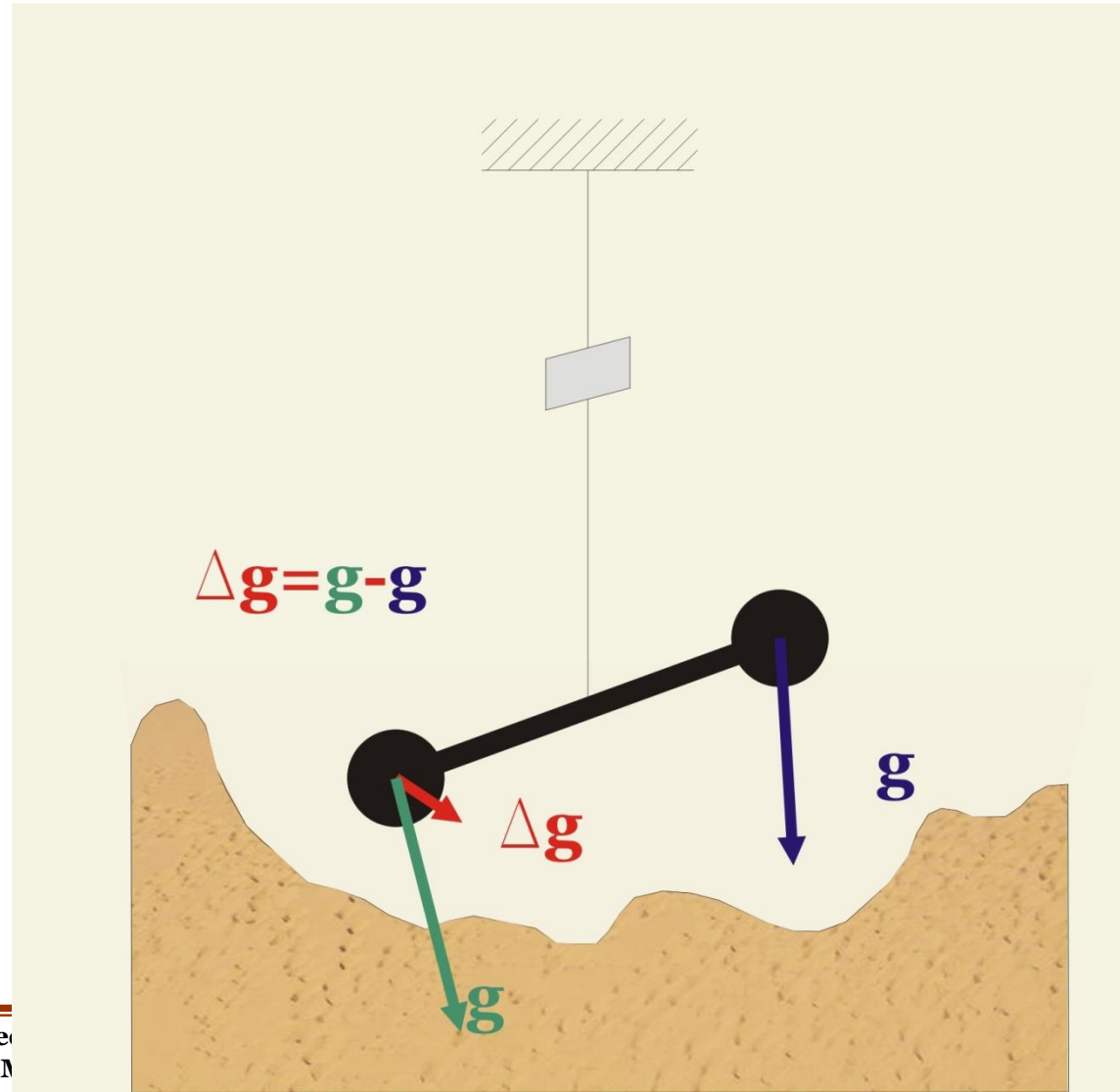
$$T_u = \begin{vmatrix} T_{xx} & T_{xy} & T_{xz} \\ T_{yx} & T_{yy} & T_{yz} \\ T_{zx} & T_{zy} & T_{zz} \end{vmatrix}$$

Gradiometry

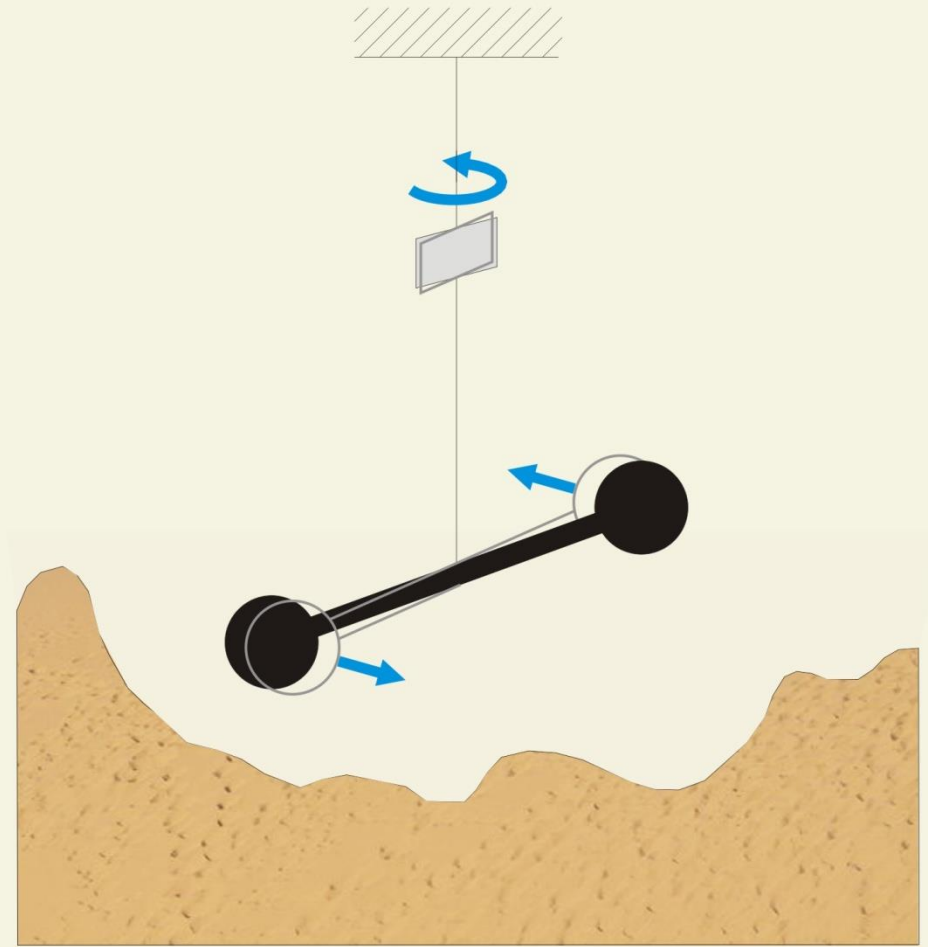
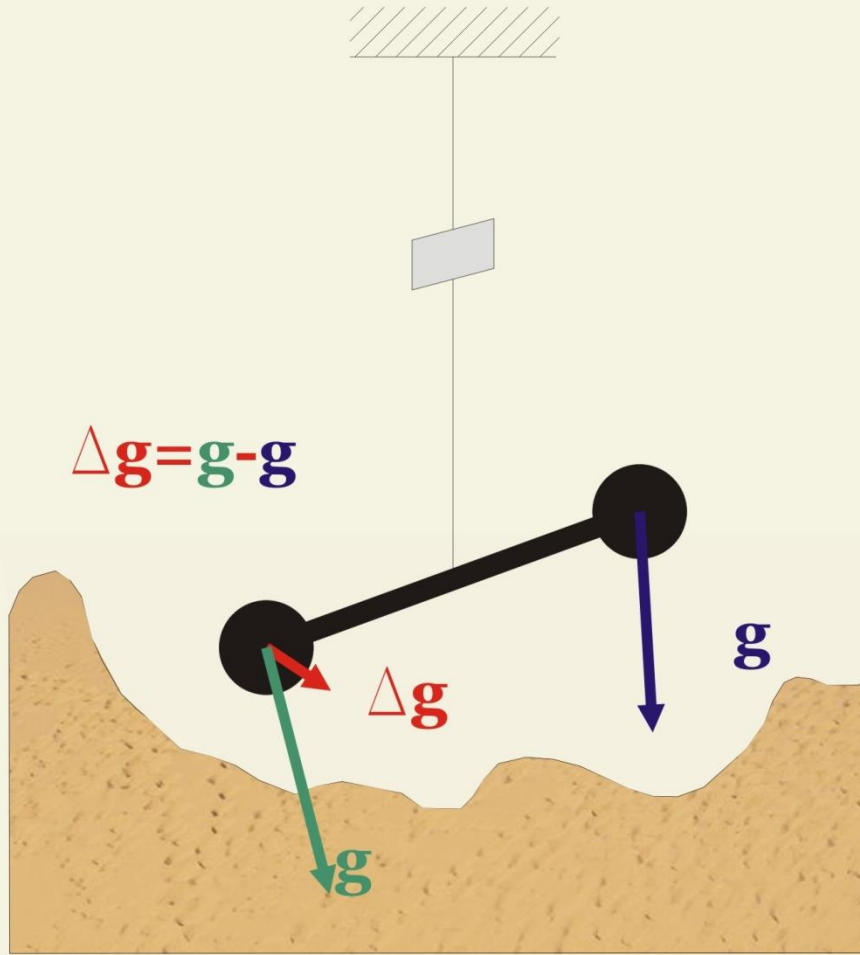
Gradiometry: observation of **gravity gradients**

$$\underline{\underline{\mathbf{E}}} = \begin{vmatrix} \mathbf{T}_{xx} & \mathbf{T}_{xy} & \mathbf{T}_{xz} \\ \mathbf{T}_{xy} & \mathbf{T}_{yy} & \mathbf{T}_{yz} \\ \mathbf{T}_{xz} & \mathbf{T}_{yz} & \mathbf{T}_{zz} \end{vmatrix}$$

The classical terrestrial gradiometer is torsion balance

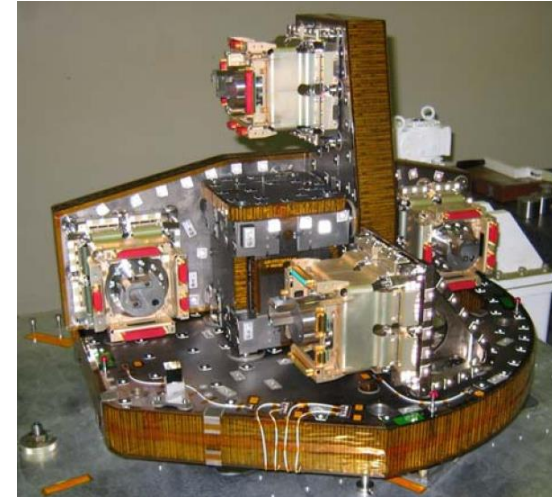
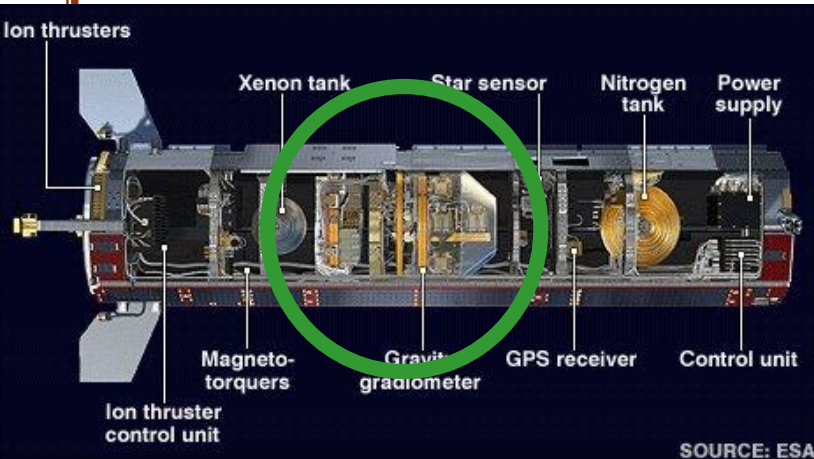
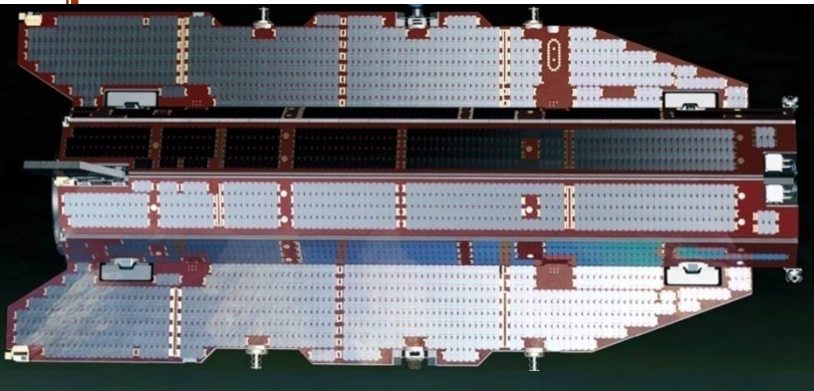


Gradiometry



GOCE gradiometer

The GOCE space gradiometer



GOCE gradiometer

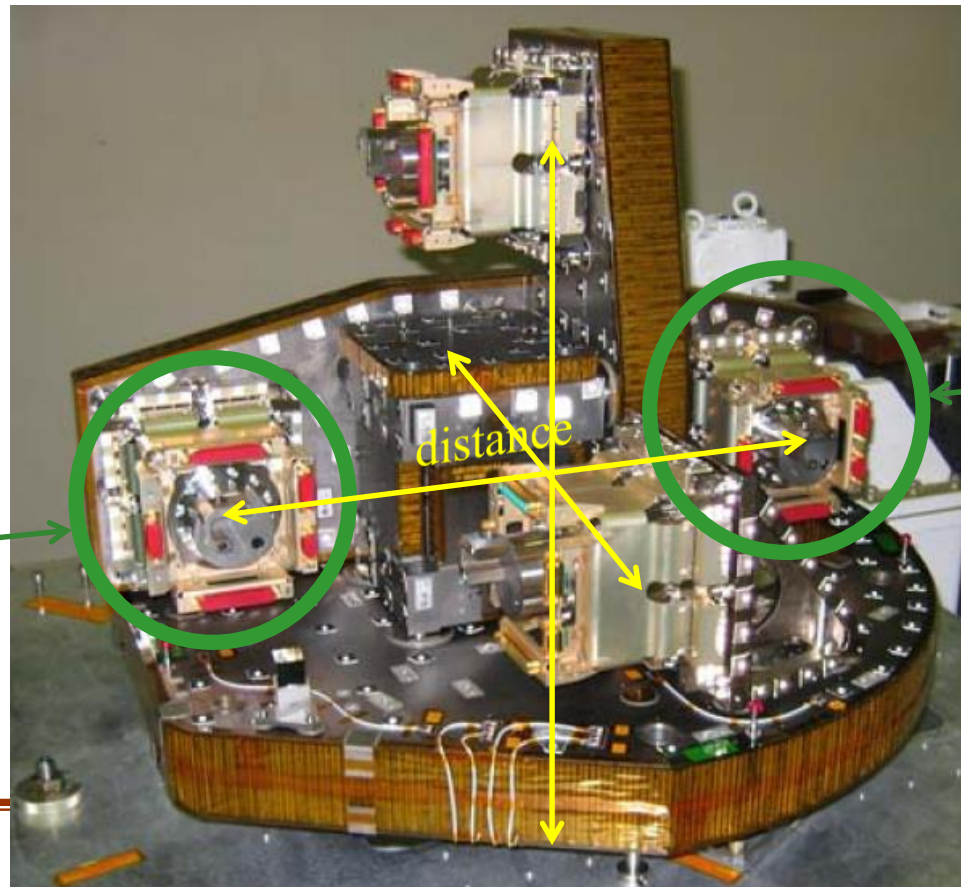
Concept of measurement:

3 pairs of *capacitive accelerometers* simultaneously takes measurements along perpendicular directions.

$$\Delta g = g_2 - g_1$$

$$\text{gradient} = \Delta g / r$$

1. accelerometer



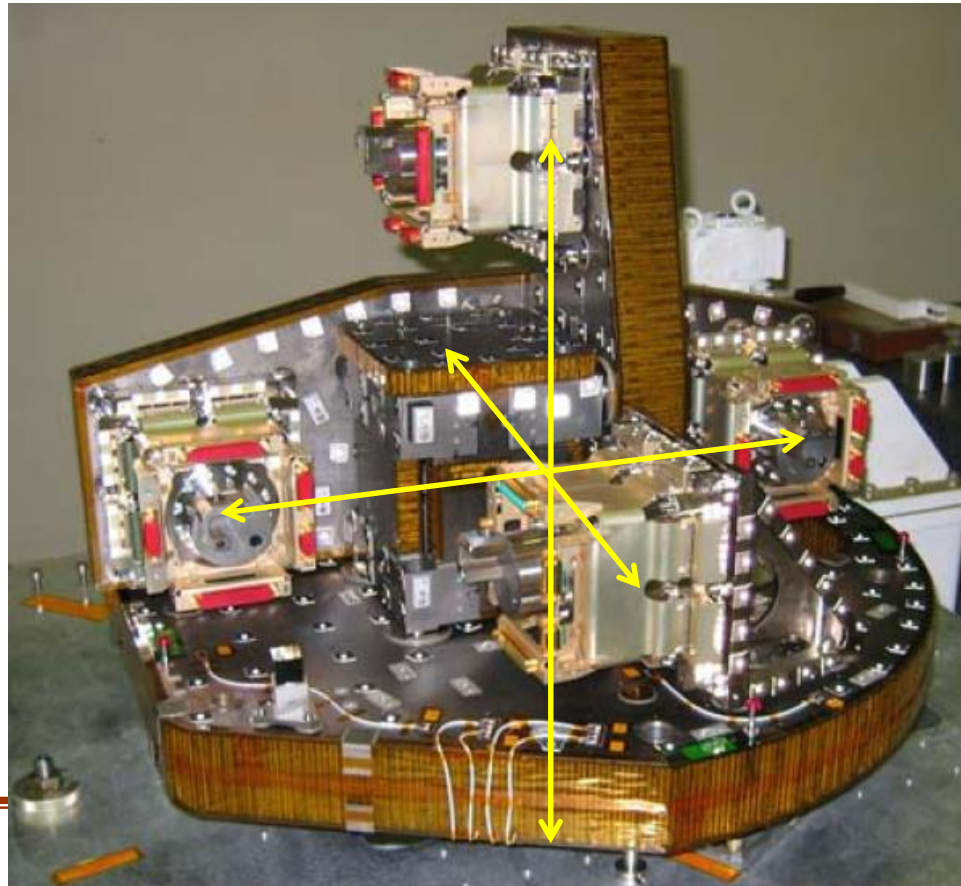
2. accelerometer

GOCE gradiometer

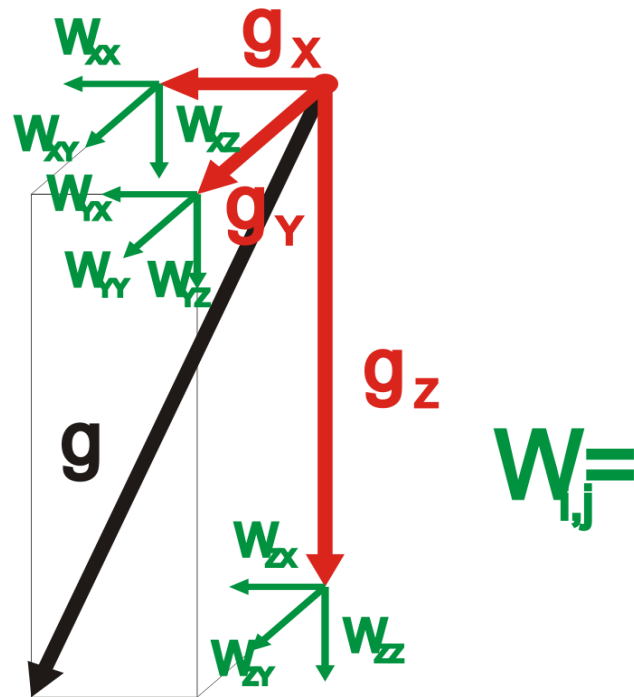
Concept of measurement:

$$E = \frac{1}{d} \cdot \begin{bmatrix} \gamma_{x2} - \gamma_{x1} & \gamma_{y2} - \gamma_{y1} & \gamma_{z2} - \gamma_{z1} \\ \gamma_{x4} - \gamma_{x3} & \gamma_{y4} - \gamma_{y3} & \gamma_{z4} - \gamma_{z3} \\ \gamma_{x6} - \gamma_{x5} & \gamma_{y6} - \gamma_{y5} & \gamma_{z6} - \gamma_{z5} \end{bmatrix} = \begin{bmatrix} V_{xx} & V_{xy} & V_{xz} \\ V_{yx} & V_{yy} & V_{yz} \\ V_{zx} & V_{zy} & V_{zz} \end{bmatrix} + \underline{\underline{\Omega}} + \underline{\underline{\dot{\Omega}}}$$

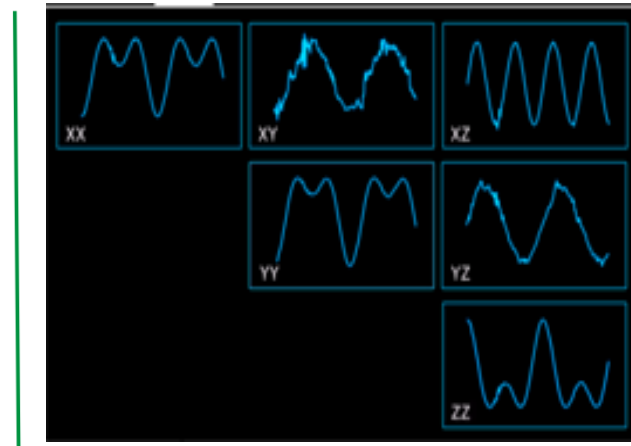
gradient = $\Delta g / r$



GOCE observable: gravity gradients

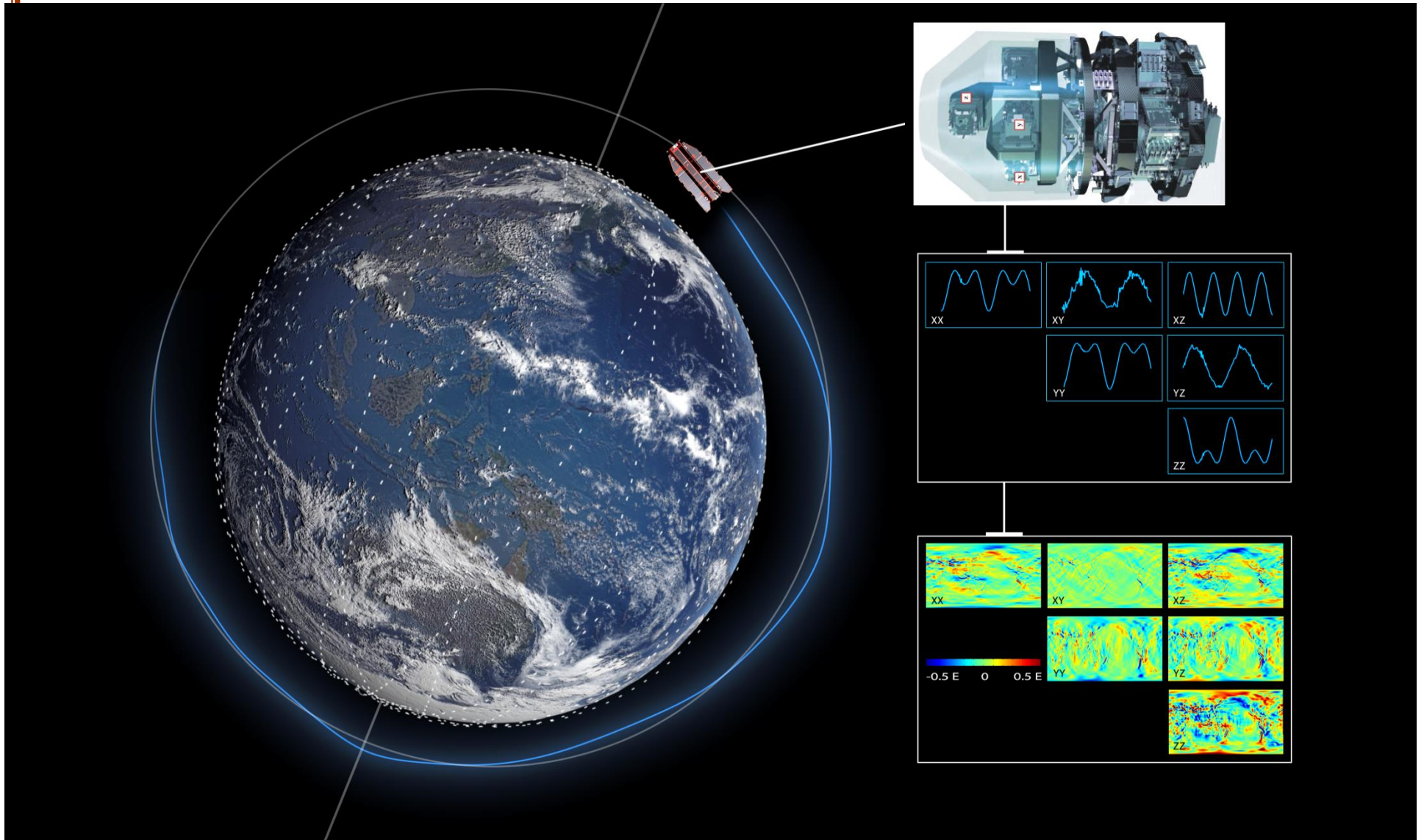


$$g = [g_x \ g_y \ g_z]$$



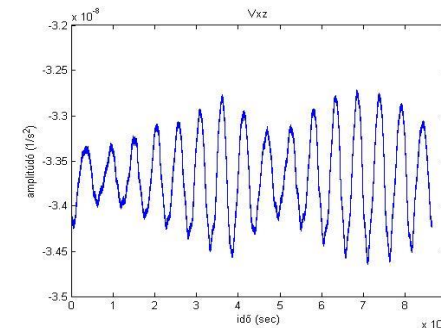
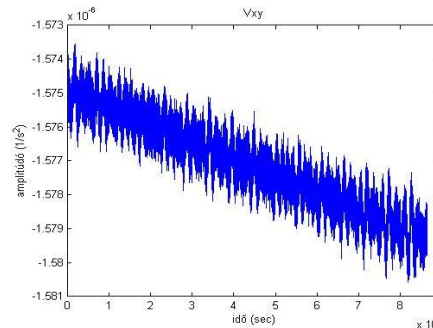
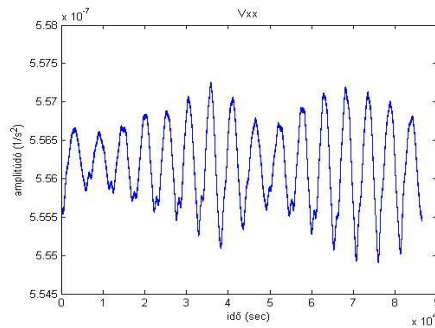
The GOCE gradiometer observes the 6 independent elements of the Gradient tensor with 1 s resolution.

GOCE observable: gravity gradients

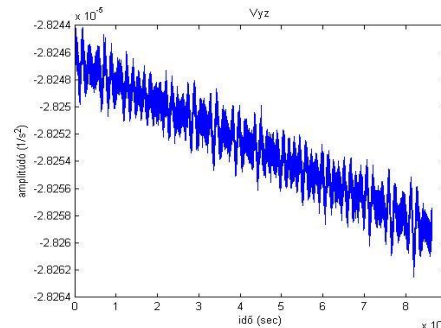
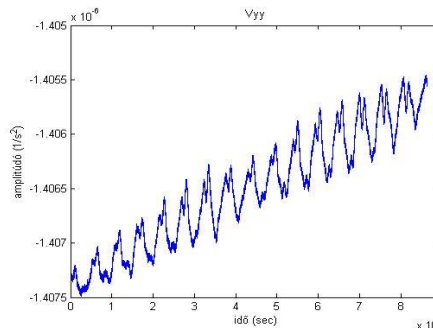


Dedicated gravity satellite missions
Mostar, 19.10.2017

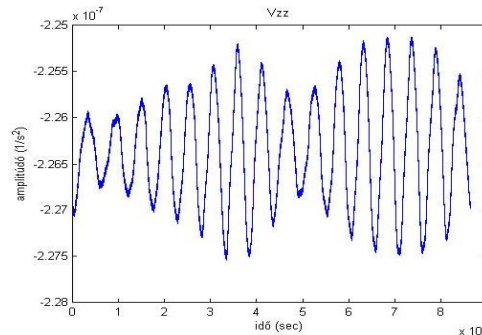
Processing GOCE gravity gradients



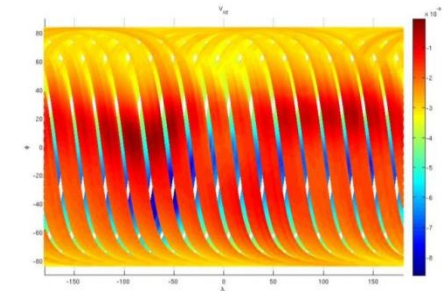
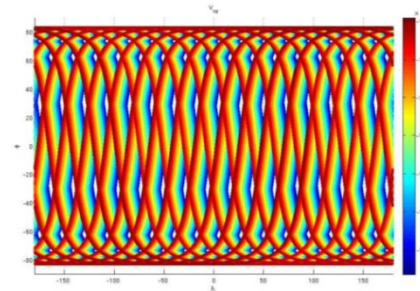
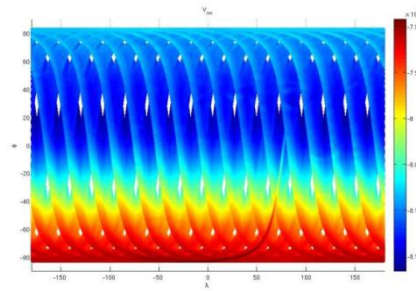
Measurement
Bandwidth (MBW):
5 – 100 mHz



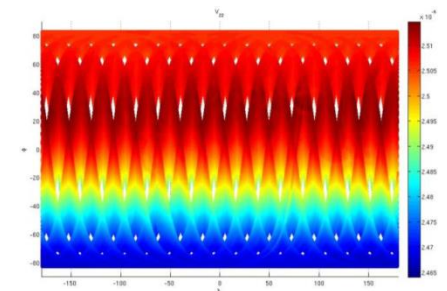
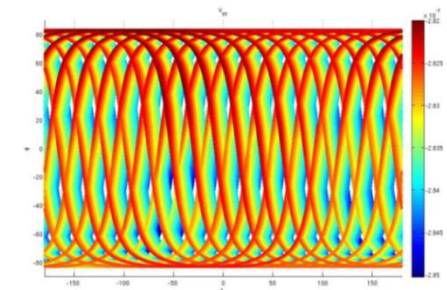
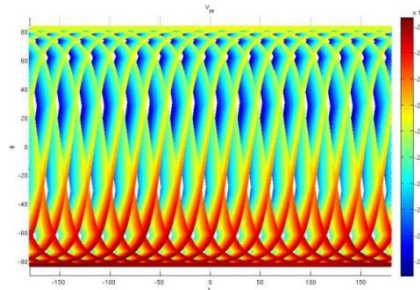
The raw observables and the
processing method should be
band limited.



Processing GOCE gravity gradients

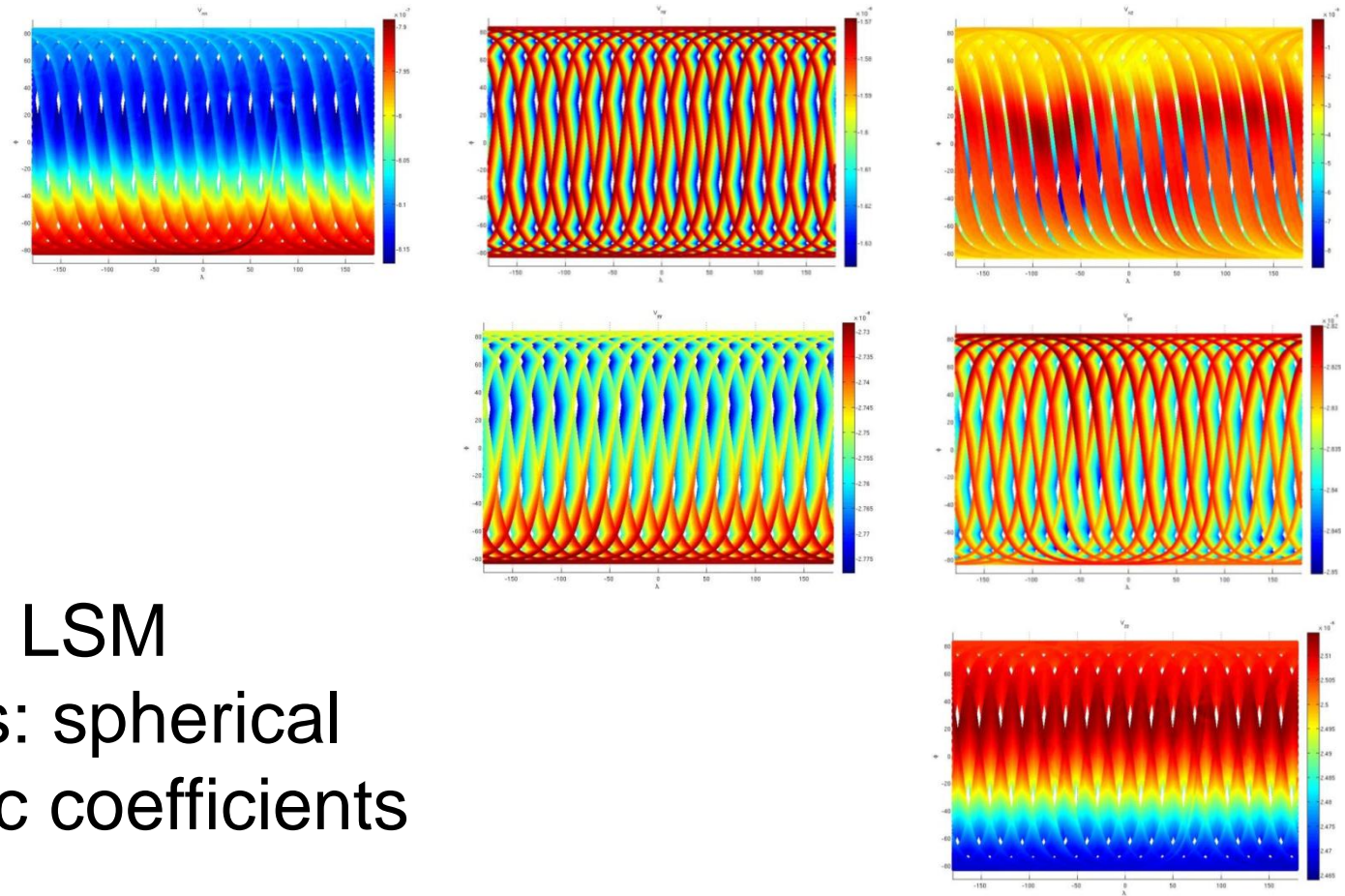


Full and
homogeneous
coverage:
2 months



200.000 epochs

Processing GOCE gravity gradients



Adjustment: LSM
Parameters: spherical
harmonic coefficients

$$V(r, \varphi, \lambda) = \frac{GM}{R} \sum_{n=0}^{\infty} \left(\frac{R}{r} \right)^{n+1} \sum_{m=0}^n (C_{nm} \cos m\lambda + S_{nm} \sin m\lambda) P_{nm}(\sin \varphi)$$



GOCE gravity field models

Based on the *International Center for Global Gravity Field Models* data, the list of the GOCE-only gravity field models:

Nr	Name	Year	Degree	Data	Reference
116	GO CONS GCF 2 SPW R1	2010	210	S(Goce)	Migliaccio et al, 2010
117	GO CONS GCF 2 TIM R1	2010	224	S(Goce)	Pail et al, 2010a
118	GO CONS GCF 2 DIR R1	2010	240	S(Goce)	Bruinsma et al, 2010
119	GO CONS GCF 2 SPW R2	2011	240	S(Goce)	Migliaccio et al, 2011
120	GO CONS GCF 2 TIM R2	2011	250	S(Goce)	Pail et al, 2011
121	GO CONS GCF 2 DIR R2	2011	240	S(Goce)	Bruinsma et al, 2010
127	GO CONS GCF 2 TIM R3	2011	250	S(Goce)	Pail et al, 2011
133	GO CONS GCF 2 TIM R4	2013	250	S(Goce)	Pail et al, 2011
134	ITG-Goce02	2013	240	S(Goce)	Schall et al, 2014
137	JYY GOCE02S	2013	230	S(Goce)	Yi et al, 2013
143	JYY GOCE04S	2014	230	S(Goce)	Yi et al, 2013
145	GO CONS GCF 2 TIM R5	2014	280	S(Goce)	Brockmann et al, 2014
149	GO CONS GCF 2 SPW R4	2014	280	S(Goce)	Gatti et al, 2014



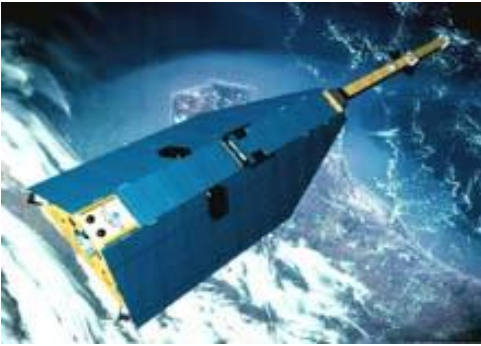
GOCE gravity field models

Based on the *International Center for Global Gravity Field Models* data, the list of combined GOCE and GRACE gravity field models:

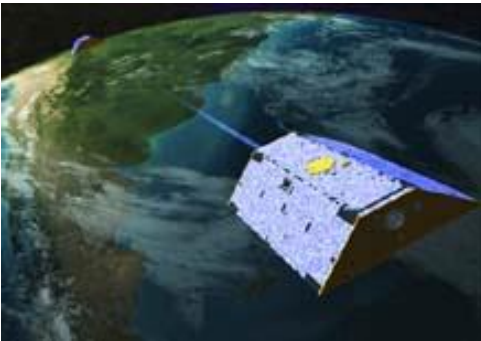
Nr	Name	Year	Degree	Data	Reference
152	GECO	2015	2190	S(Goce),EGM2008	Gilardoni et al, 2015
115	<u>GOCO01S</u>	2010	224	S(Goce,Grace)	Pail et al, 2010b
130	<u>DGM-1S</u>	2012	250	S(Goce,Grace)	Farahani, et al. 2013
136	<u>GOGRA02S</u>	2013	230	S(Goce,Grace)	Yi et al, 2013
142	<u>GOGRA04S</u>	2014	230	S(Goce,Grace)	Yi et al, 2013
123	<u>GOCO02S</u>	2011	250	S(Goce,Grace,...)	Goiginger et al, 2011
129	<u>GOCO03S</u>	2012	250	S(Goce,Grace,...)	Mayer-Gürr, et al. 2012
124	<u>EIGEN-6S</u>	2011	240	S(Goce,Grace,Lageos)	Förste et al, 2011
128	<u>GO CONS GCF 2 DIR R3</u>	2011	240	S(Goce,Grace,Lageos)	Bruinsma et al, 2010
132	<u>GO CONS GCF 2 DIR R4</u>	2013	260	S(Goce,Grace,Lageos)	Bruinsma et al, 2013
141	<u>EIGEN-6S2</u>	2014	260	S(Goce,Grace,Lageos)	Rudenko et al. 2014
144	<u>GO CONS GCF 2 DIR R5</u>	2014	300	S(Goce,Grace,Lageos)	Bruinsma et al, 2013
125	<u>EIGEN-6C</u>	2011	1420	S(Goce,Grace,Lageos),G,A	Förste et al, 2011
131	<u>EIGEN-6C2</u>	2012	1949	S(Goce,Grace,Lageos),G,A	Förste et al, 2012
139	<u>EIGEN-6C3stat</u>	2014	1949	S(Goce,Grace,Lageos),G,A	Förste et al, 2012
148	<u>EIGEN-6C4</u>	2014	2190	S(Goce,Grace,Lageos),G,A	Förste et al, 2015
151	<u>GGM05G</u>	2015	240	S(Grace,Goce)	Bettadpur et al, 2015
153	<u>GGM05C</u>	2016	360	S(Grace,Goce),G,A	Ries et al, 2016

Future satellite missions

Results of dedicated gravity missions



2 years observations of CHAMP resulted in more measurements than all in the pre-CHAMP era.



2 months observations of GRACE resulted in more measurements than all observations before GRACE.

A tool for detecting temporal gravity variations



GOCE has delivered unique spatial resolution. The contribution of GOCE on medium-wavelength can efficiently be combined with long-wavelength GRACE observations.

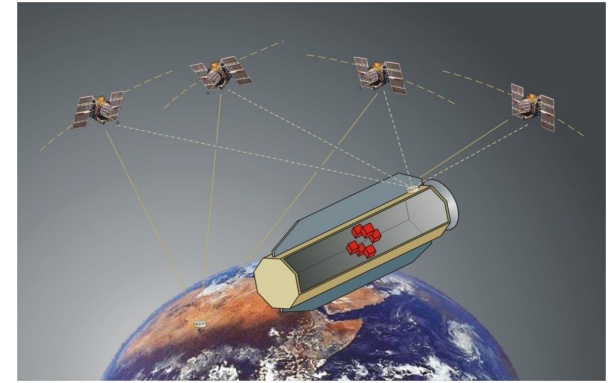
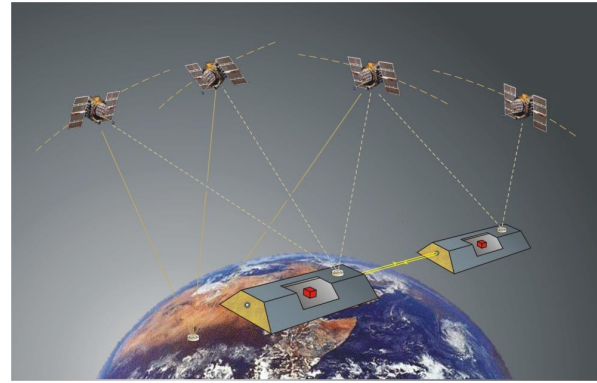
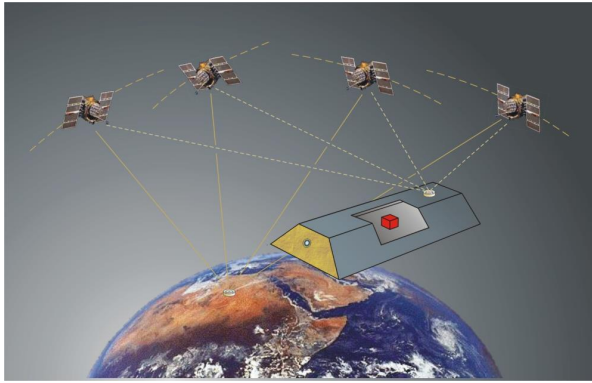
Future perspectives

Name	max. degree	spatial resolution	precision
CHAMP	70	570 km	17.27 cm
GRACE	120	330 km	18.39 cm
GOCE	250	160 km	9.02 cm
GRACE-FO	250	160 km	6.85 cm

The success of the dedicated gravity satellites calls for continuation. Particularly the GRACE-borne time series of gravity variations (with monthly resolution) is demanded to be continued.

It may be delivered by the **GRACE Follow-On** mission, which is planned to be launched in 2018.

Future perspectives



The era of CHAMP, GRACE and GOCE has nearly be gone.

Mission Elapsed Time	
Days	Hours
5694	19

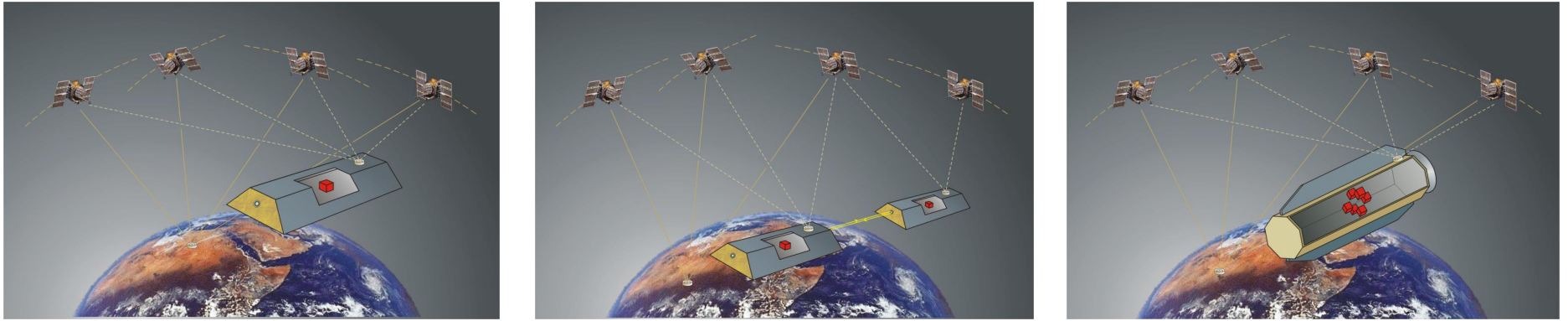
Continuation:

GRACE-FO (GRACE Follow-On)

- launch: February, 2018
- satellite: like GRACE
- orbit: like GRACE
- except: range-rate accuracy improved by 1 oom



Future satellite missions



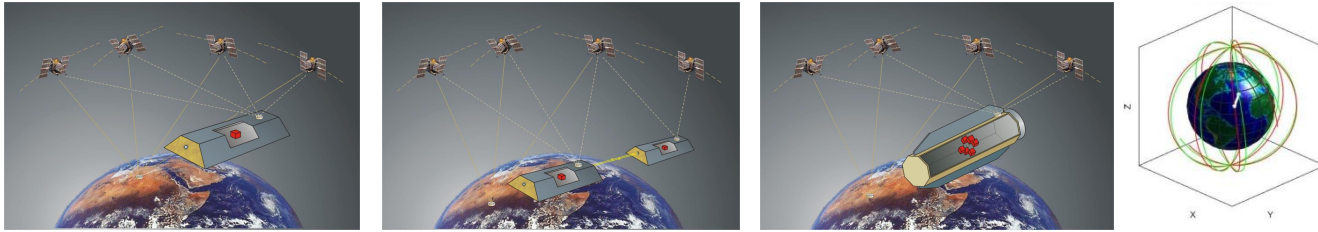
What will be after GRACE-FO?

Further concepts are under investigations

Future changes in technical limitations and perspectives:

- the range-rate observation technique may improve
- expensive satellite pair may be in the future replaced by dozen cheaper small satellites.
- etc.

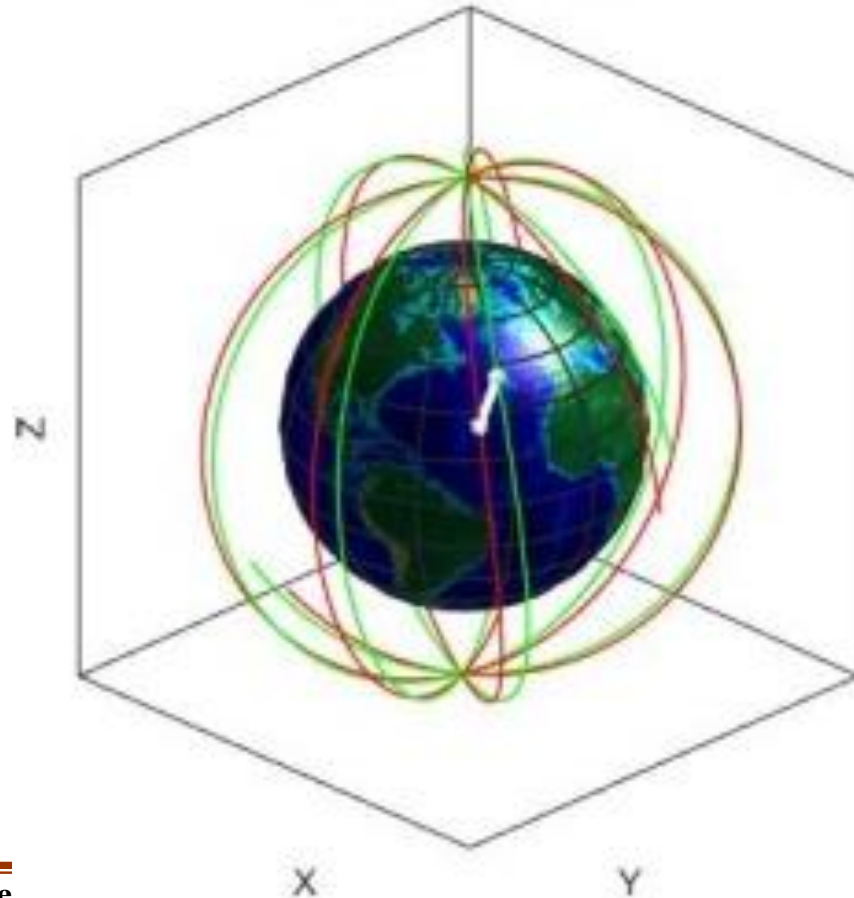
Future satellite missions



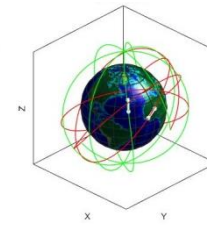
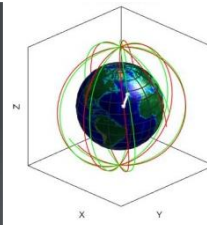
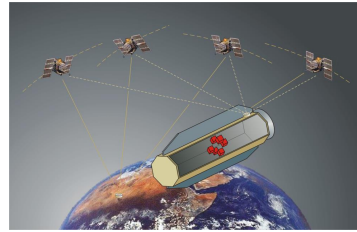
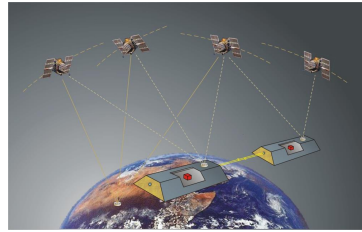
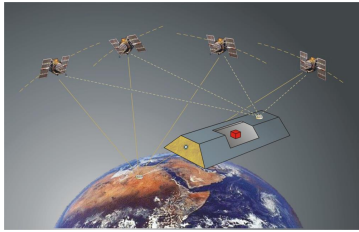
Future formations:

Pendulum

- 2 satellites
- Ω and ν differs



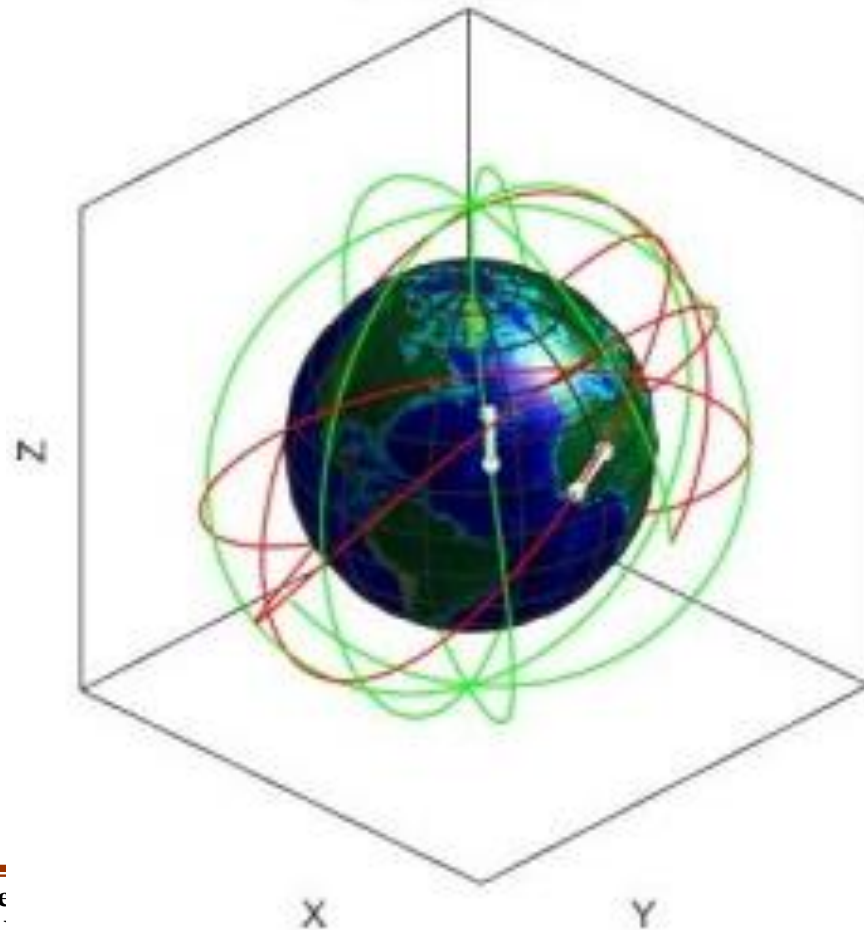
Future satellite missions



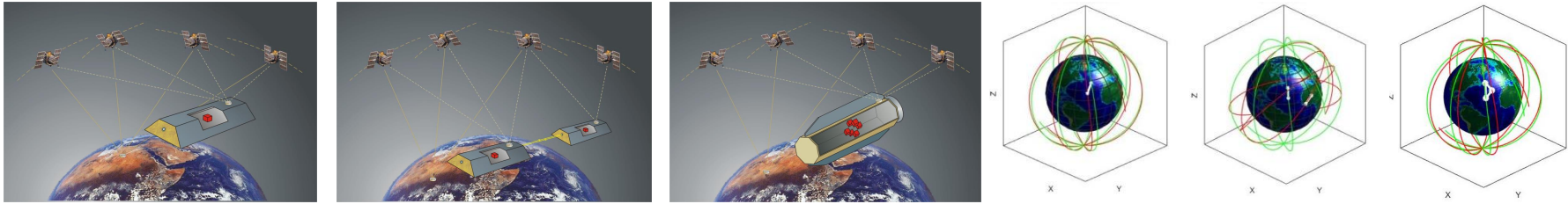
Future formations :

Bender

- 4 satellites
- 2 GRACE-pairs
- 1 pair: $i=80-90^\circ$
- 1 pair: $i=50-80^\circ$



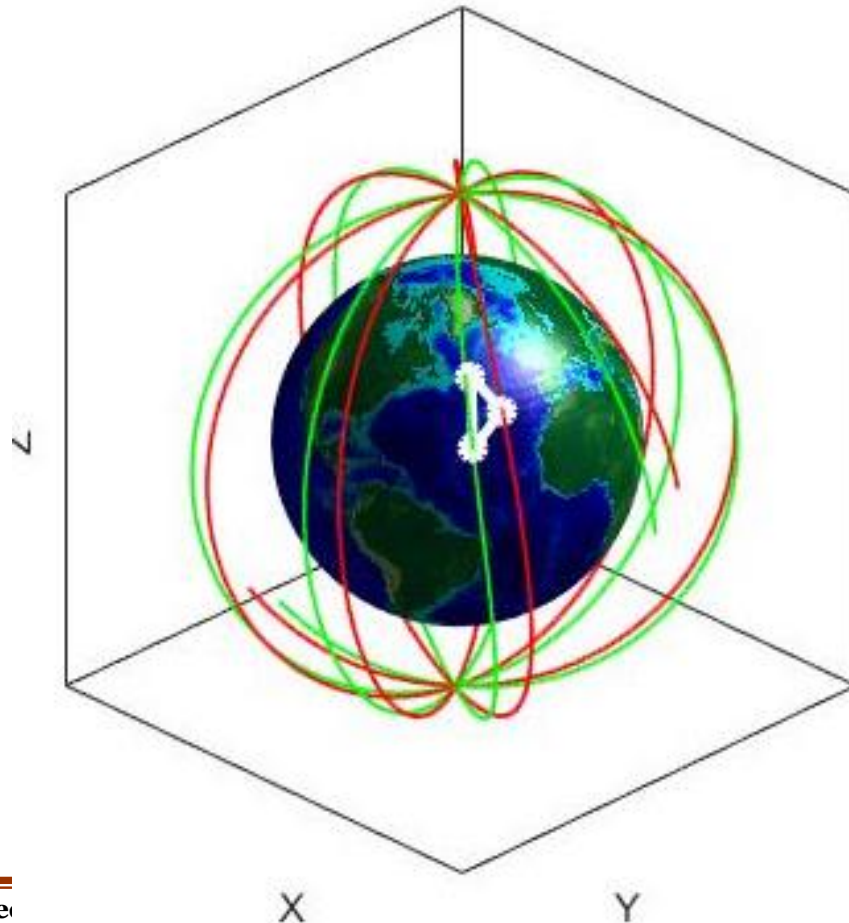
Future satellite missions



Future formations :

Tripin

- 3 satellites
- 2 of them in pair
like GRACE
- a 3rd one completes
it in to a
pendulum
formation



Dedicated gravity satellites

related issues

Issues

1. Inertial vs. Earth-fixed coordinate system
2. Involvement of models
3. Consequences of averaging

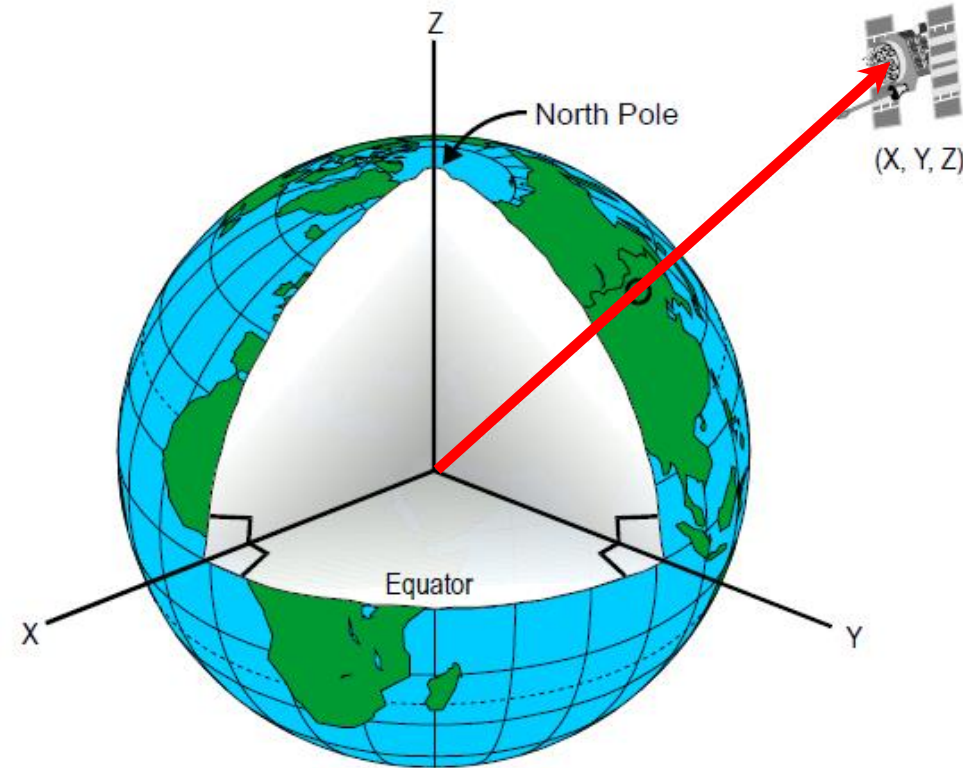
Inertial vs. Earth-fixed

Satellites are revolving around the Centre of Mass of the Earth.

The orbit of satellites is an ellipse in an **Earth-Centred Inertial** coordinate system.

Appropriate coordinate system for describing life on the surface of the Earth is **Earth-Centered Earth-Fixed** coordinate system.

Accurate transformation between them is essential!

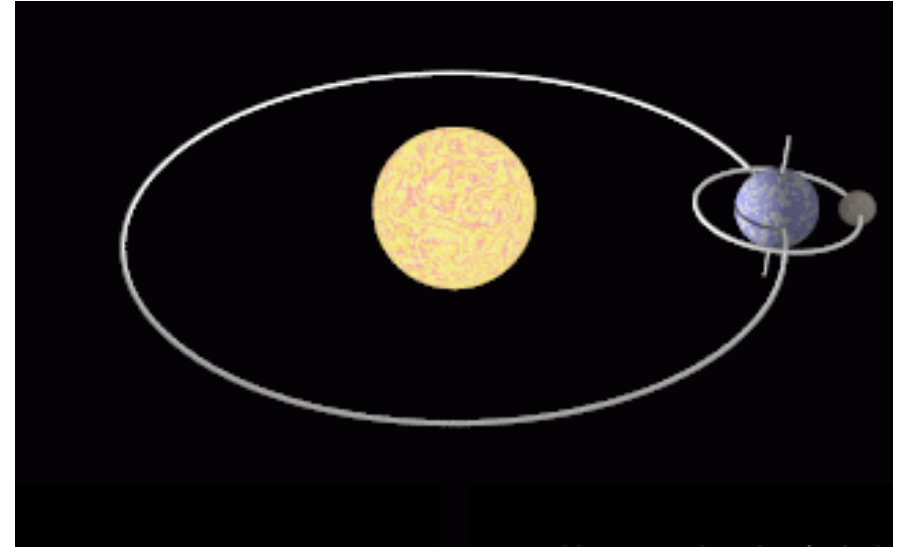


Motions of planet Earth

Determination of the Earth Orientation Parameters (EOP) is essential for processing gravity satellite data.

Main motions of the Earth:

- 1) Revolution around the Sun
- 2) Rotation around its spin axis
- 3) Precession
- 4) Nutation



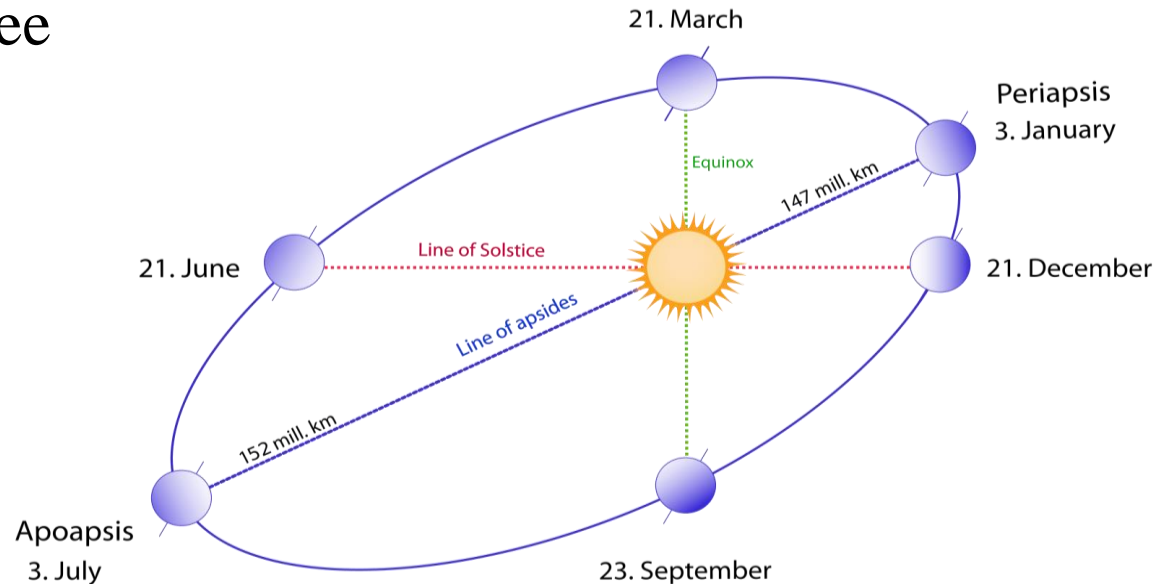
„Living on Earth may be expensive, but it includes a trip around the Sun every year for free.”

Motions of planet Earth

1) Rotation

Period: 23 hours 56 minutes 4 seconds

Axial tilt: 23.44 degree



2) Revolution

Period: 365.2422 days

Shape of the orbit: ellipse

perihelion: 147 million km

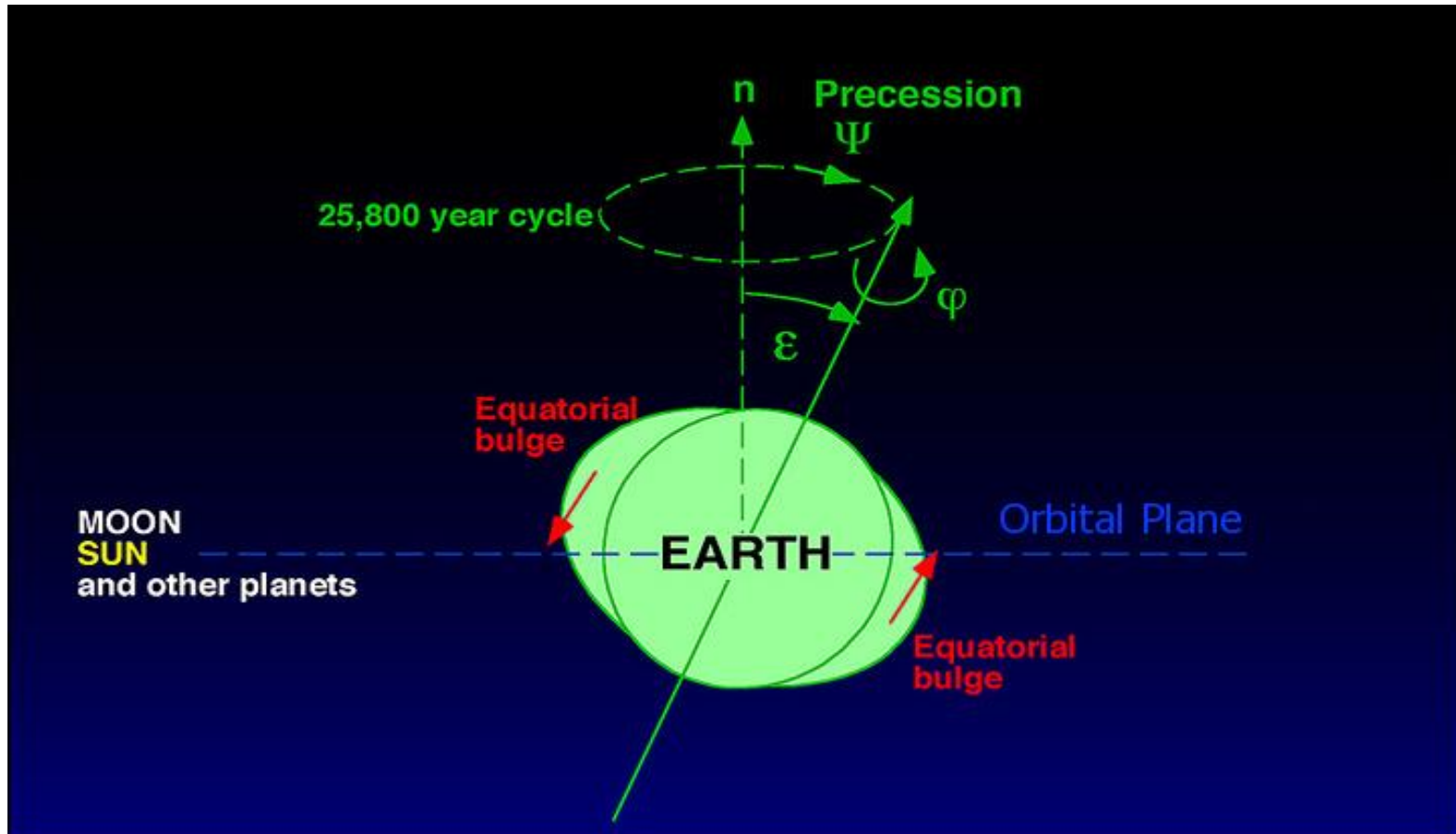
aphelion: 152 million km

mean distance: 149 597 870 700 m = 1 AU

Precession

Source: the Earth is oblate, and the Sun affects its equatorial bulge with a torque, trying to correct the axial tilt.

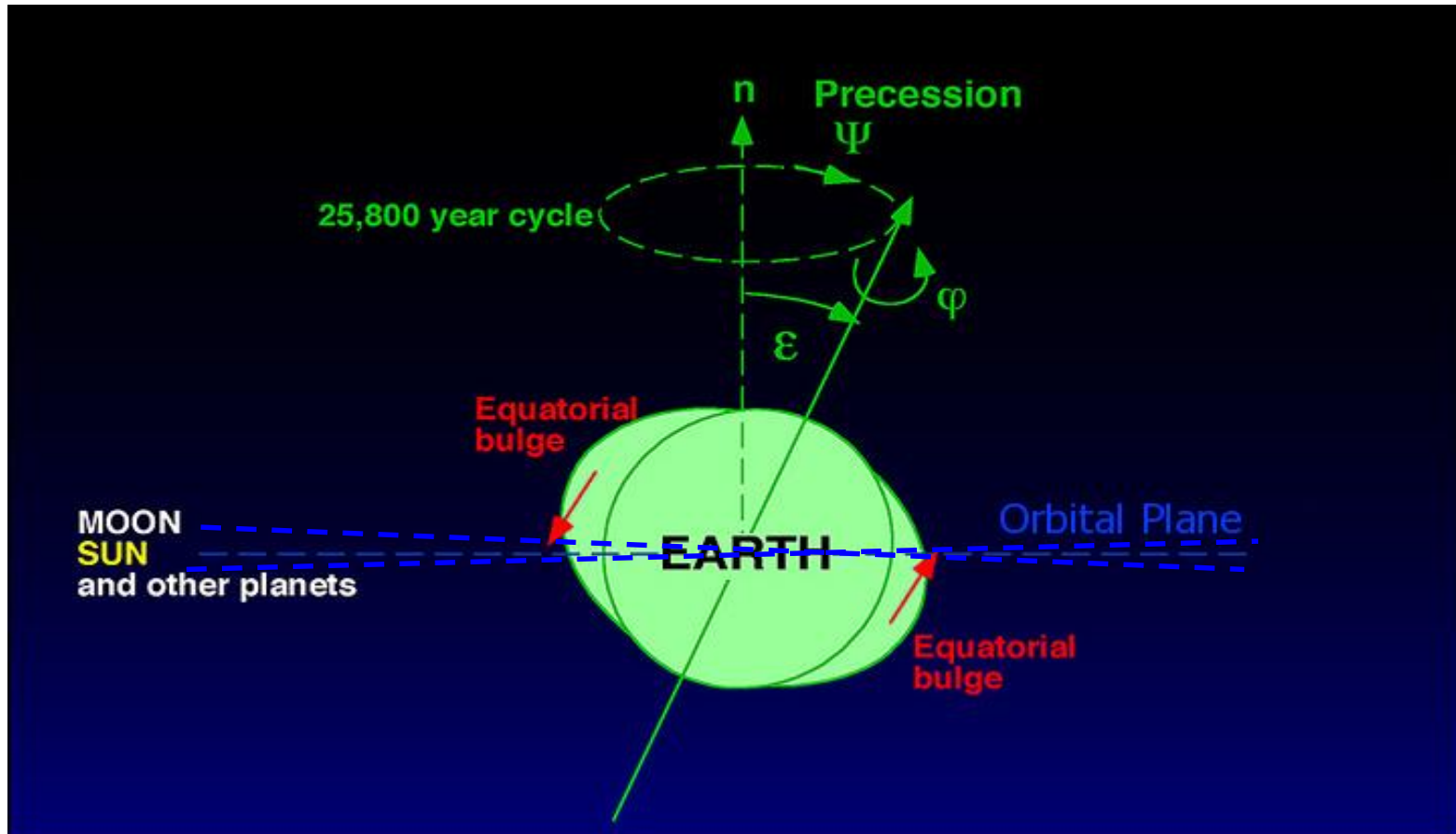
Period: appr. 26 000 years



Precession

Secondary source: the ecliptic is changing due to variations in the orbit of the other planets, varying the axial tilt of the Earth in $[22^\circ, 24.5^\circ]$.

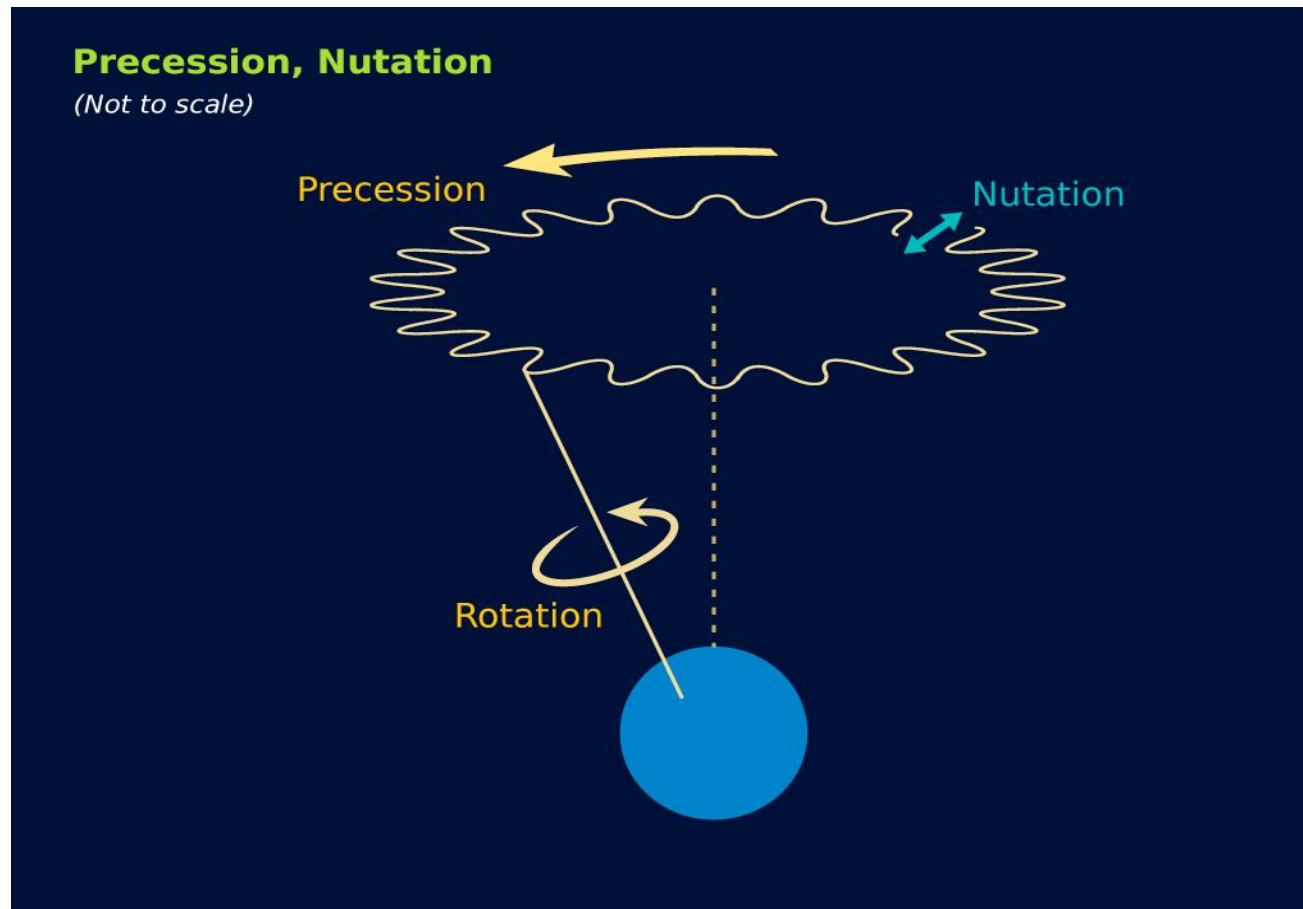
Period: appr. 40 000 years



Nutation

Source: Deviations of the precession due to the change of the relative position of the Moon and the Sun.

Periods: 18.6 years, 14 and 28 days (Moon), $\frac{1}{2}$ and 1 year (Sun)



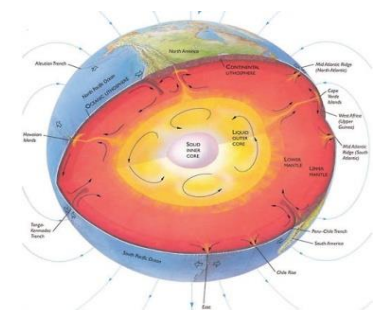
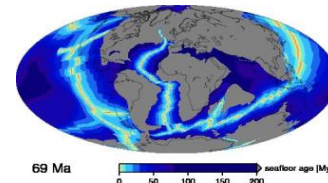
Polar motion

The Earth is a *dynamic* system.

There are mass redistribution inside and on the surface of the planet.

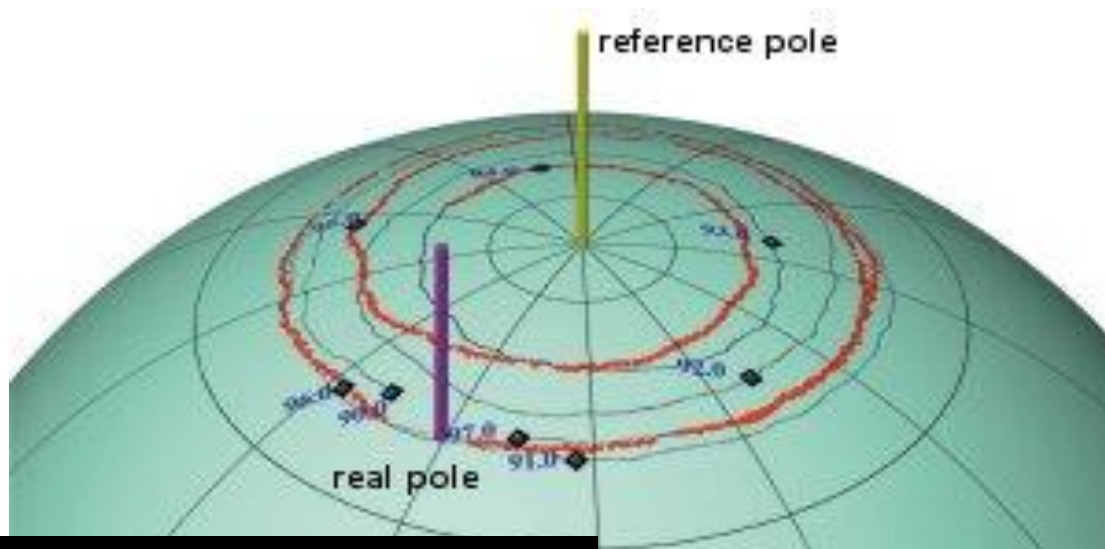
1. plate tectonics
2. mass transports of the atmosphere, hydrosphere, cryosphere and biosphere
3. mass variations of the Earth interior

These processes are constantly changing the mass distribution of the Earth, thus the inertia axis (rotational axis) is also in constant change.



Polar motion

Variations in the position of the Earth's rotation axis.

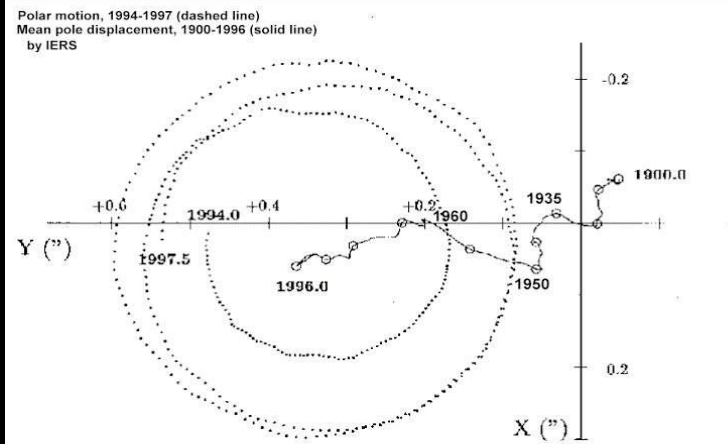
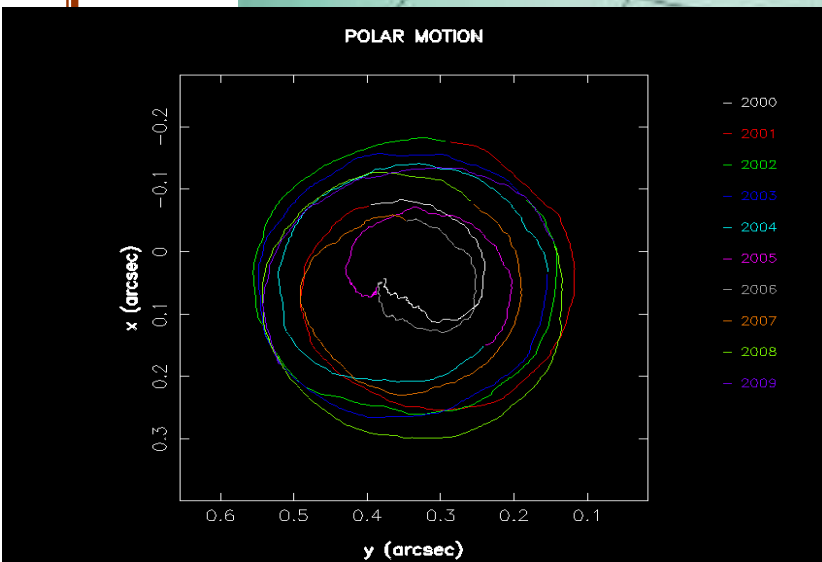


Periods:

- 12 month
- 14 month
- polar motion*
- secular
- polar wander*
- diurnal

Oppolzer terms

Component	Period [h]
K_1	23.934
O_1	25.819
P_1	24.066
ϕ_1	23.804
ψ_1	23.869
S_1	24.000



...calculated gravity satellite missions
Mostar, 19.10.2017

Motion of the planet Earth

Revolution of the Solar System: our Solar System revolves around the centre of the Milky Way

Period: 220-225 million years

Speed: 220 km/s

... Galaxies may also revolve around the centre of the Galaxy Cluster...

Summarily: The motion of the Earth from an inertial point of view looks very complex.

Q: How can we get information about this motion?

Determination of the motion of the Earth

Reference points: fix celestial bodies

Quasar: objects emitting radio-waves.

Quasars assumed to be fix in space

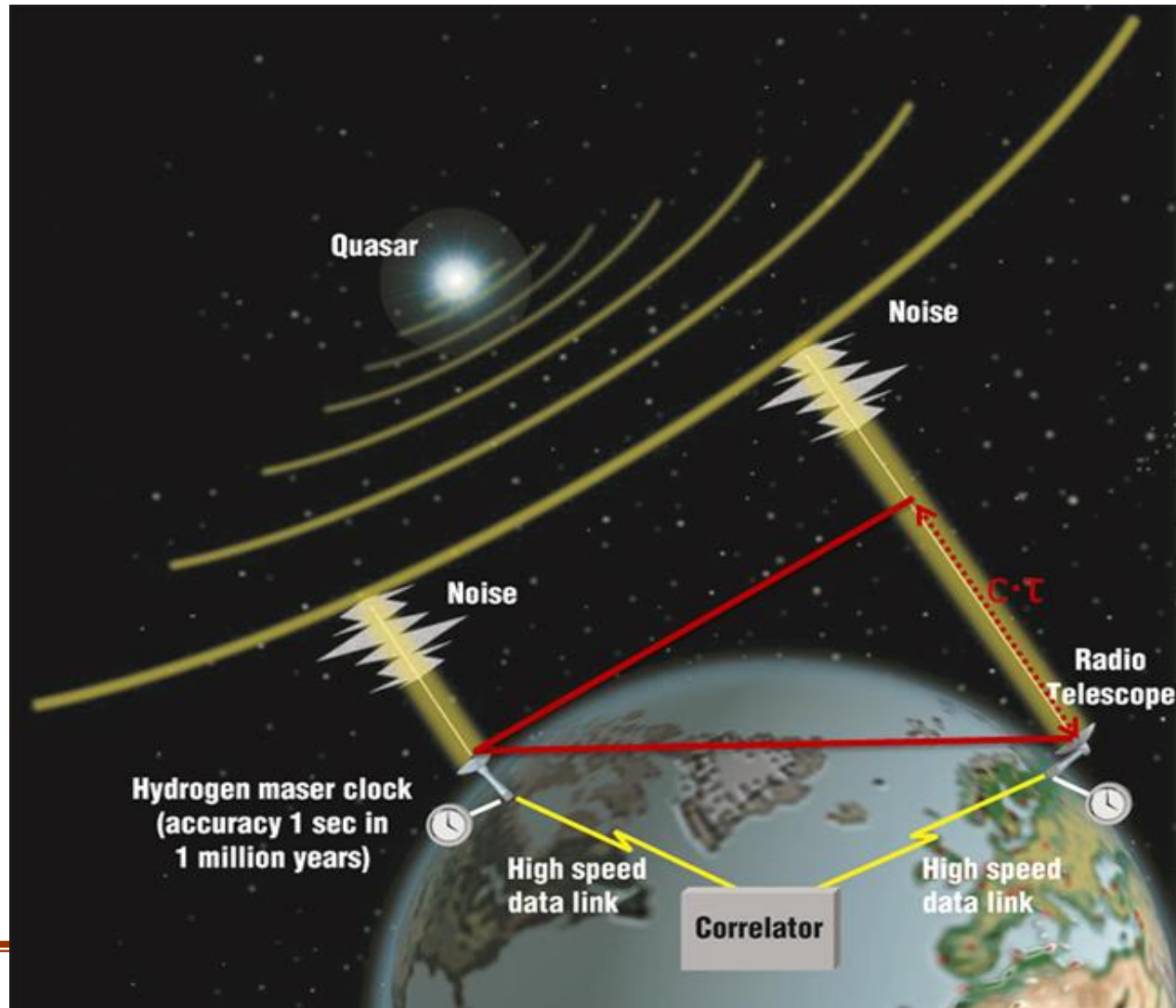
➔ they can mark a quasi-inertial coordinate system.

Measurements to quasars: VLBI (Very Long Baseline Interferometry)



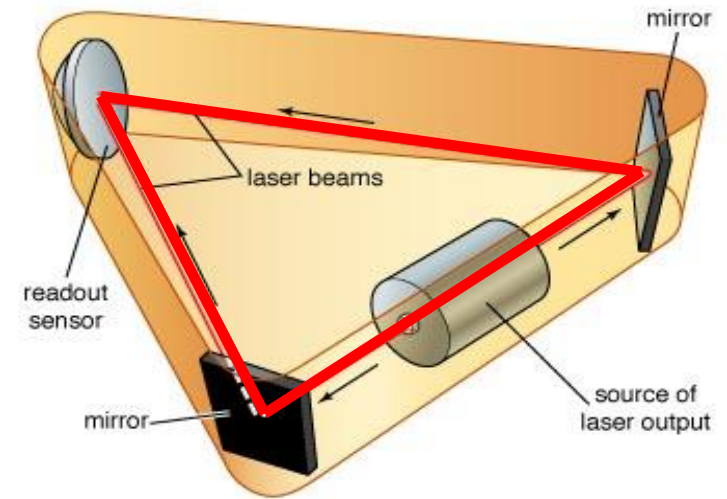
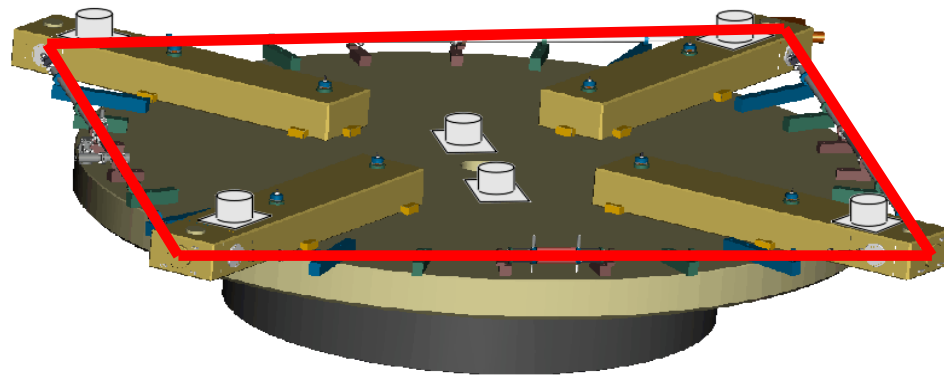
Determination of the motion of the Earth

Principle of VLBI:



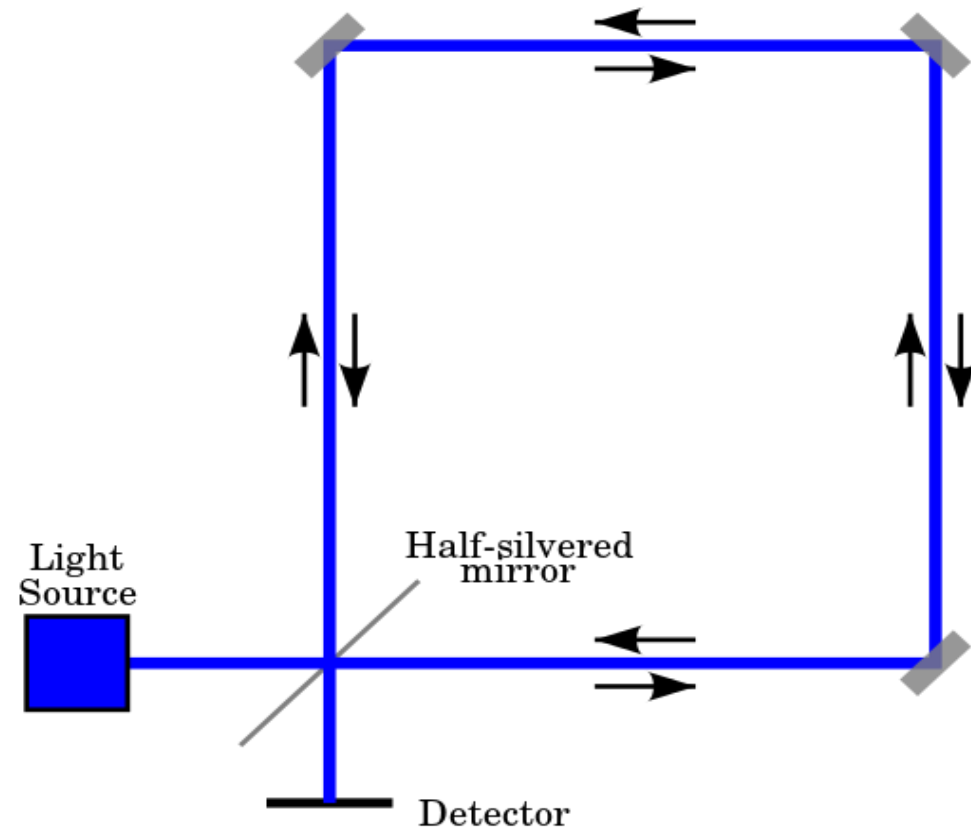
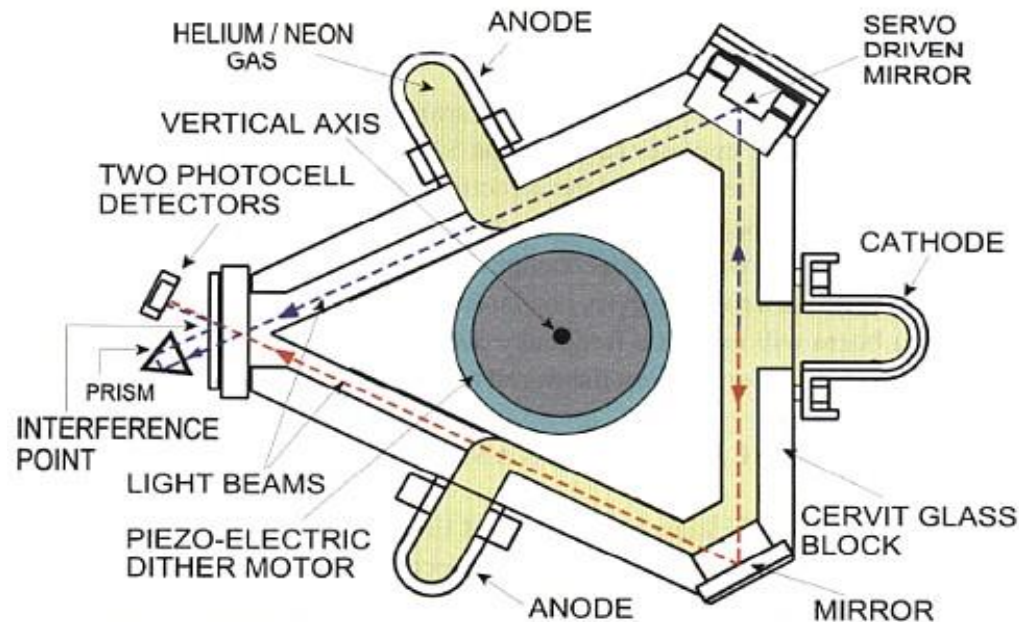
Determination of the motion of the Earth

Principle of ring lasers:



Determination of the motion of the Earth

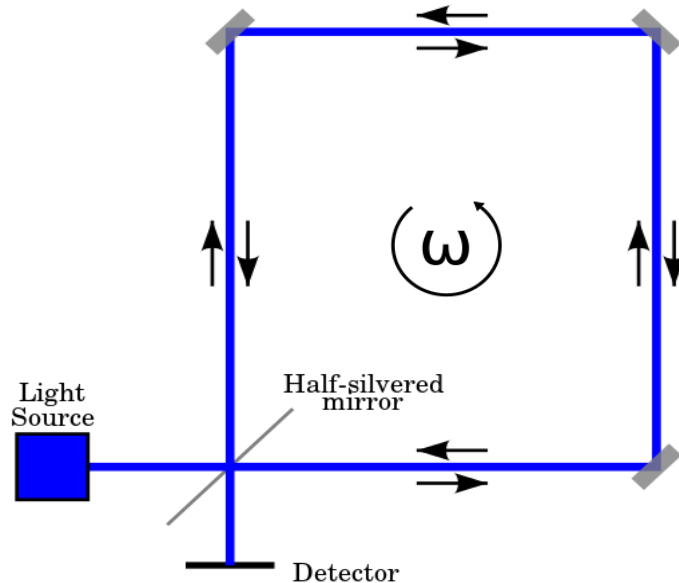
Principle of ring lasers: is based on the measurement of the Sagnac-frequency.



Determination of the motion of the Earth

Sagnac-effect: in rotating optical systems the *relative phase* or the *frequency* of a split beam (going around an area in opposite directions) is changing.

$$\delta f = \frac{4A}{\lambda P} \vec{n} \cdot \vec{\omega}$$



δf – the Sagnac frequency

A – area of the ring laser

P – periphery of the ring laser

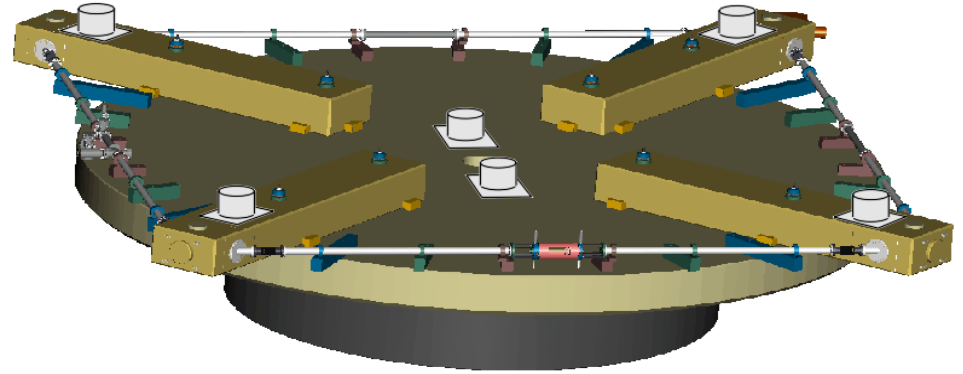
\vec{n} – normal vector of the ring laser

$\vec{\omega}$ – rotational angular velocity

Determination of the motion of the Earth

Ring lasers:

prototype instruments



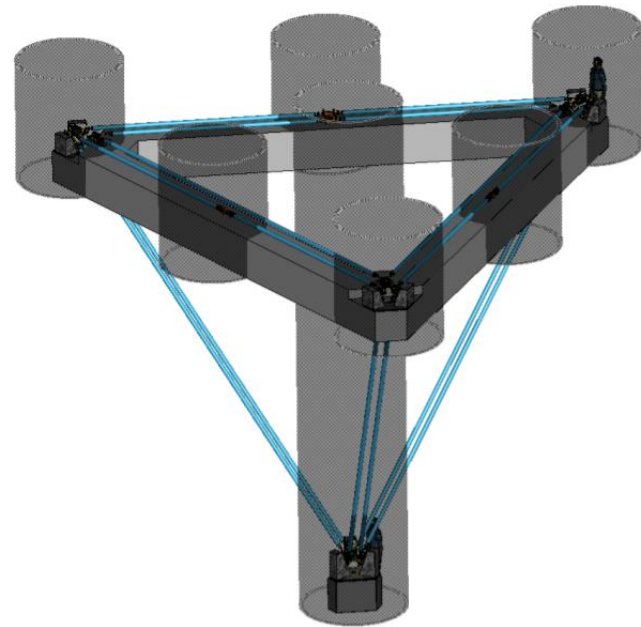
1993: C-I „Canterbury Ring”

1997: C-II

1998: G-0

2001: G „Großring”

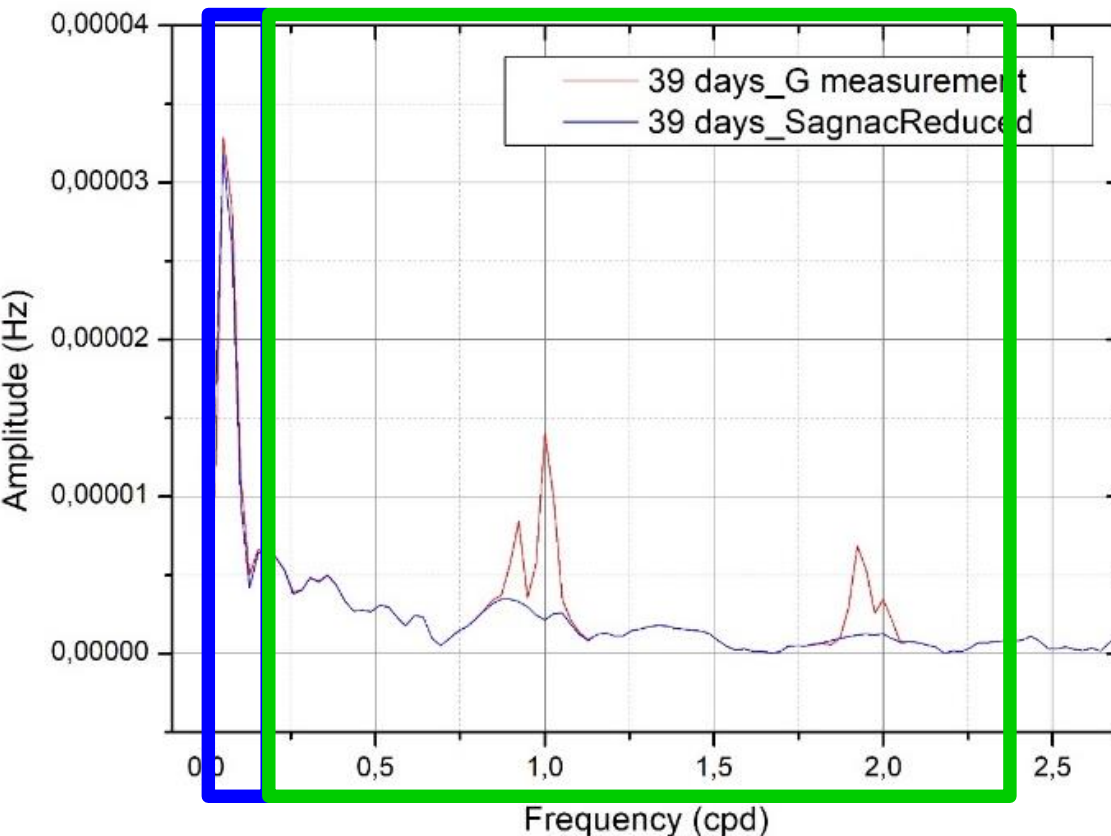
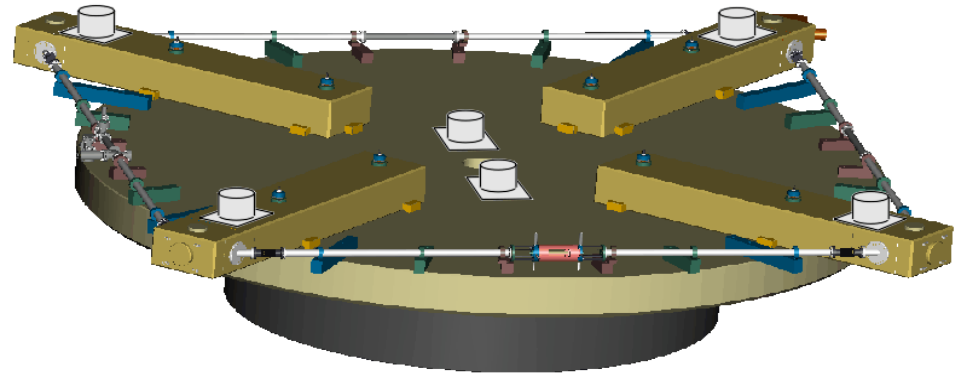
2016: ROMY Ring



Determination of the motion of the Earth

Ring lasers:

gain with ring lasers



Sub-daily periods
of Earth' motion
parameters can be
observed!

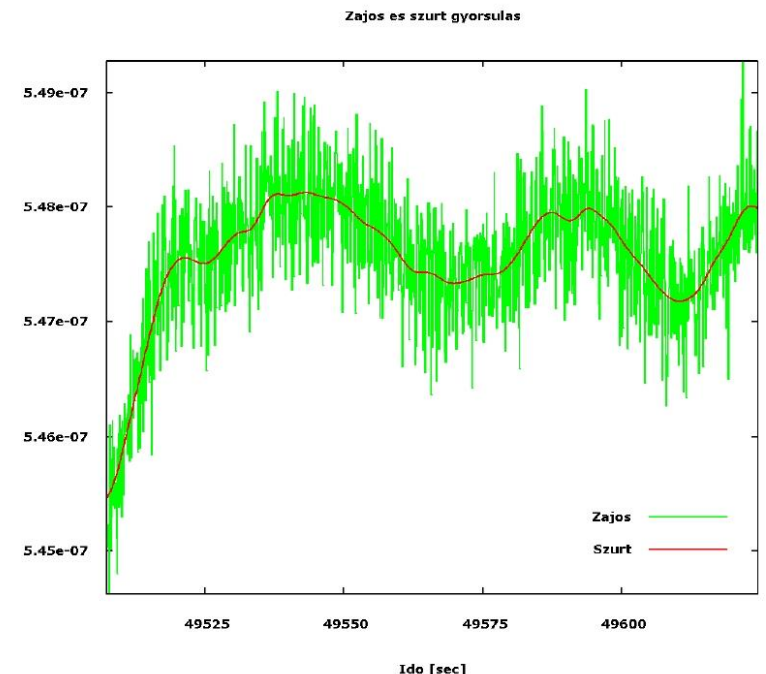
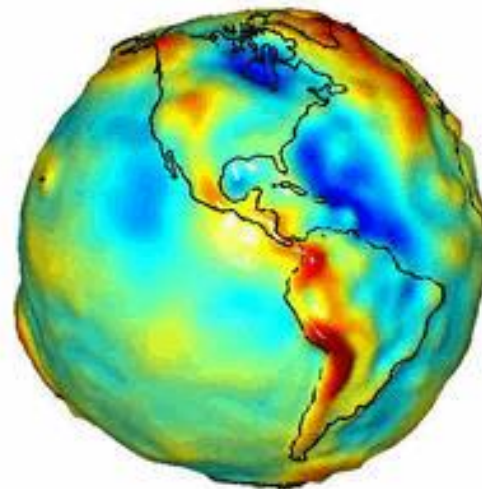
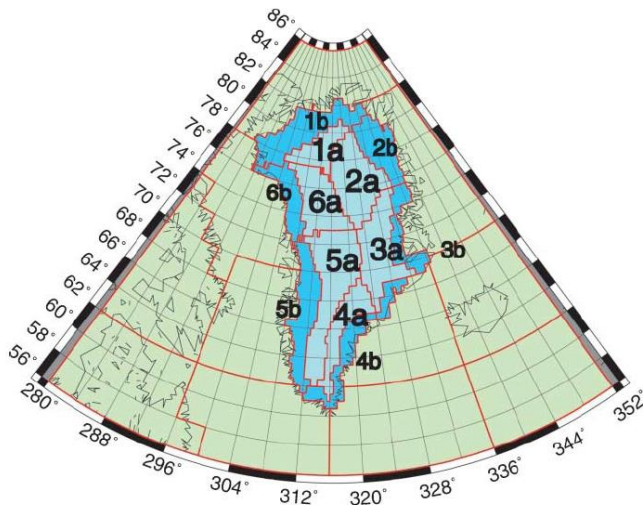
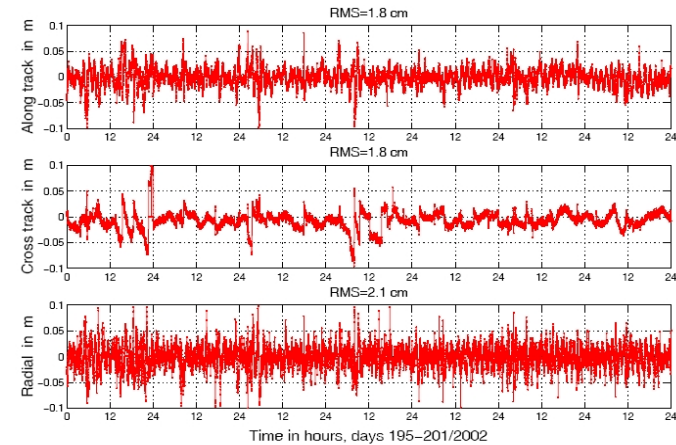
IERS EOP
ring lasers

Issues

1. Inertial vs. Earth-fixed coordinate system
- 2. Involvement of models**
3. Consequences of averaging

Processing gravity satellite observations

1. Precise Orbit Determination (POD)
based on MEASUREMENT and METHOD
2. Processing of accelerometer data
based on MEASUREMENT and METHOD
3. Gravity field determination
based on MODELS and METHOD
4. Applications of the gravity field model
based on MODELS and METHOD



Forces acting on a satellite

1. Gravity field of the Earth
2. Direct tides (gravity field of the Sun and the Moon)
based on MODEL EOP
3. Indirect tides
 - » mass variations due to the tidal forces
 - solid Earth tide based on MODEL viscosity
 - ocean tide based on MODEL ocean model
 - polar motion based on MODEL EOP
4. Non-gravitational forces based on METHOD
 - atmospheric drag
 - solar radiation pressure

Errors influencing Antarctic ice mass variation

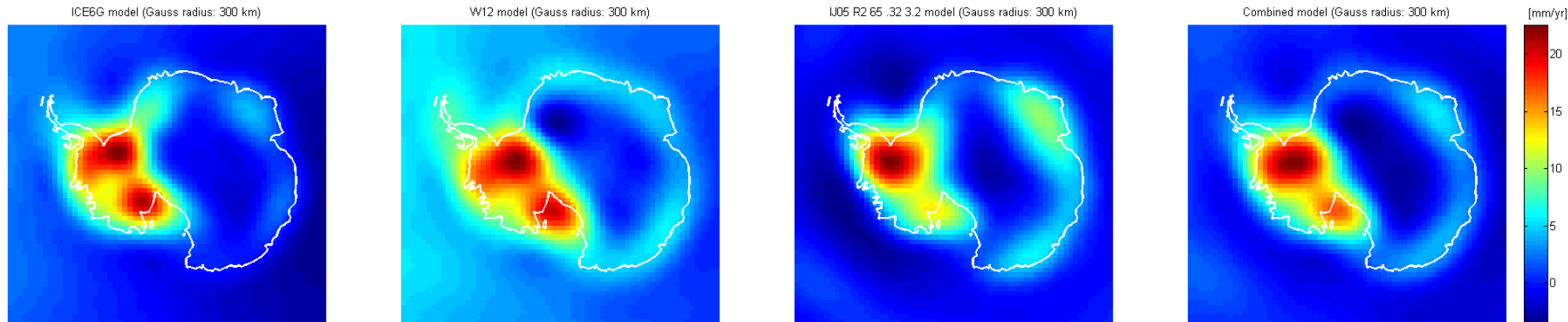
1. Separation of vertically integrated mass sources
(e.g. GIA model) MODEL dependent
- ~~2. Reduction of horizontal spatial aliasing
—(e.g. delimit regions, coasts)—~~ METHOD dependent
3. Data centre
(CSR, GFZ, JPL, etc.) MODEL dependent
4. Atmospheric correction MODEL dependent
5. Length of time span MODEL dependent
- ~~6. De-stripping method~~ METHOD dependent

Aim of the study:

Modelling **model dependent** errors of Antarctic mass change estimation.

Error estimate of Antarctic ice mass variation

1. GIA model errors



	GIA model	mean [mm/yr]	RMS [mm/yr]
1	ICE6G	5.18	± 7.89
2	W12	3.32	± 7.47
3	IJ05 R2_65_.2_1.5	2.84	± 3.52
4	IJ05 R2_65_.4_3.2	4.44	± 5.07
5	IJ05 R2_65_.32_3.2	4.31	± 4.78
6	IJ05 R2_115_.2_1.5	2.74	± 3.42
7	IJ05 R2_115_.4_3.2	4.16	± 4.83
8	IJ05 R2_115_.32_3.2	4.06	± 4.59
9	combined GIA	3.88	± 5.97

By intercomparison of frequently used GIA models, the typical difference is not less than ± 5 mm/yr.

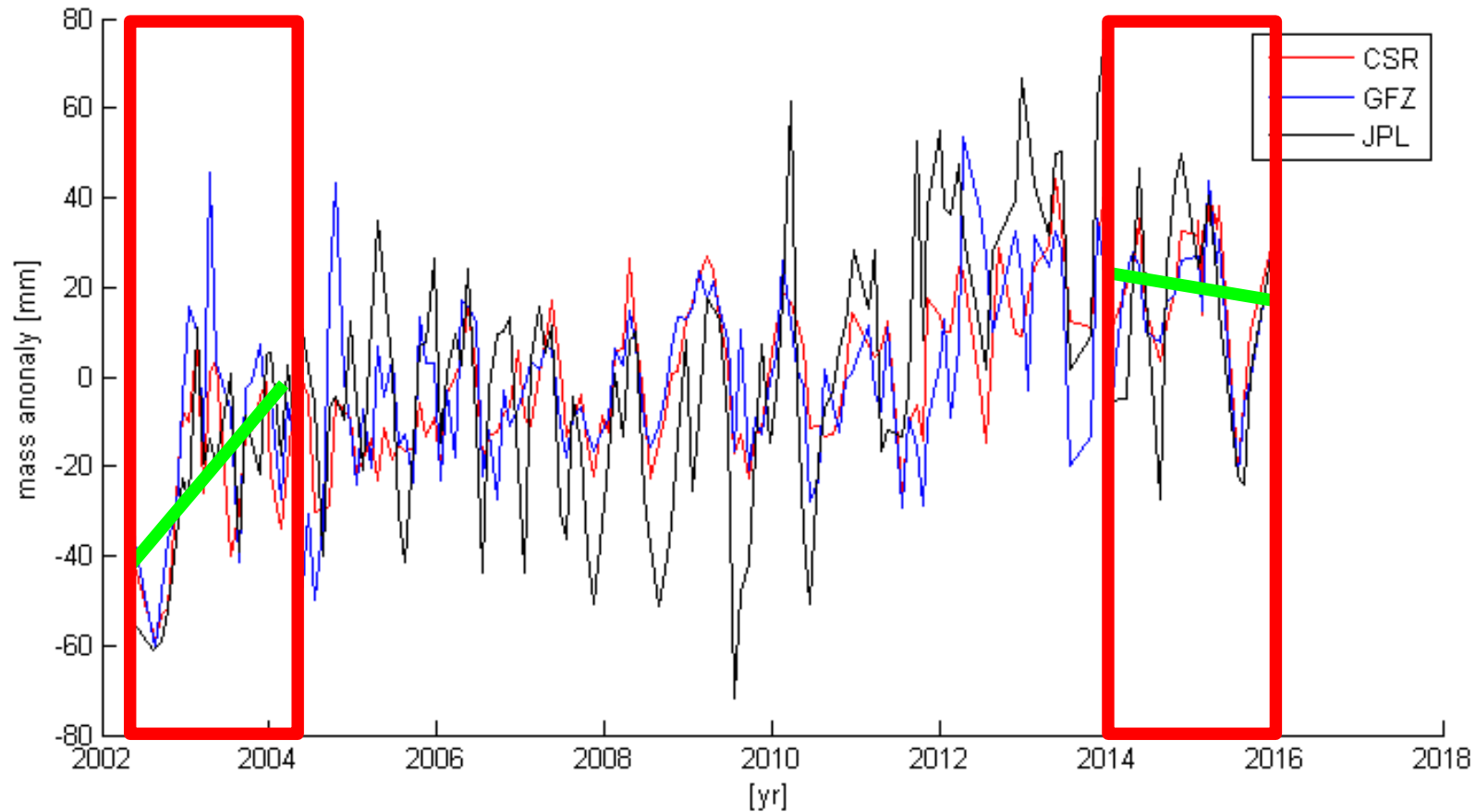
Error estimate of Antarctic ice mass variation

4. GRACE monthly solutions atmospheric correction errors over Antarctica is about $\pm 10\text{--}11$ mm/yr according to Forootan et al. (2013).



Error estimate of Antarctic ice mass variation

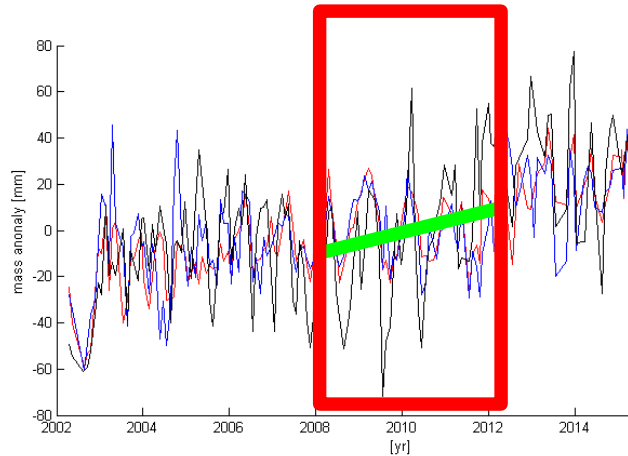
5. The error effect of the length of the time span is estimated empirically.



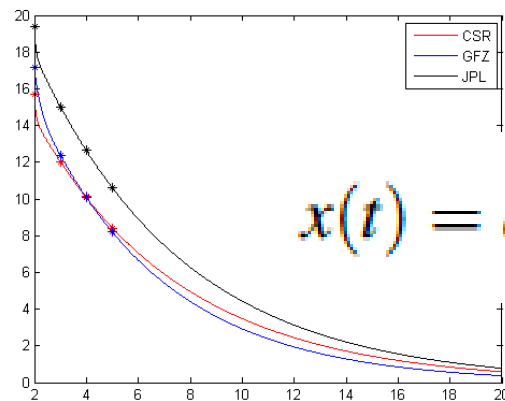
All possible trend estimates with 2, 3, 4 and 5 windows are determined.

Error estimate of Antarctic ice mass variation

5. The error effect of the length of the time span is estimated empirically.



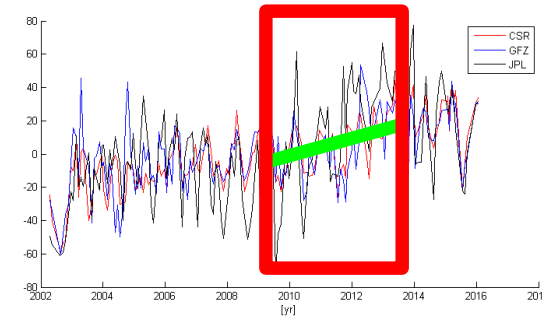
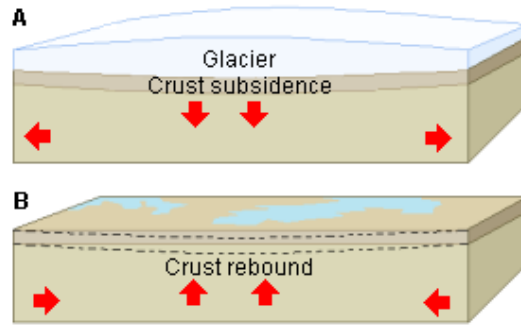
Window size	CSR	GFZ	JPL
2 years	-2.16 ± 15.73	-3.25 ± 17.18	-2.42 ± 19.41
3 years	-2.04 ± 12.00	-2.72 ± 12.38	-2.34 ± 15.01
4 years	-2.05 ± 10.13	-2.64 ± 10.07	-2.31 ± 12.66
5 years	-2.22 ± 8.41	-2.66 ± 8.20	-2.37 ± 10.59
Whole period	-2.20	-2.54	-2.28



$$x(t) = a \cdot e^{(b \cdot t)} + c \cdot e^{(d \cdot t)}$$

The extrapolation for a time span of 15 years yields an error of $\pm 1-2$ mm/yr in trend estimation.

Error estimate of Antarctic ice mass variation



GIA correction
 ± 5 mm/yr

atmospheric correction
 ± 10 mm/yr

finite length of time span
 ± 1 mm/yr

Model involved error so far (summed by error propagation law):
 ± 11.2 mm/yr

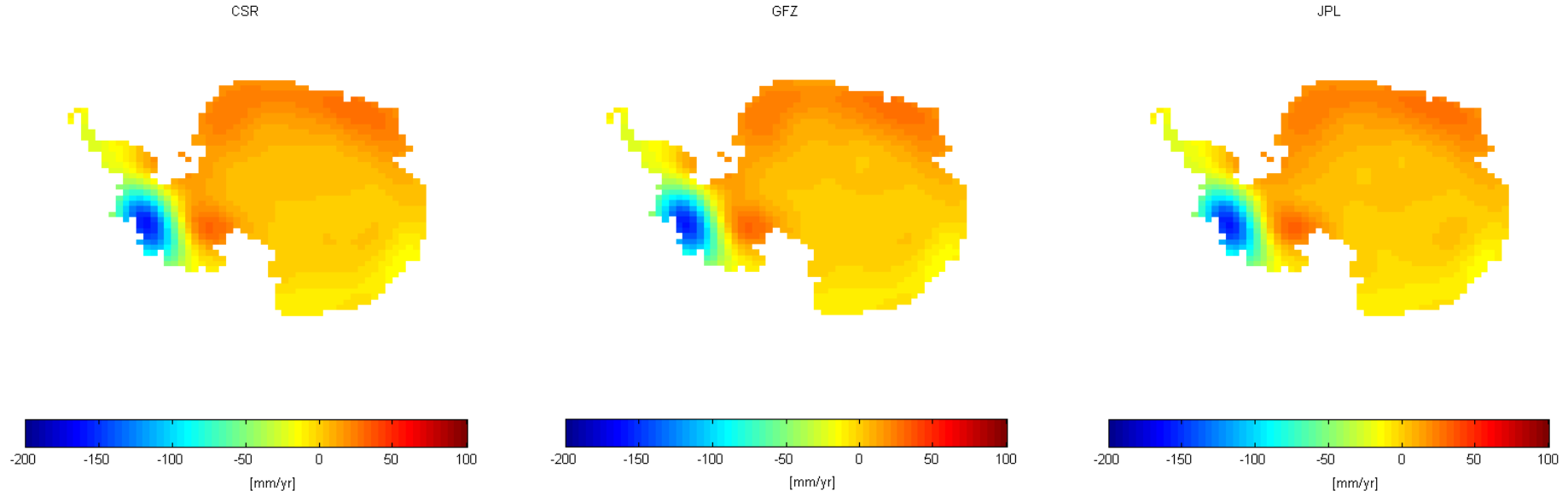
Error estimate of Antarctic ice mass variation

3. Effect of the choice of the data centre.

Investigated empirically: ice mass change estimate is reliable only if all models results in the same tendency.

$$ma(t) = A \sin(\omega_a t + \varphi_a) + B \sin(\omega_{sa} t + \varphi_{sa}) + \boxed{C} (t - t_0) + \frac{1}{2} D (t - t_0)^2 + E,$$

Linear velocity of ice mass change (melting or accumulating):



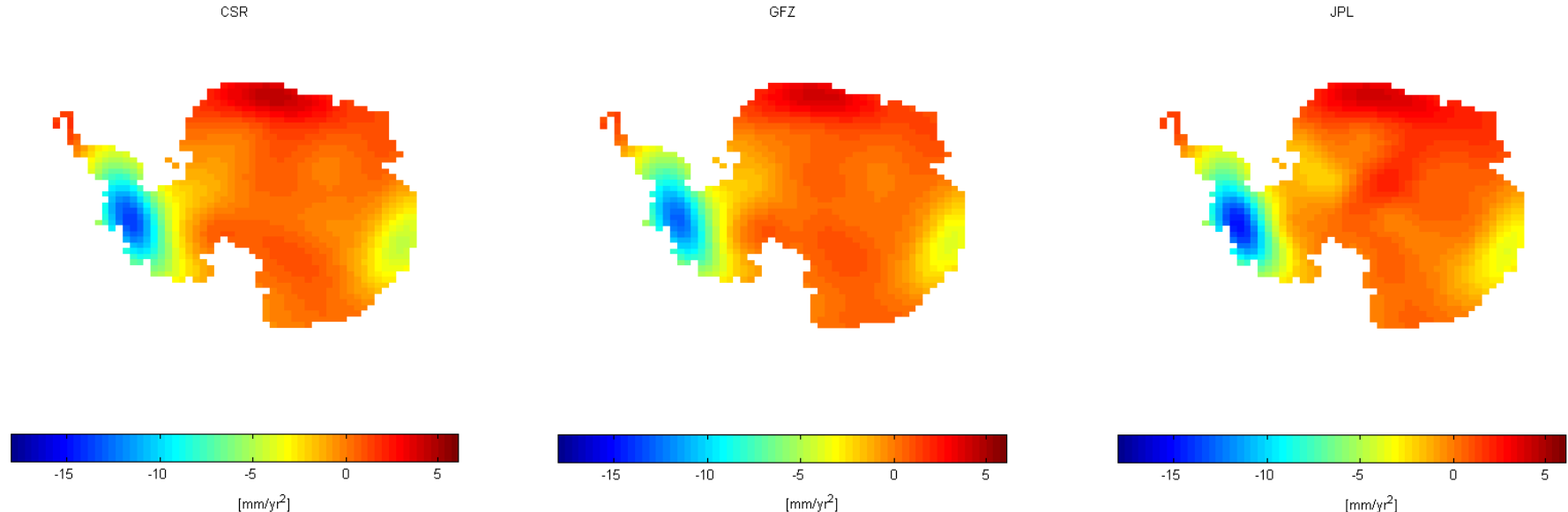
Error estimate of Antarctic ice mass variation

3. Effect of the choice of the data centre.

Investigated empirically: ice mass change estimate is reliable only if all models results in the same tendency.

$$ma(t) = A \sin(\omega_a t + \varphi_a) + B \sin(\omega_{sa} t + \varphi_{sa}) + C(t - t_0) + \boxed{D}(t - t_0)^2 + E,$$

Rate of ice mass change velocity (accelerating or decelerating):



Error estimate of Antarctic ice mass variation

3. Effect of the choice of the data centre.

Investigated empirically: ice mass change estimate is reliable only if

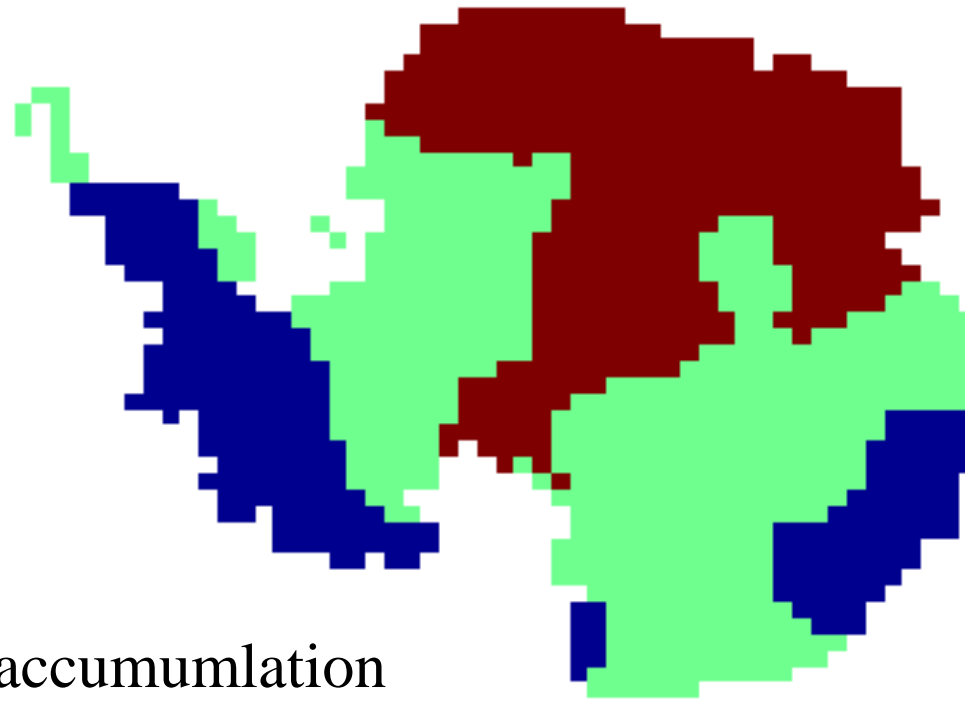





- 1 – accelerating accumulation
- 2 – decelerating accumulation
- 3 – decelerating melt
- 4 – accelerating melt

STABLE
UNSTABLE
UNSTABLE
STABLE

Error estimate of Antarctic ice mass variation

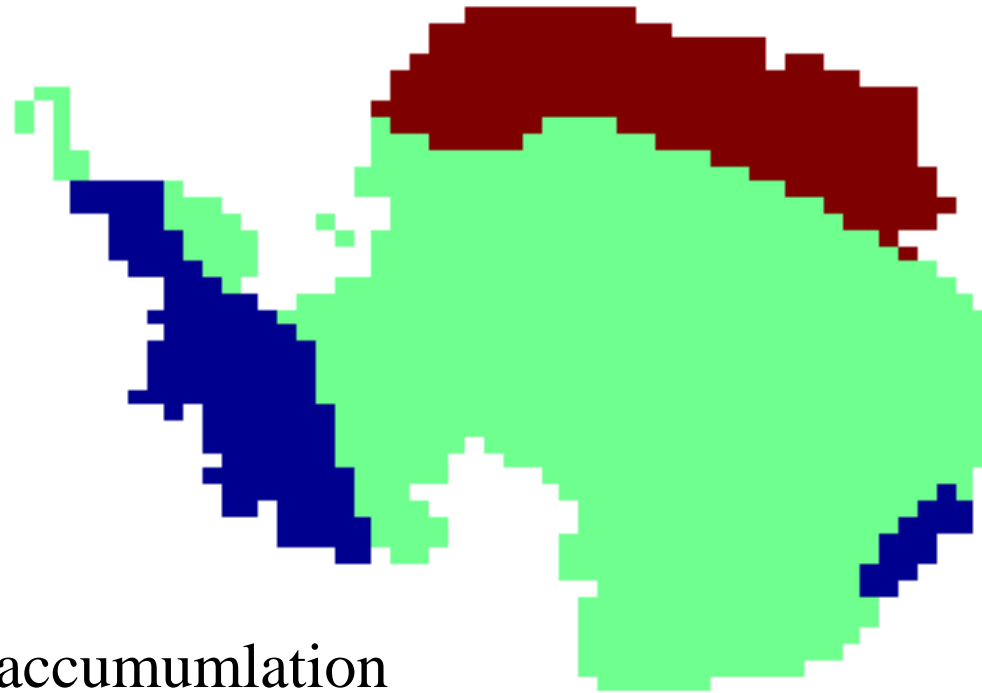
Summed model error (GIA model, atmosphere, time span): ± 11.2 mm/yr



-  – accelerating accumulation
-  – unstable process
-  – accelerating melt

Error estimate of Antarctic ice mass variation

Disregarding methodological errors, concentrating on model errors only, at most regions of Antarctica the reliability of the derived ice mass variation is found to be **uncertain**.



- accelerating accumulation
- unstable process
- accelerating melt

Error estimate of Antarctic ice mass variation

Acta Geod Geophys
DOI 10.1007/s40328-016-0185-1



ORIGINAL STUDY

Uncertainty of GRACE-borne long periodic and secular ice mass variations in Antarctica

Annamária Kiss¹ · Lóránt Földvály^{2,3}

Received: 8 April 2016 / Accepted: 14 September 2016
© Akadémiai Kiadó 2016

Abstract Glacial ice mass balance of Antarctica can be observed by the twin satellites of the gravity recovery and climate experiment (GRACE). The gravity fields with monthly resolution enable efficient detection of annual, long periodic and secular variations. The present study delivers an error estimation of the long-periodic and secular variations by determining the linear trend of the observed surface mass anomaly series. Among the error sources, the error of the timing of the trend fitting, the error of the glacial isostatic adjustment correction, and the error of the atmospheric correction of the GRACE monthly solutions are discussed. The investigation concludes that apart from West Antarctica, Wilkes Land, Queen Maud Land and Enderby Land no reliable trend estimates of ice mass variation can be expected, thus any results should be treated with care.

Keywords GRACE · Antarctica · Gravity variation · Ice mass balance · Error analysis

1 Introduction

According to the estimate by Williams and Ferrigno (1988), a quarter-century ago the Antarctic ice sheet has consisted 30,109,800 km³ volume of permanent ice over an area of 13,586,400 km². This is a huge amount of frozen water meaning 91.49 % of the total frozen water content of the Earth. The more recent Bedmap2 model (Fretwell et al. 2013) has provided an up to date estimate of the Antarctic ice sheet. According to these projects,

Annamária Kiss
kiss.annamaria@epito.bme.hu

¹ Department of Geodesy and Surveying, Budapest University of Technology and Economics, Műgyesetem rkp 3 KM 26, 1111 Budapest, Hungary

² Altha Regia Technical Faculty, Óbuda University, Budapest, Hungary

³ Geodetic and Geophysical Institute, Research Centre for Astronomical and Earth Sciences, Hungarian Academy of Science, Budapest, Hungary

Published online: 23 September 2016



For more details see:

Kiss, A., Földvály, L.:

Uncertainty of GRACE-borne long periodic and secular ice mass variations in Antarctica

Acta Geodaetica et Geophysica

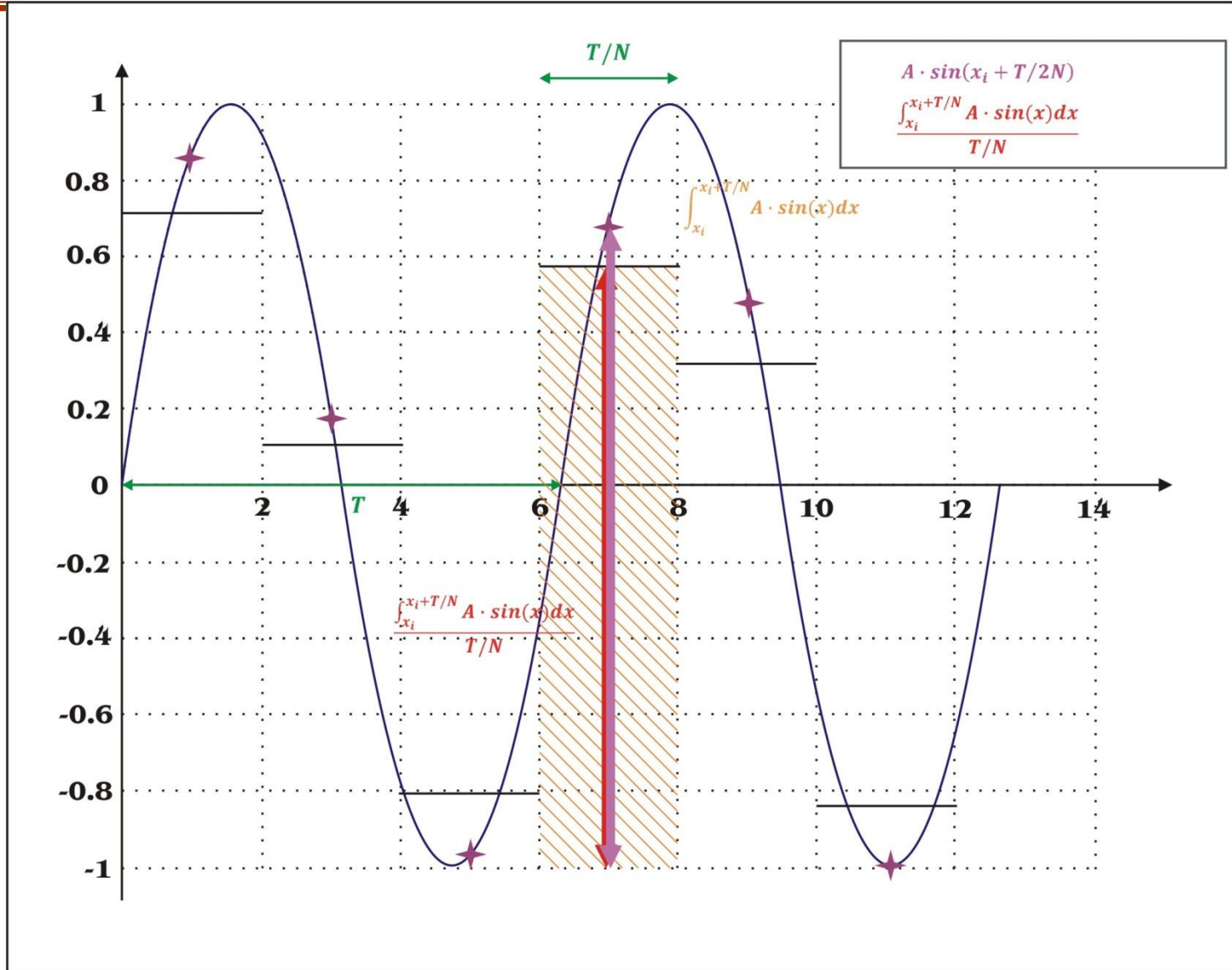
DOI: 10.1007/s40328-016-0185-1

(available online, in print)

Issues

1. Inertial vs. Earth-fixed coordinate system
2. Involvement of models
3. Consequences of averaging

Consequences of averaging



Consequences of averaging

Background:

$$f_{\text{obs.}}(x_i + \pi/N) = \frac{\int_{x_i}^{x_i + 2\pi/N} A \cdot \sin(x) dx}{\frac{2\pi}{N}}$$

$$f(x_i + \pi/N) = A \cdot \sin(x_i + \pi/N)$$

Consequences of averaging

Background:

$$\begin{aligned} \frac{f\left(x_i + \frac{\pi}{N}\right)}{f_{\text{obs.}}\left(x_i + \frac{\pi}{N}\right)} &= \frac{A \cdot \sin\left(x_i + \frac{\pi}{N}\right)}{\frac{\int_{x_i}^{x_i + \frac{2\pi}{N}} A \cdot \sin(x) dx}{\int_{x_i}^{x_i + \frac{2\pi}{N}} dx}} = \frac{\sin\left(x_i + \frac{\pi}{N}\right) \cdot \frac{2\pi}{N}}{\int_{x_i}^{x_i + \frac{2\pi}{N}} \sin(x) dx} = \\ &= \frac{\sin\left(x_i + \frac{\pi}{N}\right) \cdot \frac{2\pi}{N}}{2 \cdot \sin\left(x_i + \frac{\pi}{N}\right) \cdot \sin\frac{\pi}{N}} = \frac{\frac{\pi}{N}}{\sin\frac{\pi}{N}} \end{aligned}$$

Consequences of averaging

De-smoothing factor:

$$F(N) = \frac{f(x_i + \pi/N)}{f_{\text{obs.}}(x_i + \pi/N)} = \frac{1}{\text{sinc} \frac{\pi}{N}}$$

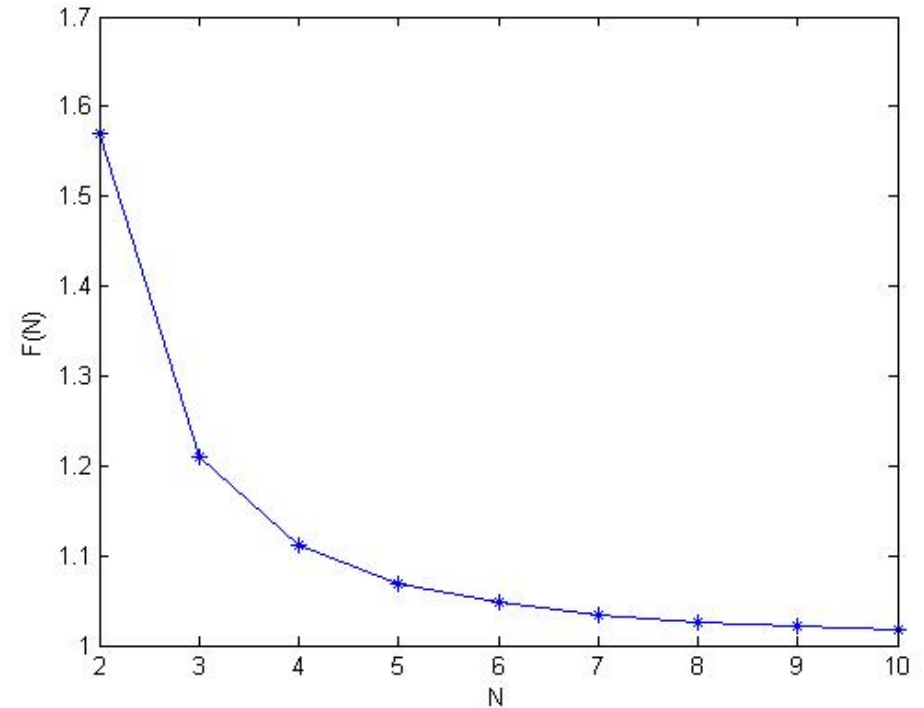
Does the smoothing effect of the averaging affects processing of geodetic observations?

Consequences of averaging

Impact of averaging:

N	$F(N)$	Error in %
2	1,5708	57,08%
3	1,2092	20,92%
4	1,1107	11,07%
5	1,0690	6,90%
6	1,0472	4,72%
7	1,0344	3,44%
8	1,0262	2,62%
9	1,0206	2,06%
10	1,0166	1,66%
11	1,0137	1,37%
12	1,0115	1,15%
24	1,0029	0,29%
48	1,0007	0,07%

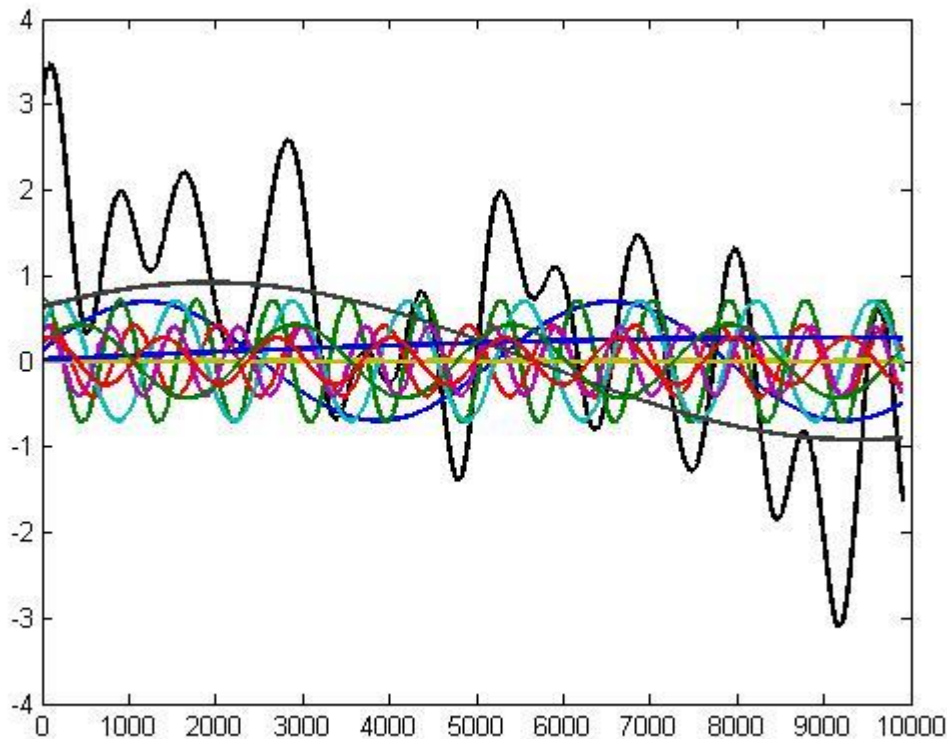
$$F(N) = \frac{f(x_i + \pi/N)}{f_{\text{obs.}}(x_i + \pi/N)} = \frac{1}{\text{sinc} \frac{\pi}{N}}$$



Consequences of averaging

Generalization of the de-smoothing formula

$$F(N) = \frac{f(x_i + \pi/N)}{f_{\text{obs.}}(x_i + \pi/N)} = \frac{1}{\text{sinc} \frac{\pi}{N}}$$



Fourier transform:

$$f(x) = \sum A_c \sin(f_c t + \varphi_c)$$

Consequences of averaging

Generalization of the de-smoothing formula

$$F(N) = \frac{f(x_i + \pi/N)}{f_{\text{obs.}}(x_i + \pi/N)} = \frac{1}{\text{sinc} \frac{\pi}{N}}$$

Factor F_c belonging to f_c :

$$F_c = \frac{1}{\text{sinc} \frac{\pi f_c}{f_o}}$$

where $f_c = \frac{1}{T/N}$ and $f_o = \frac{1}{T}$

Fourier transform:

$$f(x) = \sum A_c \sin(f_c t + \varphi_c)$$

$$f(x) = \sum F_c A_c \sin(f_c t + \varphi_c)$$

Application of de-smoothing for geodesy




$$F(N) = \frac{f(x_i + \pi/N)}{f_{\text{obs.}}(x_i + \pi/N)} = \frac{1}{\text{sinc} \frac{\pi}{N}}$$

1. Temporal variations of gravity
2. Satellite-borne observations
3. Spherical harmonic synthesis and analysis
4. Digital Terrain Models

Application of de-smoothing for geodesy

Temporal variations of gravity:

- 
1. Temporal variations of gravity
 2. Satellite-borne observations
 3. Spherical harmonic synthesis, analysis
 4. Digital Terrain Models

Periodic variations:

$$f(t) = A \sin(\omega t + \varphi) + Bt + C$$

Used for the monthly solutions of GRACE:

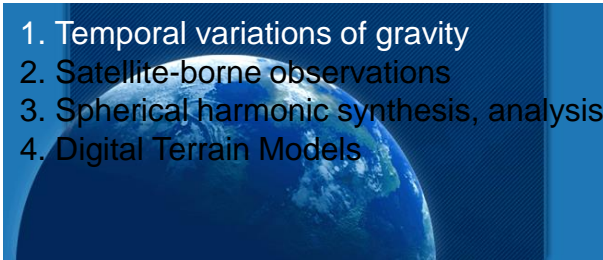
$$f(t) = A_1 \sin(\omega_1 t + \varphi_1) + A_2 \sin(\omega_2 t + \varphi_2) + A_3 t$$

T = 1 year yields N=12 samplings

T = 1/2 year yields N=6 samplings

Application of de-smoothing for geodesy

Temporal variations of gravity:

- 
1. Temporal variations of gravity
 2. Satellite-borne observations
 3. Spherical harmonic synthesis, analysis
 4. Digital Terrain Models

$$f(t) = A_1 \sin(\omega_1 t + \varphi_1) + A_2 \sin(\omega_2 t + \varphi_2) + A_3 t$$

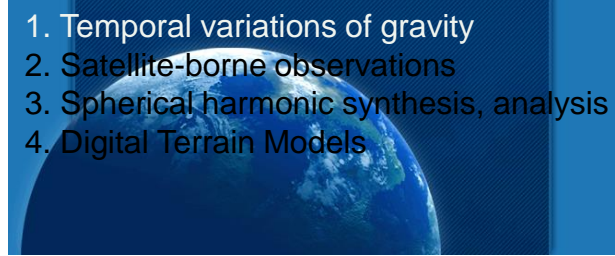
replaced to

$$f(t) = \mathit{sinc}\left(\frac{\pi}{12}\right) A_1 \sin(\omega_1 t + \varphi_1) \\ + \mathit{sinc}\left(\frac{\pi}{6}\right) A_2 \sin(\omega_2 t + \varphi_2) + A_3 t$$

Application of de-smoothing for geodesy

Temporal variations of gravity:

N	$F(N)$	Error in %
2	1,5708	57,08%
3	1,2092	20,92%
4	1,1107	11,07%
5	1,0690	6,90%
6	1,0472	4,72%
7	1,0344	3,44%
8	1,0262	2,62%
9	1,0206	2,06%
10	1,0166	1,66%
11	1,0137	1,37%
12	1,0115	1,15%
24	1,0029	0,29%
48	1,0007	0,07%

- 
1. Temporal variations of gravity
 2. Satellite-borne observations
 3. Spherical harmonic synthesis, analysis
 4. Digital Terrain Models

Antarctic ice mass loss

period	without	with
annual	11.06 kg/m ²	11.19 kg/m ²
semi-ann.	4.83 kg/m ²	5.06 kg/m ²

Application of de-smoothing for geodesy

Satellite-borne observations:

1. Temporal variations of gravity
2. Satellite-borne observations
3. Spherical harmonic synthesis, analysis
4. Digital Terrain Models

The velocity of satellites is some km/s



Observations along a satellite's orbit can not be referred to any exact location in space.



Application of de-smoothing for geodesy

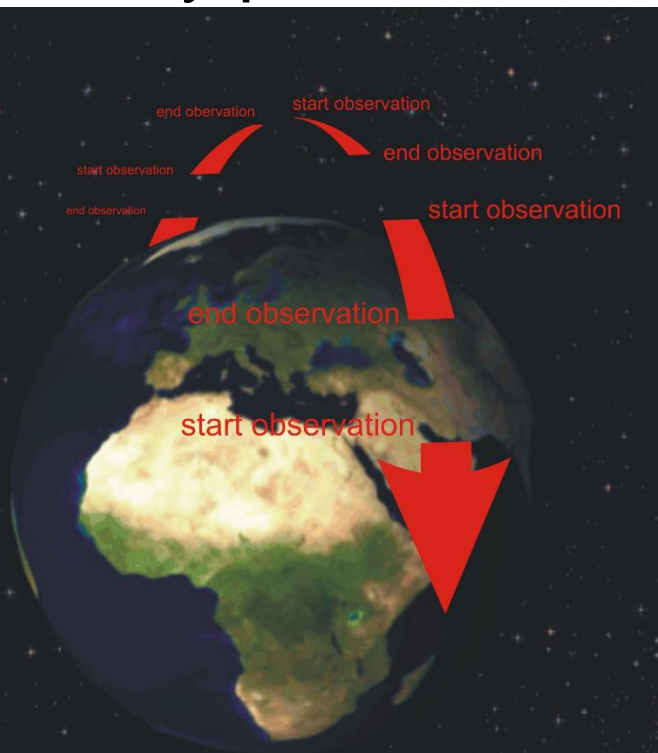
Satellite-borne observations:

1. Temporal variations of gravity
2. Satellite-borne observations
3. Spherical harmonic synthesis, analysis
4. Digital Terrain Models

Nearly polar orbits are often applied for geosciences (except: navigational satellites). Thus on-board observations are affected by N-S-N periodicity.



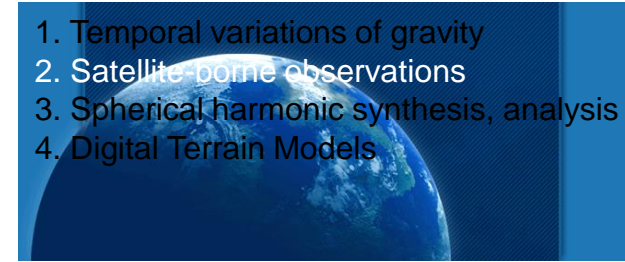
Usually the largest variation can be found at the orbital frequency.



Application of de-smoothing for geodesy

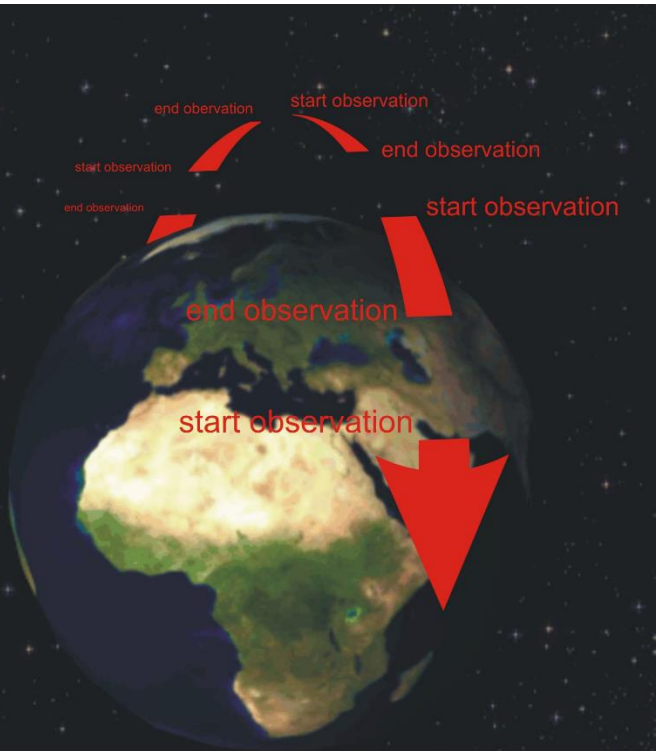
Satellite-borne observations:

1. Temporal variations of gravity
2. Satellite-borne observations
3. Spherical harmonic synthesis, analysis
4. Digital Terrain Models



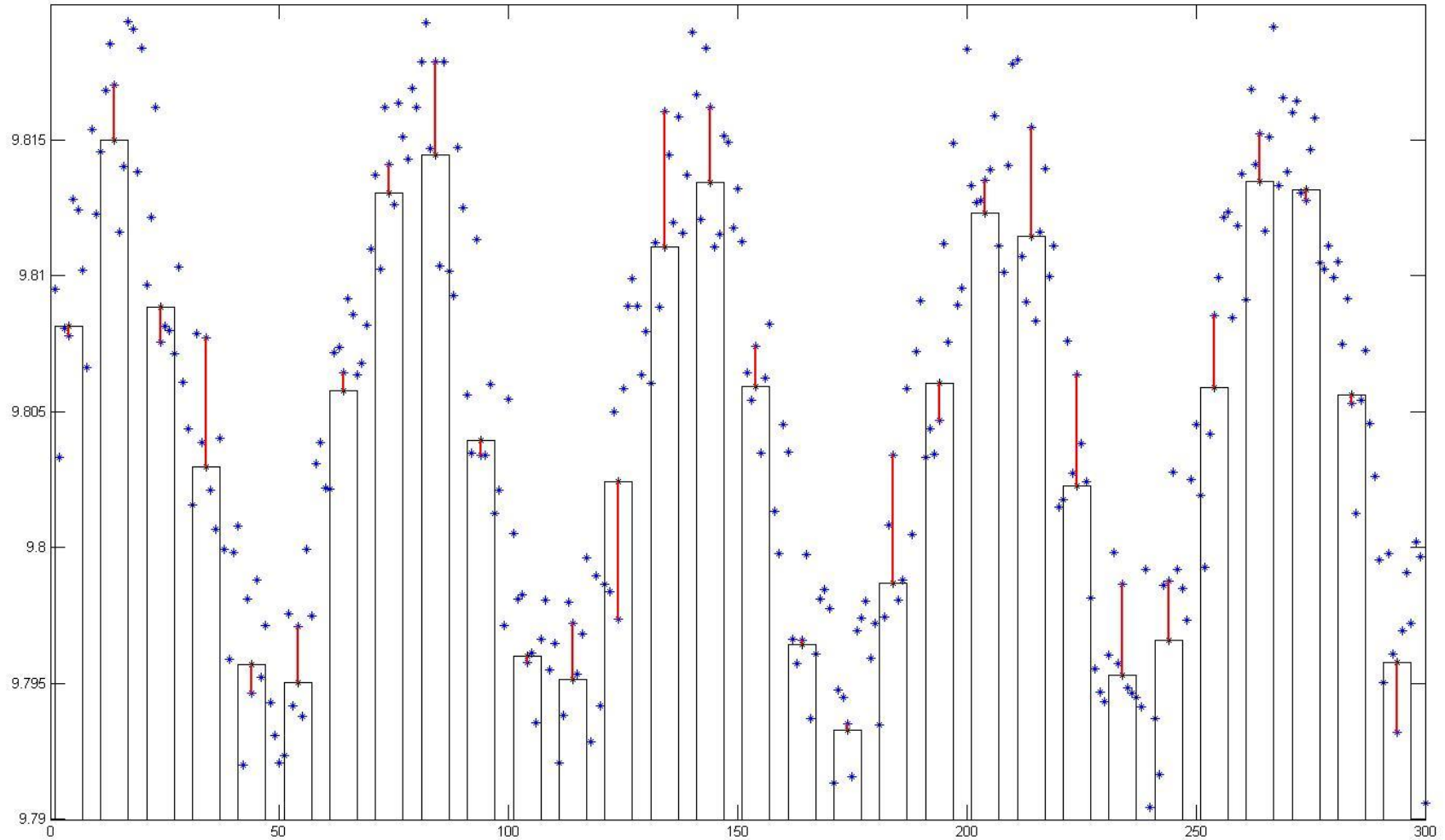
Correction only for the orbital frequency may be sufficient.

$$F_c = \frac{1}{\text{sinc} \frac{\pi f_{\text{orbit}}}{f_o}} = \frac{1}{\text{sinc} \frac{\pi \Delta t}{T_{\text{orbit}}}}$$



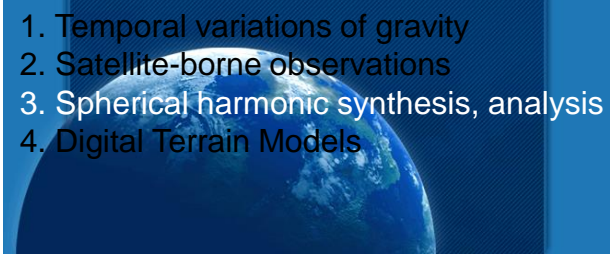
Application of de-smoothing for geodesy

- signal (periodic+noise)
- averaging
- | difference



Application of de-smoothing for geodesy

Spherical harmonic synthesis / analysis

- 
1. Temporal variations of gravity
 2. Satellite-borne observations
 3. Spherical harmonic synthesis, analysis
 4. Digital Terrain Models

Spherical harmonic
representation of potential:

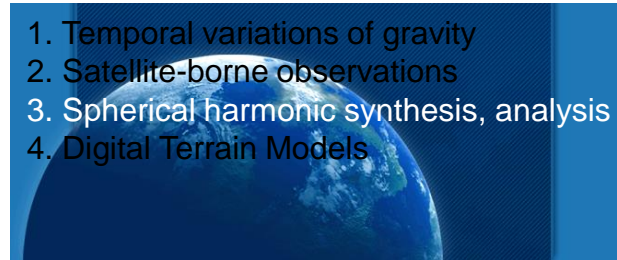
$$V = \frac{kM}{r} \sum_l \left(\frac{R}{r}\right)^l \sum_m (\bar{C}_{lm} \cos m\lambda + \bar{S}_{lm} \sin m\lambda) \bar{P}_{lm}(\psi)$$

Analysis: using a model $(\bar{C}_{lm}, \bar{S}_{lm}, kM)$ to calculate potential (or $T, N, \Delta g, T_i, T_{ij}$, etc.) at an arbitrary r, ψ, λ .

Synthesis: determination of a model $(\bar{C}_{lm}, \bar{S}_{lm}, kM)$ based on observations $(T, N, \Delta g, T_i, T_{ij})$ at r, ψ, λ .

Application of de-smoothing for geodesy

Spherical harmonic synthesis / analysis

- 
1. Temporal variations of gravity
 2. Satellite-borne observations
 3. Spherical harmonic synthesis, analysis
 4. Digital Terrain Models

Spherical harmonic
representation of potential:

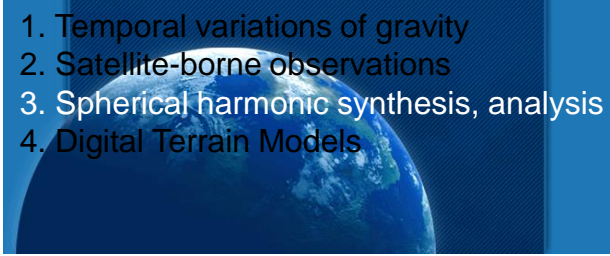
$$V = \frac{kM}{r} \sum_l \left(\frac{R}{r}\right)^l \sum_m (\bar{C}_{lm} \cos m\lambda + \bar{S}_{lm} \sin m\lambda) \bar{P}_{lm}(\psi)$$

Frequent inconsistency in practice:

1. pixel (block) averages used as point data.
2. point-wise grid data referred to blocks.

Application of de-smoothing for geodesy

Spherical harmonic synthesis / analysis

- 
1. Temporal variations of gravity
 2. Satellite-borne observations
 3. Spherical harmonic synthesis, analysis
 4. Digital Terrain Models

Properly:

1. pixel (block) averages use point-wisely:

$$V = \frac{kM}{r} \sum_l \left(\frac{R}{r}\right)^l \sum_m F_{\psi\lambda} (\bar{C}_{lm} \cos m\lambda + \bar{S}_{lm} \sin m\lambda) \bar{P}_{lm}(\psi)$$

2. using point-wise grid data to blocks:

$$V = \frac{kM}{r} \sum_l \left(\frac{R}{r}\right)^l \sum_m \frac{1}{F_{\psi\lambda}} (\bar{C}_{lm} \cos m\lambda + \bar{S}_{lm} \sin m\lambda) \bar{P}_{lm}(\psi)$$

Application of de-smoothing for geodesy

Spherical harmonic synthesis / analysis

Spherical harmonic representation:

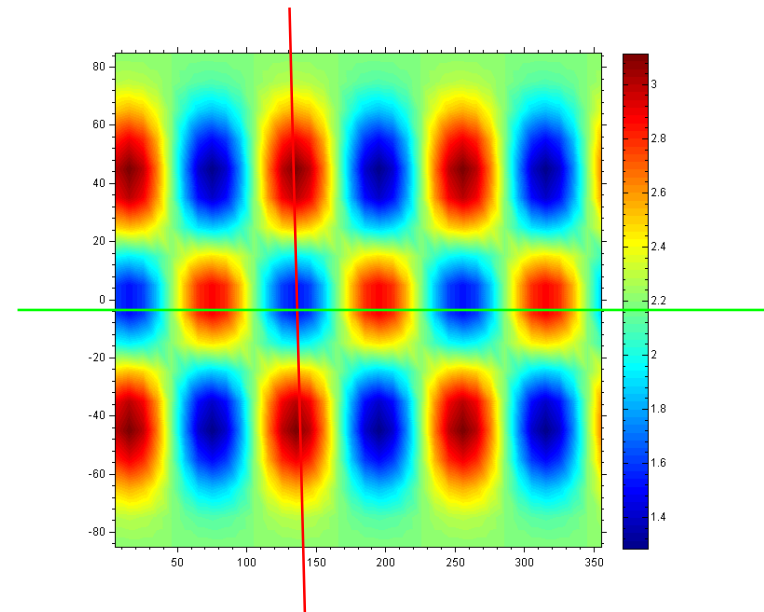
1. Temporal variations of gravity
2. Satellite-borne observations
3. Spherical harmonic synthesis, analysis
4. Digital Terrain Models

$$V = \frac{kM}{r} \sum_l \left(\frac{R}{r}\right)^l \sum_m (\bar{C}_{lm} \cos m\lambda + \bar{S}_{lm} \sin m\lambda) \bar{P}_{lm}(\psi)$$

$$F_{\psi\lambda} = F_{\psi} \cdot F_{\lambda}$$

$$F_{\lambda} = \frac{1}{\text{sinc}\left(\frac{m\Delta\lambda}{2\pi}\right)}$$

$$F_{\psi} = f(l, m, \psi)$$



Application of de-smoothing for geodesy

Digital Terrain Models:

DTMs smooths extremes.



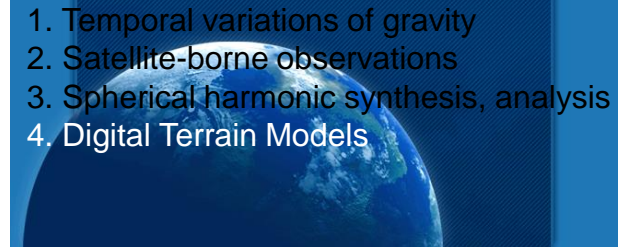
Point-wise extreme cannot be restored by de-smoothing,
but it can be reduced.

DTMs using r, ψ, λ can apply:

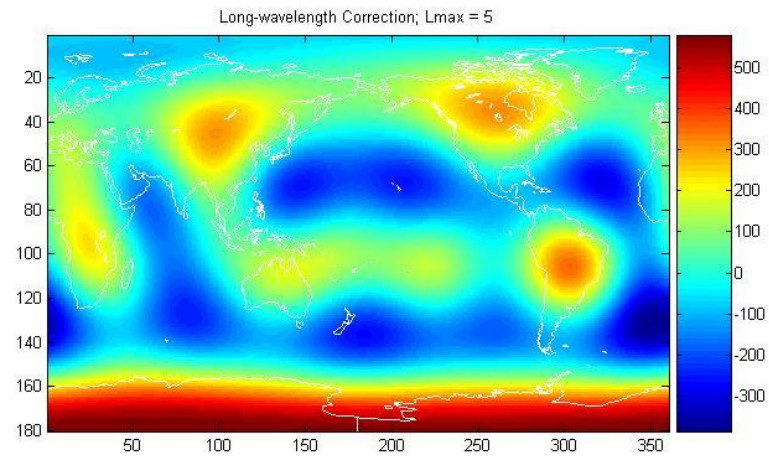
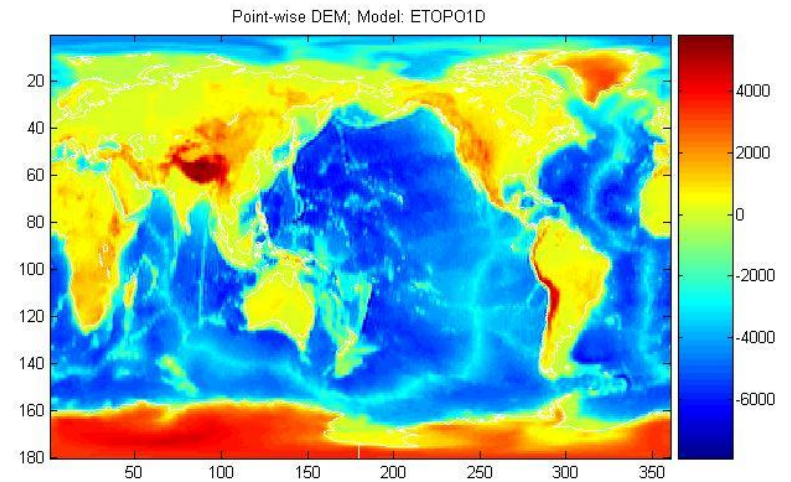
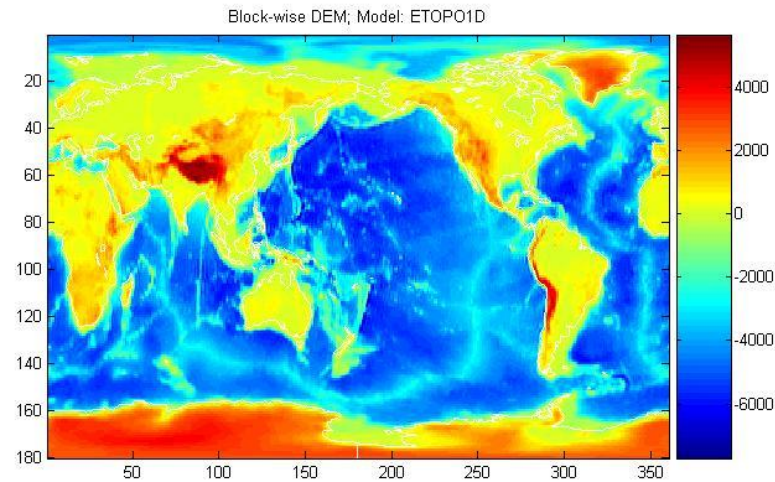
$$F_{\psi\lambda} = F_{\psi} \cdot F_{\lambda}$$

DTMs using topocentric x, y, z coordinates can apply:

$$F_{xy} = F_x \cdot F_y = \frac{1}{\text{sinc}(f_c \Delta x)} \cdot \frac{1}{\text{sinc}(f_c \Delta y)}$$

- 
1. Temporal variations of gravity
 2. Satellite-borne observations
 3. Spherical harmonic synthesis, analysis
 4. Digital Terrain Models

Application of de-smoothing for geodesy



Application of de-smoothing for geodesy

Desmoothing of averaged periodical signals for geodetic applications

Lóránt Földvály

Institute of Geoinformatics, Alba Regia Technical Faculty, Óbuda University, Pálosalma u 1–3, H-8000 Székesfehérvár, Hungary.
E-mail: foldvally.lorant@amk.uni-obuda.hu

Accepted 2015 February 23. Received 2015 February 21; in original form 2014 July 18

SUMMARY

In general, observations are normally considered to refer to an epoch in time, however, observations take time. During this time span temporal variations of the observable alias the measurement. Similar phenomenon can be defined in the space domain as well: data treated to refer to a geographical location often contains integrated information of the surroundings. In each case the appropriate signal content can partially be recovered by desmoothing the averaged data. The present study delivers the theoretical foundation of a desmoothing method, and suggests its use on different applications in geodesy. The theoretical formulation of the desmoothing has been derived for 1-D and 2-D signals, the latter is interpreted on a plain and also on a sphere. The presented case studies are less elaborated, but intended to demonstrate the need and usefulness of the desmoothing tool.

Key words: Time-series analysis; Fourier analysis; Spatial analysis; Satellite geodesy; Geopotential theory; Time variable gravity.

1 INTRODUCTION

In the discussion of Fourier series and transforms, continuous and discrete cases are distinguished. In the discrete case, the function of interest is assumed to be sampled at discrete epochs over a finite record length, and the transform is defined by the well-known formulas of discrete Fourier transform (DFT) converting back and forth between time and frequency domain (cf. Smylie 2013):

$$g(f) = \Delta t \sum_{k=-n}^n G(k) e^{i2\pi f t(k)} \quad (1)$$

$$G(k) = \Delta t \sum_{j=-n}^n g(f) e^{-i2\pi f t(j)} \quad (2)$$

where $g(f)$ is the time-series sampled at $t(f)$ epochs, $G(k)$ is its counterpart in the frequency domain at $f(k)$ frequencies. (Notations of this section based on that of the second chapter of Smylie (2013), which chapter provides a most recent, comprehensive introduction on Fourier series and transforms.)

When the Fourier transform is derived for continuous functions by increasing the record length to infinity, $T \rightarrow \infty$ (equivalently $\Delta f = 1/T \rightarrow 0$) and increasing the sampling rate indefinitely, $n \rightarrow \infty$ (equivalently $\Delta T \rightarrow 0$) the Fourier integral is yielded:

$$g(t) = \int_{-\infty}^{\infty} G(f) e^{i2\pi f t} df \quad (3)$$

$$G(f) = \int_{-\infty}^{\infty} g(t) e^{-i2\pi f t} dt \quad (4)$$

In the latter case, the effect of a finite record length is treated by convolving the continuous function with a boxcar filter (a.k.a. rectangular function, brick-wall filter, Mulgrew *et al.* 2003) or some more elaborated filters in the time domain. The convolution in the frequency domain is a multiplication, as so, the filtering is equivalent to a multiplication of the Fourier transform with a sinc function, the Fourier equivalent of the boxcar filter.

Considering either discrete or continuous Fourier series, in the theory of Fourier transforms the sampling of the time-series (which is obtained by measurements) is considered to take no time. More precisely, this premise is derived by assuming the time span of a sample made to converge to zero, that is $\Delta T \rightarrow 0$ (cf. chapter 2.4.3. of Smylie 2013). In fact, a measurement does take time. Either it is short or long, it is a finite length of time. As so, it is rather improper to consider it to refer to a single epoch. Several measurement types are obviously affected by temporal averaging (e.g. absolute gravity measurements are obtained from huge number of repeated drops), others are implicitly contaminated by temporal aliasing (e.g. satellite geodetic techniques). For most measurement types the time span of the measurement does not affect the result, so the measurement reasonably can be referred to a single epoch. In this study, examples are investigated, when the time span of the measurement is comparable with certain periods of the observable signal.

The adequate way of considering the sampling process is to convolve the continuous time-series with a boxcar function for the time span of the sampling, ΔT at every epoch, instead of forming its product with a finite Dirac comb (Smylie 2013). Note that within the ΔT interval the distribution of the signal can be of variable characteristics. In this study the simplest case is assumed, when during

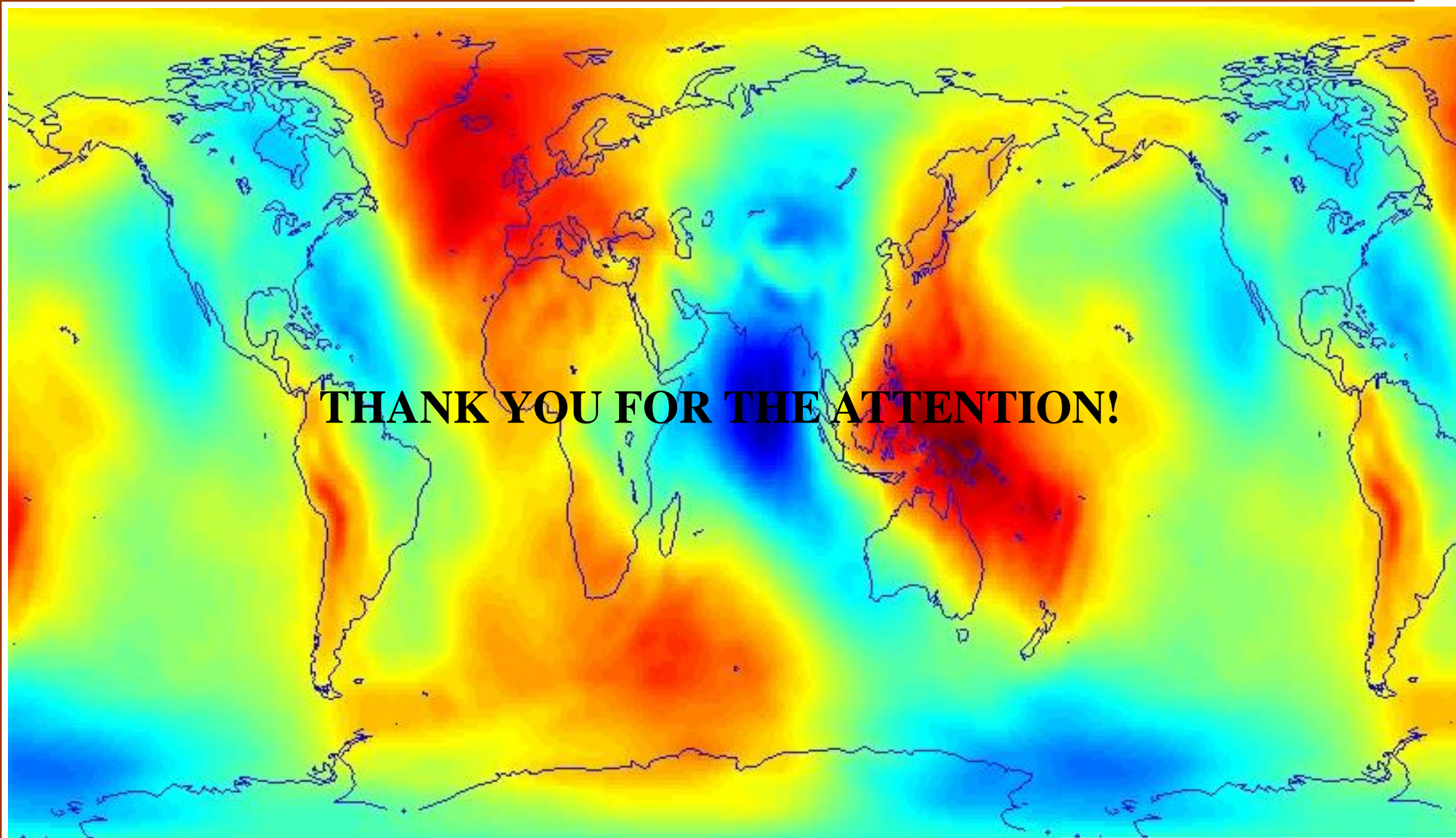
For more details see:

Földvály, L.:

Desmoothing of averaged periodical signals for geodetic applications

Geophys. J. Int. 201, 1235–1250
(2015)

DOI: 10.1093/gji/ggv092



THANK YOU FOR THE ATTENTION!

**Dedicated gravity satellite missions
Mostar, 19.10.2017**